



National Library of Canada
Collections Development Branch

Canadian Theses on
Microfiche Service

Bibliothèque nationale du Canada
Direction du développement des collections

Service des thèses canadiennes
sur microfiche

NOTICE

The quality of this microfiche is heavily dependent upon the quality of the original thesis submitted for microfilming. Every effort has been made to ensure the best quality of reproduction possible.

If pages are missing, contact the university which granted the degree.

Some pages may have indistinct print especially if the original pages were typed with a poor typewriter ribbon or if the university sent us a poor photocopy.

Previously copyrighted materials (journal articles, published tests, etc.) are not filmed.

Reproduction in full or in part of this film is governed by the Canadian Copyright Act, R.S.C. 1970, c. C-30. Please read the authorization forms which accompany this thesis.

**THIS DISSERTATION
HAS BEEN MICROFILMED
EXACTLY AS RECEIVED**

Ottawa, Canada
K1A 0N4

AVIS

La qualité de cette microfiche dépend grandement de la qualité de la thèse soumise au microfilmage. Nous avons tout fait pour assurer une qualité supérieure de reproduction.

S'il manque des pages, veuillez communiquer avec l'université qui a conféré le grade.

La qualité d'impression de certaines pages peut laisser à désirer, surtout si les pages originales ont été dactylographiées à l'aide d'un ruban usé ou si l'université nous a fait parvenir une photocopie de mauvaise qualité.

Les documents qui font déjà l'objet d'un droit d'auteur (articles de revue, examens publiés, etc.) ne sont pas microfilmés.

La reproduction, même partielle, de ce microfilm est soumise à la Loi canadienne sur le droit d'auteur, SRC 1970, c. C-30. Veuillez prendre connaissance des formules d'autorisation qui accompagnent cette thèse.

**LA THÈSE A ÉTÉ
MICROFILMÉE TELLE QUE
NOUS L'AVONS REÇUE**

FLAME PHOTOMETRIC DETECTION/
OF SELECTED ORGANOMETALLIC COMPOUNDS

by

CHRISTOPHER G. FLINN

Submitted in partial fulfillment
of the requirements for the Degree of
DOCTOR OF PHILOSOPHY IN CHEMISTRY

at Dalhousie University
Halifax, Nova Scotia, Canada

DATE

Sept 6, 1979

TABLE OF CONTENTS

	Page
1. Introduction	1
1.1 General Introduction	1
1.2 Use of Optical Spectroscopic Methods for G.C. Detection	2
1.2.1 Atomic Absorption Spectroscopy	2
1.2.2 Infrared and Raman Spectroscopy	3
1.2.3 Discharge Detectors	4
1.2.4 Ultraviolet Absorption and Ultra- violet Fluorescence Detectors	5
1.2.5 Cool Flame Chemiluminescence	6
1.3 Use of Flames as Emission Sources for Gas Chromatography	7
1.4 History of the Flame Photometric Detector	8
1.4.1 The Salet Phenomenon	8
1.4.2 The Bredy-Chaney (Melpar, Mikrotek, Tracor) FPD	9
1.4.3 Melpar Detector Limitations	10
1.4.4 Other FPD Designs	12
1.5 FPD: Characterization and Applications	14
1.5.1 General Characteristics	14
a) The Flame	14
b) Chemiluminescence	15
c) Optimization of Detector Parameters	15

	Page
1.5.2 Characteristics of Sulfur Emission . . .	16
a) Spectrum	16
b) Mechanism of Emissions	18
c) Coping with Quadratic Response . . .	19
d) Sulfur in the Background: Wanted and Unwanted	20
e) The Hydrocarbon Quenching Problem	22
1.5.3 Characteristics of Phosphorous Emission	22
a) Spectrum	22
b) Mechanism of Emission	24
c) General Characteristics	24
1.5.4 Applications	25
a) Pesticide Residue Analysis	25
b) Sulfur in Complex Hydrocarbon Mixtures	25
c) Air Pollution	26
d) Miscellaneous Applications	27
1.5.5 Flame Photometric Detection of Ele- ments Other than P and S	28
a) Air-Hydrogen Flames - Chemiluminescence	28
b) Oxyhydrogen Flames: Thermal Emission	28
1) Organoboron compounds	28
2) Chromium chelates	29
c) Sensitized Flames	29
1) The Beilstein detector	29

	Page
2) Indium-Sensitized Flames	30
3) Sodium-Sensitized Flames	30
1.6 Choice of Species to Investigate	31
1.6.1 General Discussion	31
1.6.2 Tin Compounds	33
a) Uses and Environmental Concerns	33
b) Analytical Methodology	36
1.6.3 Selenium Compounds	37
a) Uses and Environmental Concerns	37
b) Analytical Methodology	39
1.6.4 Germanium Compounds	39
a) Uses and Environmental Concerns	39
b) Analytical Methodology	40
1.6.5 Tellurium Compounds	40
a) Uses and Environmental Concerns	40
b) Analytical Methodology	41
1.7 Gas Chromatography of Compounds of Tin, Selenium, Germanium and Tellurium	41
1.7.1 Tin	41
1.7.2 Selenium	45
1.7.3 Germanium	45
1.7.4 Tellurium	46

	Page
2. Experimental	47
2.1 Shimadzu FPD: Construction and Operation	47
2.2 Reagents and Gases	50
2.3 Detector Design Modifications: Flame Enclosure Geometry and the Use of Masks	51
2.3.1 Modified Flame Enclosures for Tin Detection	51
2.3.2 Masks for Bisected Flame Enclosures	53
2.3.3 Masks for Geometric Selectivity	55
2.4 Optimization of Detector Parameters	55
2.5 A Simple Method for Determination of a "Spectrum" using a Flame Photometric Detector	57
2.6 Doping Arrangements	59
2.6.1 Carbon Disulfide (Sulfur) Doping	59
2.6.2 Hydrogen Chloride and Hydrogen Bromide Doping	59
2.6.3 Methane Doping	61
2.6.4 Silane Doping	61
2.7 Hydride Generation	65
3. Organotins: Detection, Derivatization and Application to Environmental Samples	67
3.1 Development of a Photometric Tin Detector: A Brief History	67
3.2 Characterization and Optimization of the Photometric Tin Detector	70

	Page
3.2.1 Spectral Characteristics	70
3.2.2 Flow Rate Optimization	73
3.2.3 Detector Performance	75
3.2.4 Hydrocarbon Interference: Methane Coping	78
3.2.5 Detector Poisoning	80
3.2.6 Effect of Quartz Flame Enclosure Geometry	86
3.3 The Tin Emission Mechanism: Surface vs. Gas- Phase Luminescence	86
3.3.1 Visual Observation	88
3.3.2 The Bisected Enclosure and the Masks for Geometric Selectivity	89
3.3.3 Effect of the Height of the Bisecting Tube Above the Flame on Tin and Sulfur, Using China Ink Masks	90
3.3.4 A Dual-Masked Bisected Quartz Flame Enclosure for Geometrically Selective Monitoring of FPD Emissions	91
3.3.5 Assessment	93
3.4 The Quartz Wool Tin Detector (QWTD)	96
3.5 Derivatization of Labile Tin Compounds	97
3.5.1 Organotin Hydrides	97
a) Reaction Conditions	101
1) Importance of Solvent	102
2) Reaction Rate	102
3) Other Parameters	104
b) Chromatography	104

	Page
3.5.2 Organotin Halides	106
a) R_3SnX	107
b) R_2SnX_2 and $RSnX_3$	107
c) Important Considerations and Parameters	109
3.5.3 Application to Environmental Samples: Future Work	112
4. Organoselenium Photometric Response	114
4.1 Development of a Selenium Photometric Detector .	114
4.2 Characterization and Optimization of the Selenium Photometric Detector	114
4.2.1 Spectral Characteristics	114
4.2.2 Flow-Rate Optimization	117
4.2.3 Detector Performance	117
4.2.4 Hydrocarbon Interference: Methane Doping	118
5. The Interchalcogen Effect: S-Se-Te	124
5.1 Discovering the Interchalcogen Effect	124
5.2 Characteristics of CS_2 (Sulfur) Doping	125
5.3 Development of Mathematical Models for Sulfur and Selenium Response Under Sulfur Doping Conditions	133
5.3.1 Sulfur	133
5.3.2 Selenium	138
5.4 Search for the Interchalcogens (SeS , TeS , $SeTe$)	143
5.4.1 What is the Cause of the "Interchalcogen Effect"?	143
5.4.2 Search for Spectral Evidence	144

	Page
6. Germanium Photometric Response	152
6.1 Surface-Induced Emission	152
6.1.1 Initial Investigation	152
6.1.2 Spectral Characteristics	153
6.1.3 Flow Rate Optimization	155
6.1.4 Detector Performance	157
6.2 Gas-Phase Luminescence	158
6.2.1 Spectral Characteristics	158
6.2.2 Flow Rate Optimization	162
6.2.3 Detector Performance	162
6.3 Tin and Germanium in the FPD: A Comparison	165
7. Selectivity	168
8. Conclusions	173
Appendix	175
References	185

LIST OF FIGURES

<u>Figure number</u>	Page
1. Sulfur "Spectrum" - 320 nm to 504 nm	17
2. Phosphorous "Spectrum" - 450 nm to 800 nm	23
3. Schematic of the Shimadzu FPD	48
4. Modified Flame Enclosures for Tin Detection.	52
5. Masks for Bisected Flame Enclosure	54
6. Masks for Geometric Selectivity	56
7. Flow Schematic for CS ₂ Doping	60
8. Flow Schematic for HCl or HBr Doping	62
9. Flow Schematic for CH ₄ Doping	63
10. Flow Schematic for SiH ₄ Doping	64
11. Flow Schematic for Organotin Reduction with Silane	66
12. Tin Emission Spectra - 300 nm to 650 nm, in Both "Normal" and "Overloaded" Conditions Using a Constricted Quartz Flame Enclosure	72
13. Sensitivity Versus Air and Hydrogen Flow Rates for Two Tin Emissions	74
14. Tin Detector Performance - an Overall View	76
15. Detector Sensitivity - Temperature-Programmed Chromatography of Five Organotin Compounds at the 10 pg and 1 pg Levels	79
16. Effect of Methane Doping on Tin Response - using a Constricted Quartz Flame Enclosure	81
17. Detector Poisoning	82
18. Dependence of Tin Compound Peak Shape on Quartz Flame Enclosure Geometry	84
19. Chromatography in the Saturation Region of the Calibration Curve of Various Tin Compounds	87

	Page
20. Variation of Tin and Sulfur Response with the Height of the Bisecting Tube above the Flame Cup	92
21. Ratio of "Gas-Phase" vs. "Surface" Emissions for Tin, Germanium and Sulfur Response Via a Dual-Masked Bisected Quartz Flame Enclosure	94
22. Temperature-Programmed Chromatography of a 4-Component Mixture with Detection on Both Surface and Gas-Phase Selective Channels of a Dual-Masked Bisected Quartz Flame Enclosure	95
23. Calibration Curves for Tetrapropyltin using the Quartz Wool Tin Detector and a Normal Pyrex Flame Enclosure	98
24. Chromatography of 100 Femtograms of Tetrapropyltin using the Quartz Wool Tin Detector	99
25. "Yield" of Tributyltinhydride Versus Time of Reaction for the Reduction of tributyltin Oxide with Silane	103
26. Chromatography of tripropyltin Oxide and tributyltin Oxide as Chlorides at the 1 pg Level	108
27. Chromatography of Butylstannic Acid, Dibutyltin Oxide and Tributyltin Acetate as Chlorides at the 1 ng Level	110
28. Selenium "Spectrum" - 300 nm to 630 nm	115
29. Calibration Curves for Methylselenole and Possible Interfering Species using a 484 nm Interference Filter and a Constricted Quartz Flame Enclosure	119
30. Temperature-Programmed Chromatography of Four Selenium Compounds at 1 and 10 ng Levels	120
31. Response of Selected Compounds Versus Amount of Methane Added to the Carrier Gas	121
32. Calibration Curves for Methylselenole and Possible Interfering Species Using a 484 nm Interference Filter, a Constricted Quartz Flame Enclosure and Methane Doping	123
33. The Effect of Different CS ₂ Doping Levels on	

	Page
the Calibration Curves of Diphenylsulfide, Diphenylselenide and Octadecane	126
34. The Effect of Various CS ₂ Doping Levels on the Calibration Curve of Dibutyltellurium	128
35. Linearization of Sulfur and Selenium Response Via CS ₂ Doping	130
36. Effect of Sulfur Background on the Response of 2 ng of Diphenylsulfide and 20 ng of Diphenyl- selenide	137
37. Comparison of Calculated and Experimental Cali- bration Curves for Diphenylsulfide and Diphenyl- selenide under Sulfur Doping	139
38. Representation of a Selenium Peak on a Sulfur Background	145
39. A Comparison of Detector Spectral Output: A Sulfur "Spectrum", a Selenium "Spectrum" on a Large Sulfur Background and a Pure Selenium Spectrum	148
40. A Comparison of a Detector Spectral Output: A Tellurium "Spectrum" on a Large Sulfur Back- ground and a Pure Tellurium "Spectrum"	149
41. A Comparison of Germanium, Tin and Background Spectra Using a Bisected Quartz Flame Enclosure	154
42. Germanium Detector Performance: An Overall View	157
43. Comparison of Germanium "Spectra" in Surface- Induced and Gas-Phase Emission Modes	159
44. Tin and Germanium "Spectra" in the Gas-Phase - 200 nm to 800 nm, Optimized for "GeH" Emission	161
45. Tin and Germanium "Spectra" above 600 nm - "High Resolution"	163
46. Sensitivity Versus Air and Hydrogen Flow Rates for "GeH" Emission	164
47. Calibration Curves for Tetrabutylgermane and Tetrabutyltin Using a 650 nm Interference Filter	166

48. Illustration of Selectivity Measurements
between Calibration Curves. Case 1: Both
Linear, Case 2: Both Quadratic Case 3:
One Linear, One Quadratic 169

LIST OF TABLES

<u>Table No.</u>		Page
1.	Flame Photometric Detection Limits	78
2.	Comparison of Tin and Sulfur Response Using a Masked Bisected Flame Enclosure in "Side-on" and "End-on" Viewing Modes . . .	90
3.	Detection Limit of Tin Using the Quartz Wood Tin Detector	97
4.	Typical Linear Calculations of Analyte Content by the Internal Standard Technique	131

ABBREVIATIONS AND SYMBOLS

AAS	- atomic absorption spectroscopy
AC	- alternating current
Chrom W	- Chromosorb W
const	- constant
DC	- direct current
DFO	- Department of Fisheries and Oceans
ECD	- electron capture detector
EPA	- Environmental Protection Agency
FID	- flame ionization detector
FPD	- flame photometric detector
g	- grams
HAFID	- hydrogen atmosphere flame ionization detector
ID	- inner diameter
IR	- infrared
IUPAC	- International Union of Pure and Applied Chemistry
MDA	- minimum detectable amount
MECA	- molecular emission cavity analysis
μ g	- microgram
μ l	- microliter
min	- minute
ml	- milliliter
mm	- millimeter
MS	- mass spectroscopy

MTES - metastable transfer emission spectroscopy
n- - normal
OD - outer diameter
PM - photomultiplier
ppb - parts per billion
ppm - parts per million
psi - pounds per square inch
QWTD - quartz wool tin detector
sec - second
t- - tertiary
UV - ultraviolet
WHO - World Health Organization

Acknowledgement

I am deeply indebted to my most knowledgeable supervisor, Dr. Walter A. Aue, who guided and directed the research on which this thesis is based. I am truly grateful for the friendship and support, both moral and scientific, of Dr. Velupillai Paramasigamani, his wife, Kalyani, and Dr. Zbigniew Mielniczuk. Special mention goes to Dr. Shubhender Kapila, Michael Siy and Juergen Mueller (the master glassblower) for all their help. I would like to thank my family for providing the kind of care and understanding necessary for my well-being and success.

Finally, I would like to acknowledge the support of the Izaak Walton Killam Scholarship Fund and the National Research Council during my studies.

Dedication

To the Flinn's

To the Newman's

To the Haggerty's

To the Stone's

Abstract

A dual-channel flame photometric detector (Shimadzu) was adapted for the detection of organic compounds of tin, selenium, tellurium and germanium as separated by gas chromatography.

Tin was found to yield extremely efficient luminescence on a quartz surface that had been suitably treated and positioned above the flame. Several experiments were carried out to confirm that the luminescence was indeed induced by the surface. The minimum detectable concentration of tin was 5.3×10^{-16} g/sec. A reduction method using SiH_4 , and a halogenation method based on conditioning the gas chromatograph with HCl or HBr were developed for derivatizing labile tin compounds in order to exploit the sensitivity of the detector for environmental trace analysis.

Selenium photometric response was found to closely parallel that of sulfur. Increasing the selectivity of selenium versus sulfur was accomplished using methane doping. The mutual enhancement of response among the chalcogens led to chemical linearization of their exponential response. A mathematical treatment of the linearization of sulfur and selenium response by sulfur doping was carried out, as well as a spectroscopic search for proof of the existence of the molecules, SeS and TeS .

The photometric response of germanium compounds in the detector was found to closely resemble that of tin,

with an analogous, surface-induced response and a similar gas phase hydride emission spectrum. A discussion of the use and mis-use of the word, selectivity, with respect to the so-called selective detectors is also presented.

1. Introduction

1.1 General Introduction

Gas chromatography has become an indispensable tool for separating complex mixtures of organic compounds. A variety of detectors have been developed to provide qualitative and quantitative analysis of the separated compounds. They are of the general type, such as the Flame Ionization Detector (FID), or of the selective type, such as the Electron Capture Detector (ECD). Selective detectors can be used to aid in the identification as well as in the quantitation of organic compounds containing important heteroatoms. To realize the importance of selective detectors, one need only to recall that the environmental concerns over DDT and the Freons were precipitated by use of the ECD.

A good selective detector must be able to "see" the heteroatom of interest in a complex sample matrix and detect it at trace levels. This is important because compounds containing heteroatoms, such as organometallics, are often present at trace (ppm) and ultratrace (ppb) levels. Even at such low concentrations compounds may show biological activity, sometimes both beneficial and detrimental. Such biological activity is known to be greatly affected by speciation of a particular element, i.e., the chemical structure associated with it. Gas chromatography with selective detection can often answer the qualitative question: What species is present?, in addition to providing the usual quantitative data.

1.2 Use of Optical Spectroscopic Methods for GC Detection

The various processes of absorption or emission of light are the basis of optical spectroscopy. Techniques based on these processes can yield structural information about a compound and identify elements or molecular fragments in its breakdown products. Various dispersive devices such as interference filters and monochromators induce selectivity to optical spectroscopy by alleviating the ever-present problem of interfering species, or by resolving the spectroscopic information into recognizable patterns. A great deal of effort has gone into the marriage of such widely divergent techniques as infrared spectroscopy (IR) and atomic absorption spectroscopy (AAS) to gas chromatography. This has resulted in a family of selective detectors which are capable of providing reliable qualitative and quantitative information for a broad range of applications. A general review of these detectors, stressing their advantages and disadvantages, is provided here as a necessary background for the subject of this thesis.

1.2.1 Atomic Absorption Spectroscopy

Atomic absorption spectroscopy is a truly specific detection method for a large number of elements. Hence identification of the unknown is possible in many cases because of the very narrow linewidth specificity of atomic resonance radiation. Both flame (1-7) and non-flame (6-14) atomic absorption techniques have been applied to GC detection. Non-flame techniques are orders of magnitude more

sensitive than flame techniques, but are much more difficult to master. Parris et al. (15) have undertaken a detailed study of chemical and physical parameters of non-flame atomic absorption coupled with GC. Typically AAS has been used in conjunction with hydride generation or methylation techniques to determine volatile compounds separated by gas chromatography.

1.2.2 Infrared and Raman Spectroscopy

These molecular, hence complementary techniques can be coupled with a gas chromatograph to provide important qualitative information (16-30). The eluted GC component can be trapped or held in the cell by stop-flow or cryogenic techniques, and the spectrum scanned. For small samples, the low sensitivity of infrared spectrometers sometimes necessitates collecting the total eluted substance (batch) rather than recording only a portion of it during the course of its elution ("on-the-fly"). Fourier transform spectrometers permit scanning of components on-the-fly (27-29) because of their superior speed and sensitivity.

Since strong absorptions occur in this spectral region at wavelengths specific for functional groups, versatile group-specific detectors have been made available, whose selectivity can be easily altered. A number of these group-specific detectors can be arranged in tandem and made to produce multichannel chromatograms identifying the functionality of eluting peaks. Considerable improvement in sensitivity and cell constant of IR detectors has recently

4
been made by Hausdorff (25,26).

A further interesting development in GC-IR has been made by Kreuzer (30). Unlike previous detectors, his device used an IR laser radiation source and an optoacoustic detector. He reported that the combination results in a sensitivity at least 1000 times better than previously reported systems. The detector works on the basis of sound waves generated by the absorption of an amplitude-modulated IR beam and measured directly by a microphone. The microphone was kept cool for optimum performance. The excellent sensitivity of this detector could enable it to complement GC-MS (in areas where mass spectroscopy fails to distinguish between compounds, e.g. isomers).

1.2.3. Discharge Detectors.

Various types of discharge detectors have been developed which are based on monitoring the emission spectra of compounds eluted from a gas chromatograph and fragmented and excited in a high-energy plasma. Such plasmas are produced by radio (31,32) or microwave (33-53) generators or the more conventional DC and AC power supplies (54,55). Helium is most often used as a discharge gas, followed by argon. The mechanism of molecular degradation and excitation is attributed to ionized or metastable rare gas atoms, to electron bombardment, and possibly to thermal excitation processes. A scanning monochromator is typically used to monitor the emission.

MacCormack, Teng and Cooke (33) first reported the use of a microwave-stimulated plasma emission detector for organic compounds containing phosphorous, sulfur and halogens as well as for permanent gases. The detector showed a linear dynamic range of 2×10^4 and selectivity from two to four orders of magnitude versus hydrocarbons. Considerable work has been done to optimize this type of detector with regard to plasma stability, reduced background emission and increased emission intensity. Dagnall et al. (42) extended its use to volatile metal chelates of aluminum, chromium, copper, iron, scandium, gallium and vanadium. It is possible that, in the future, these discharge detectors will be improved and used on a wider range of other organic and heteroorganic compounds.

1.2.4 Ultraviolet Absorption and Ultraviolet Fluorescence Detectors

The detection of column effluents by ultraviolet spectroscopy has been largely confined to liquid chromatography where it has been indispensable. For gas chromatography one can trap samples, dilute them with solvent and measure them in a conventional UV spectrometer. Hought and Baalhuis (56) combined a second derivative ultraviolet spectrometer and a gas chromatograph for on-the-fly analysis. Obviously, only compounds with large extinction coefficients can be usefully analysed by GC-UV.

The techniques of UV-fluorescence have been applied more successfully to gas chromatography (57-61). It has

proven sensitive (nanogram range) and selective to polynuclear aromatic systems. The detection systems range from fast-scanning fluorescence spectrometers (58), photomultiplier tubes with wide-band pass filters (61), to SIT image Vidicon tubes (59) that can provide background correction.

1.2.5 Cool Flame Chemiluminescence

The phenomenon of chemiluminescence has been known for a long time; the burning of white phosphorous in air and the glow of marsh gas are two prime examples. Only recently, though, has it been used as an analytical technique; for the most part finding application in gas analysis and air pollution monitoring (62,63). The reactions of ozone with organic species such as olefins and sulfur compounds have been used as a detector for gas chromatography (65,65). Olefinic and sulfur-containing compounds give high responses which can be optimized by adjustment of detector temperature and ozone flow rate.

A very sensitive method for the determination of oxygen based on P_4-O_2 chemiluminescence has been developed by Aue et al. (66). The cold flame of phosphorous has been further developed as a selective detector for GC effluents, based on the fact that organic molecules compete in the complex reaction mechanism of this flame with widely different efficiencies and thereby quench its luminescence (67).

1.3 The Use of Flames as Emission Sources for Gas Chromatography

Grant (68) suggested the use of flame emission for the detection of organic compounds separated by gas chromatography. His detector was based on the increase in the total emission of a hydrocarbon/air flame without wavelength discrimination caused by the combustion of column effluents. The high background emission of such flames restricted the sensitivity of the detector considerably.

Zado and Juvet (69) used an oxy-hydrogen flame with a Beckmann atomizer-burner to detect metal chelates, metal halides and organic compounds. A monochromator system with narrow slits enabled the detector to monitor atomic lines to give a high degree of selectivity. The detector could also be operated in a non-selective mode for organic compounds and elements giving no distinct emission lines, by providing an alternate, direct light path between the burner and the photomultiplier tube with a simple filter chosen to eliminate radiation from the hydroxyl bands of the flame. The non-selective mode proved superior in providing sensitivity for species with broad emission bands. Juvet and Durbin (70) gave a more detailed characterization of the operation and performance of this detector in the selective mode.

Braman (71) employed the cooler air-hydrogen flame using interference filters for selectivity for the GC detection of organic compounds. Spectra were recorded for

all species of interest e.g. aliphatics, aromatics, amines, sulfur and phosphorous-containing compounds, in order to determine which interference filter could be used. The sensitivity was in the microgram range for organics and in the nanogram range for heteroorganics. Braman also studied the effect of structure on spectral response of organic compounds for qualitative information.

Recently Belcher et al. (72) evaluated the use of Molecular Emission Cavity Analysis (MECA) as a gas chromatographic detector. MECA is based on molecular emissions produced in a cavity suitably placed in an air-hydrogen flame and has been applied to the determination of several types of heteroorganic and inorganic compounds (73, 74). The authors feel that the MECA detector is more versatile than a conventional flame photometric detector and indicate that, although its sensitivity is not as good, considerable improvement in this area could be made by a thorough optimization of detector parameters.

1.4 History of the Flame Photometric Detector

1.4.1 The Salet Phenomenon

Chemiluminescence phenomena produced by the cool air-hydrogen flame operating in a hydrogen-rich atmosphere led to the development of what is widely known as the flame photometric detector (FPD). Over 100 years ago, Salet (75) discovered that if a cold object is placed near the core of a low-temperature, fuel-rich hydrogen flame, an intense blue or green emission is observed near the surface of the

object depending on whether a sulfur or a phosphorous compound is introduced. These emissions arise from the S_2 and HPO molecules formed in the flame gases chilled by the relatively cool surface of the object. Nearly 100 years later, Brody and Chaney (76) developed the first GC detector based on this phenomenon.

1.4.2 The Brody-Chaney (Melpar, Mikrotek, Tracor) FPD

Essentially, the Tracor FPD is a combination of a flame ionization detector and an optical system consisting of a filter and a sensitive, low-noise photomultiplier tube. The column effluent is premixed with air (sometimes with oxygen) and fed into the burner, which is surrounded by four openings supplying hydrogen. The fuel-rich flame burns inside a metal cup or flame shield on top of the burner nozzle. This effectively prevents the emission of the luminous primary zone from reaching the photomultiplier tube. A quartz window separates the filter and PM tube from the flame gases. The optical parts are thermally insulated by an adaptor made from modified teflon. In addition, the adaptor is provided with aluminum fins for extraneous cooling. Early models did not have the teflon adaptor. They did, however, include a mirror opposite the optical system to increase the light throughput for single channel operation. This turned out to be wishful thinking and the mirror was later discarded.

The detector was sensitive to sub-nanogram amounts of phosphorous compounds and could detect as little as a nano-

gram of sulfur compounds. The selectivity of the detector was concentration dependent, but ranged from 3 to 4 orders of magnitude versus hydrocarbons. Sulfur response was quadratic, with only two orders of magnitude linearity on a log-log plot; phosphorous response, however, was linear for about 4 decades.

1.4.3 Melpar Detector Limitations

The Melpar FPD was not without its problems. The flame was extinguished when one microliter or more of organic solvent eluted from the column. Hydrocarbons eluting from the column at the same time as a sulfur compound depressed its response. The original detector had an upper detector temperature limit of 165°C to prevent damage to the optics. Since patent protection assured a captive market, the companies taking over the Melpar patent, Mikrotek and then Tracor, did not improve to any significant extent the original Brody and Chaney design, but relied on FPD users for further progress.

Proper insulation of the optics was ensured by means of water-cooled copper coils placed between the flame region and the PM tube. This allowed the detector to be operated in excess of 250°C.

The flame-out problem was attacked by a variety of means, including simple modifications of the detector and its flow system (77-79) as well as new detector designs (80-82). The simplest approach was to vent most of the solvent, leaving enough to give a solvent peak but not

enough to extinguish the flame. Burgett and Green (79) simply reversed the hydrogen and air inlets and found improved detector performance.

Moye (81) built a non-extinguishing FPD, using a modified acetylene torch tip as a burner. The column effluent passed through the centre tube while the hydrogen and air were premixed and flowed through the outer tube. Moye explained the "non-extinguishing" property by the modes of gas mixing in the detector. The solvent can't flash back through the torch because there is no oxygen to support combustion.

Gibbons and Goode (82) describe another permutation of detector design, where the column effluent was mixed with the fuel gas forming a hydrogen-hyperventilated flame. A similar modification can be seen in the Shimadzu FPD which will be described later in the experimental section.

The problem of hydrocarbons quenching detector emission has been dealt with by separating the processes of compound degradation and chemiluminescent emission. Rupprecht and Phillips (83) first developed a dual-flame photometric detector. The purpose of the first flame was to combust the compounds eluting from the column to CO_2 and SO_2 , and the purpose of the second, to produce the desired emission. The quenching effect on emission by CO_2 is negligible when compared to that exerted by the hydrocarbons themselves. This made prior separation of sulfur compounds and hydrocarbons unnecessary for the analysis of sulfur

compounds in gas, fuel and petroleum samples. Varian has recently developed a commercial model of a dual-flame photometric detector (84); it has shown great promise in the area of reliable quantitation of sulfur compounds (85). The only drawback of the dual-flame detector is its somewhat lower sensitivity, possibly because of the dilution of the sample with considerable quantities of flame gases.

1.4.4 Other FPD Designs

A lot of work was done by various investigators to improve the Brody-Chaney design and to increase the flexibility and reliability of flame photometric analysis.

Hasinski (80) designed a detector which used a thermal insulation plate to separate the luminescence and burner regions. The insulating plate could easily be replaced with others of different size to change the geometry of the detector itself. It allowed thermal control of both parts of the detector, that is, the burner could be maintained at high temperature while the luminescence block could be kept as low as 100°C (necessary to prevent the condensation of water). The separation of the detector parts influenced parameters such as background emission (hence noise) and detector sensitivity to carbon. If stoichiometric conditions were met, then up to 30 μ l of solvent could be injected without extinguishing the flame over a wide range of flow rates.

Joonson and Loog (86) developed a detector with specific combustion and emission chambers, which improved

the selectivity of phosphorous and sulfur versus hydrocarbons. Air or oxygen was introduced through a series of orifices in the combustion chamber, each of which produced a flame burning in a hydrogen-rich atmosphere. Compounds from the column were mixed with the hydrogen stream and decomposed in the combustion chamber. The flow of flame gases, supplemented by an inert gas, swept the reacting substances into the second chamber for S_2 and HPO emission. No "flame-outs" resulted for up to 50 μ l of injected sample.

The Pye FPD was introduced in 1974 and has been characterized by Greenhalgh and Wilson (87). Hydrogen and the column effluent were premixed and encountered the air only at the burner tip. Unlike in most FPD designs, the entire flame was viewed by the PM tube.

A number of photometric detectors, although not combined with a gas chromatograph, provided some insight into detector design. Aldous et al. (88) studied a reducing air-hydrogen diffusion flame that used a large, open-tube pyrex burner in place of a standard circular emission burner head. It could be used with aqueous or organic matrices. A nebulizer capable of producing a very fine, uniform mist could be satisfactorily used; on the other hand, a pre-burning stage for organic liquids of low-sulfur content was needed to oxidize the sulfur to SO_2 .

The effect of a shield, which surrounded the emission zone of the flame, was investigated by Veillon and Park (89).

They used shields of different dimensions and materials - e.g. borosilicate glass, fused silica, copper and stainless steel. Basically they found that the shield was necessary to produce chemiluminescence but that its dimensions and composition were not important. Syty and Dean (90) found different optimum shield dimensions for sulfur versus phosphorous emission.

Von Haub et al. (91) designed a burner which had a split flame. The emission zone of the flame had a quartz shield which was cooled by running water, to prevent radiation-less decomposition of excited HPO species. No use for detection purposes was made of the second flame burning on top of the quartz shield.

1.5 FPD: Characterization and Applications

1.5.1 General Characteristics

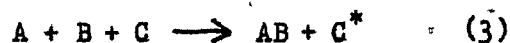
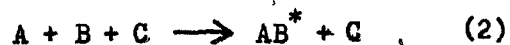
(a) The Flame

The heart of the flame photometric detector is the fuel-rich air-hydrogen flame. The energetics of the flame are such that little thermal emission can occur, the flame temperature being low compared to such flames as air-acetylene. As a result the flame has a low level of background emission. Even the well-known OH band at 301.0 nm is very weak. As one approaches a stoichiometric flame, the background emission increases and the detector noise increases as well. The probability of thermal emission increases as the flame becomes more energetic. The primary zone of the flame is the main source of background emission

and it is usually blocked from view of the PM tube. The primary zone serves to decompose the column effluent into small molecular fragments while the secondary zone and the relatively cool region above it provide the emission.

(b) Chemiluminescence

Emission from species such as S_2 and HPO occurs by chemiluminescence, not by thermal emission. Basically chemiluminescence is light emitted due to a chemical reaction, and can be of the following types:



Two-body association or recombination reactions producing electronically excited states are characterized by the "recombination" continuum emitted in the radiative stabilization of the association complex. Three body reactions, on the other hand, give rise to discrete spectral features. The third body removes some of the excess vibrational energy from the newly formed, electronically excited molecule, leaving it in one of its discrete vibrational states. Reactions in the gas phase involving excited electronic states have been reviewed by Laidler and Shuler (92).

(c) Optimization of Detector Parameters

The detector must be optimized for sensitivity (best signal-to-noise ratio) and selectivity (versus known interferences). Such optimization involves the choice of

flow rates, detector geometry, filter, PM tube, etc. One normally uses an interference filter for selectivity purposes, but the choice of a filter also affects sensitivity. It relates to spectral characteristics, e.g. sharpness of bands, number of prominent peaks, presence of continuum emission, wavelength range, etc. The selectivity of the detector using an interference filter depends on the particulars of the transmission profile (percent maximum transmission, band width at half height), its ability to cut off spectral regions above and below the chosen maximum wavelength, and the degree of spectral overlap with the bands of interfering species. If there is little interference and sensitivity is the major concern, the detector can be operated without a filter (93). It is interesting to note that the FPD's selectivity for P and S versus hydrocarbons is only slightly lowered by running it in such an "open-mode" (93).

1.5.2 Characteristics of Sulfur Emission

(a) Spectrum

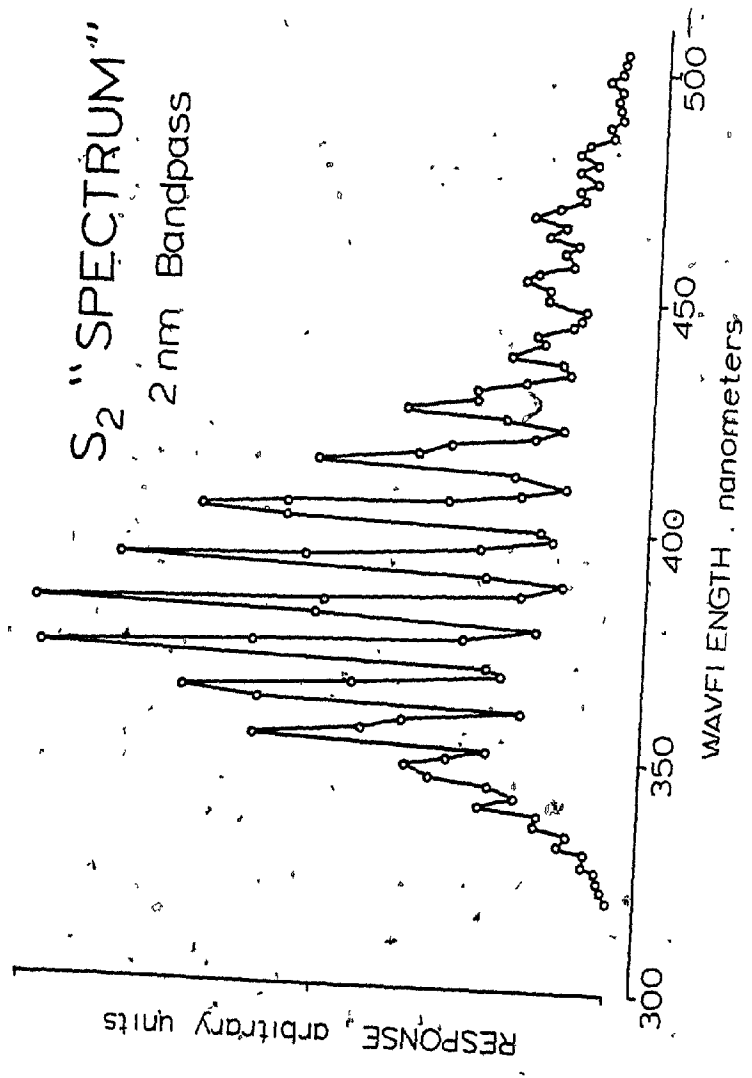
Sulfur emits the well-known S_2 spectrum as seen in Figure 1. It consists of a large number of closely-spaced, sharp bands from about 300 nm to 600 nm. The most intense of the bands lie close to the strongest one at 394 nm. Because of its very broad S_2 spectrum, sulfur can interfere in the analysis of other species by flame photometric detection. The most notable example is the "cross-talk" of sulfur compounds during an analysis for phosphor-

17

Figure 1

Sulfur "Spectrum" - 320 nm to 504 nm

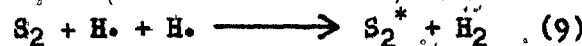
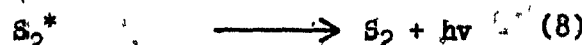
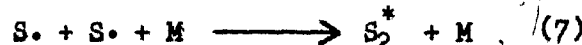
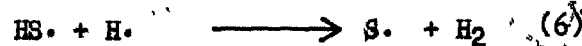
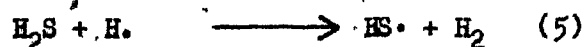
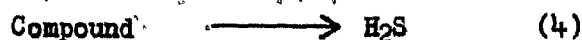
2 nm bandpass



ous compounds using a 526 nm interference filter. This problem can be alleviated by dual-channel operation of the detector and has been dealt with electronically by Johnson and Loog (86). It has been common practice to use an interference filter with maximum transmission at 394 nm although the 394 nm band has no particular advantage over any of the other nearby bands.

(b) Mechanism of Emission

From the spectrum, it is clear that S_2 is the emitting species for sulfur response. The mechanism leading to this emission must produce enough energy to satisfy the chemiluminescence requirement. Sugiyama et al. (94) proposed the following mechanism:



Reaction (7) seems to be clearly favoured because its kinetics require that the response be proportional to the square of the concentration of sulfur atoms, e.g.

$$R \text{ prop. } [S_A]^n \quad n = 2 \quad (10)$$

R = FPD response, peak height

S = sulfur in analyte injected

and, in actual practice, sulfur compounds do show quad-

ratio response. Equation (9) is also thermodynamically feasible (as are possibly other reaction schemes).

There has been a great deal of controversy over whether or not sulfur response and the slope of the calibration curve is dependent on the structure and oxidation state of the sulfur atoms in the chromatographed compound. Several authors (95-97) have concluded that sulfur response is strongly dependent on compound type with the exponent "n" ranging from 1.5 to 2.0. Kakemoto and Maruyama (98) however, countered that response depended only on the number of sulfur atoms in a molecule and not on its chemical structure, provided all experimental conditions were kept constant for the comparison (including retention time, i.e. chromatographic peak width).

(c) Coping with Quadratic Response

For the analyst a linear response is an ideal, a non-linear one a headache. It generally means that larger errors can be expected and that more care must be taken to keep all conditions constant.

Coping with non-linear sulfur response has involved many different approaches. The simplest and most tedious is to plot frequent log-log calibration curves. This is time-consuming and not very popular. The calibration curve can be electronically linearized if the response exponent is precisely known using a variable-exponent linearizer module (99). Some commercial linearizers (100,101) assume the exponent to be precisely 2. As was previously men-

tioned, there has been a lot of controversy over whether or not the response exponent is really 2 for all sulfur compounds. With this in mind, the potential error using such commercial linearizers could be large and has been studied by Burnett et al. (102).

If sulfur response is not truly quadratic, then the approach of Attar et al. (103) using the equation

$$R = \frac{A}{R_m \left(\frac{n-1}{n} \right)} \quad (11)$$

A = peak area R_m = peak height,

R = linearized response n = response exponent

can be used. However, if sulfur response is quadratic, then either the standard addition method as shown by Marcelin (104) can be used, or the relationship

$$R = \sqrt{R_m} \cdot W \quad (12)$$

W = peak width at half height

can be plotted as outlined by Kakimoto (98) for a linear calibration curve.

(d) Sulfur in the Detector Background: Wanted and Unwanted

According to the kinetics of sulfur emission, a continuous amount of a volatile sulfur compound could be added to the detector in order to enhance the response of any sulfur compound injected on top of this background. This feature of a square law detector was pointed out by

Crider and Slater (105).

In fact one very annoying problem in the analysis of sulfur compounds by flame photometric detection has been the frequent but irreproducible "linearization" of the lower end of the calibration curve. This has been used by Maitlen et al. (106) for insecticide residue analysis. Moss (107) commented that the effect "may be used for detecting small unwanted backgrounds...due to detector contamination or column bleed". The effect could easily be produced by a volatile, sulfur-containing impurity in one of the supply gases.

It is obvious that improvements in detection limits can be obtained by providing a suitable sulfur background (105,107,108). One can also envisage the linearization of sulfur calibration curves by chemical means, that is, by creating a pseudo-first order reaction by providing a suitably large sulfur background. The idea seems promising as it should eliminate the problem of irreproducible data from the low end of the calibration curve, and produce an extended range of linear response. The practicality of the method would depend on how easy a constant sulfur background could be introduced, and how much the expected increase in detector noise would raise the minimum detectable limit. Such an investigation was undertaken and proved to have a much wider scope than anticipated. The results are presented in Chapter Five.

(e) The Hydrocarbon Quenching Problem

One of the problems associated with the Brody and Chaney FPD and others of similar design has been the depression of sulfur response by co-eluting hydrocarbons. Dual flame methods (83,84) as previously discussed, reduce this effect considerably. One can also monitor the GC effluent simultaneously with a flame ionization detector either as a built-in part of the FPD or used in parallel with it in an effluent splitter arrangement (107). This would warn the analyst of any large amount of interfering hydrocarbon, but would not solve the problem. Sugiyama *et al.* (109) stated that the effect can be explained by deactivation of the excited S_2 species by its combination with an organic compound and/or its degradation products. There are other possible explanations such as the absorption of some sulfur emission by hydrocarbon degradation products, the scavenging of sulfur atoms or other species in the flame that take part in the reaction scheme (such as hydrogen atoms), or a resultant change in flame temperature.

1.5.3 Characteristics of Phosphorous Emission

(a) Spectrum

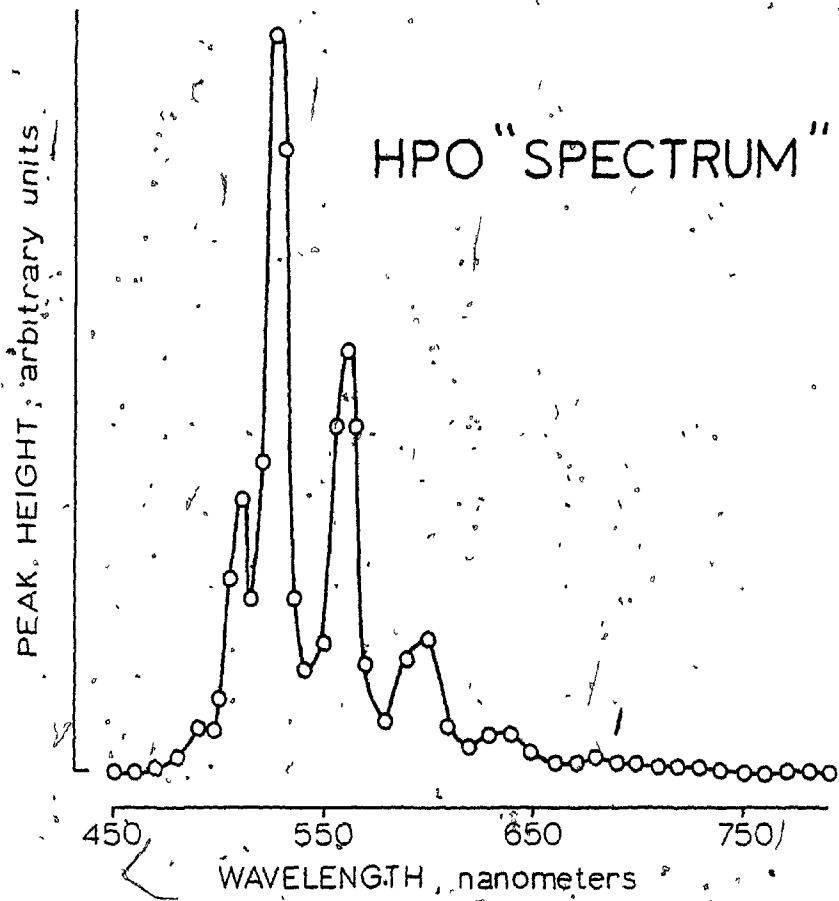
Phosphorous compounds produce a characteristic green luminescence consisting of three main bands on a broad continuum located for the most part between 500 and 600 nm (See Figure 2). Most of the emission is due to the three strong bands of HPO as described by Gilbert (110). A 526 nm interference filter, isolating the strongest of these

23

Figure 2

Phosphorous "Spectrum" - 450 nm to 800 nm

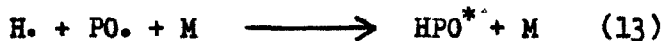
8 nm bandpass



bands, is normally employed for selectivity purposes.

(b) Mechanism of Emission

The mechanism of phosphorous response is not known as well as that of sulfur response in the FPD. Linear calibration curves are obtained, in agreement with the assumption of the one-phosphorous-species HPO as the main emitter. Again, because the emission is chemiluminescent and observed in cool flame regions, any proposed mechanism must account for the energy of emission by reaction only. Syty and Dean (90) favour the reaction of



whereas Gilbert (110) argues in favour of



He states that this reaction has just the right energy to produce excited HPO , that H_2 is a major component, and that the hydrogen flame gases are abnormally high in OH . No doubt other possible reactions exist, but the true reaction scheme may be difficult to establish.

(c) General Characteristics

The flame photometric detection of phosphorous compounds usually requires flow conditions different from those used for sulfur. Because the FPD is more sensitive to phosphorous than to sulfur, the flow conditions for dual channel operation are chosen close to the optimum for sulfur. Two detectors which have the same optimum flow rate for sulfur and phosphorous are the dual-flame

detector of Patterson (84) and the FPD designed by Joanson and Loog (86). Coincidence of optimum flow rates are particularly advantageous for single-channel detectors where one can change a P to an S-channel by changing filters only. The detector shows linear response to phosphorous-containing compounds over four orders of magnitude and its selectivity versus hydrocarbons is in excess of 10^4 .

1.5.4 Applications

(a) Pesticide Residue Analysis

The use of the flame photometric detector in various applications has mushroomed because of its good sensitivity and selectivity. Since Brody and Chaney first applied their detector to the analysis of pesticides containing sulfur and/or phosphorous (76, 111-127), the FPD has steadily grown in popularity. Dual-channel operation has proved invaluable for qualitative purposes as well. One can calculate the P/S ratio for thiophosphates by dividing the phosphorous response by the square root of the sulfur response (128). This can help to indicate the actual P/S ratio in the molecule and, when used in conjunction with retention times, can aid in peak identification.

(b) Sulfur in Complex Hydrocarbon Mixtures

The FPD has been used as a qualitative and quantitative detector in the analysis of oils and oil products such as gasoline (83, 129-132), as well as hydrocarbon gases such as natural gas and cooking gas (133, 134). Its sensitive and selective response to sulfur enables it to.

be used in "fingerprinting" of oils and oil spills (130). The distribution of sulfur compounds can be found using very little sample. Total sulfur can be determined by combustion of the sulfur compounds to SO_2 (83,129) and determination by FPD. Dual-flame photometric detectors are very valuable for obtaining quantitative data in applications where the sulfur compounds elute on a complex background of hydrocarbons.

(c) Air Pollution

The FPD has found a place in air pollution monitoring (97,135-145). Sulfur-containing gases such as H_2S , COS , CS_2 , SO_2 and various mercaptans are common air pollutants, generated by combustion and certain chemical processes e.g. those used in Kraft mills. Aside from high local concentrations, for instance around a coal-fired power plant or a pulp and paper manufacturing facility, they are usually present as trace quantities in air and hence require a detector with high sensitivity. Most of the problems related to the analysis of these gases by flame photometric detection, are due to their poor chromatographic properties and high chemisorptive activity. Because of this reactivity, the chromatographic system must be made as inert as possible and the column must be properly deactivated.

A second problem is making accurate calibration standards of these gases. The most accepted method makes use of permeation tubes. The desired level of the calibration gas is controlled by the nitrogen flow rate over the perm-

selective polymer. Preconcentration of analyte gases on solid adsorbents like gold-coated glass beads is sometimes used to gain increased sensitivity (135,136). The determination of phosphine (e.g. from the fumigation of grain) can also be performed by GC-flame photometric detection (146).

(d) Miscellaneous Applications

The FPD has been used to determine elemental phosphorous (147) and elemental sulfur (148) in conjunction with gas chromatography. The volatility of these elements makes them amenable to GC. Darlage *et al.* (149) used an FPD for the analysis of coal sulfur where the sulfur was converted to SO_2 before analysis. The analysis of the pesticide manganese ethylenebis (dithiocarbamate) has been carried out by a conventional CS_2 evolution method (150)

Sulfur-containing flavour components of foods such as coffee and tea have been analysed by head-space sampling prior to gas chromatography and flame photometric detection (151,152). Robison and Hilton (153) indirectly determined zinc phosphide by converting it to phosphine, followed by GC-FPD analysis.

The FPD has potential medical applications as well. The combination of breath sampling techniques and flame photometric detection (154-156) can allow doctors to determine whether or not a patient has certain diseases. For example, the concentration of methyl mercaptan was reported to be significantly elevated in the breath of

patients with hepatic cirrhosis. The technique appears to hold great promise for the future.

1.5.5 Flame Photometric Detection of Elements Other Than P and S

(a) Air-Hydrogen Flames: Chemiluminescence

The cool air-hydrogen flame has been found to give chemiluminescent emission from compounds containing other heteroatoms. Crider (157) used a large air/H₂ flame and monitored chemiluminescent emission from organic halides at various detector operating conditions. This technique proved reasonably sensitive to compounds containing iodine and bromine but not fluorine or chlorine.

Dagnall and co-workers studied chemiluminescence produced by a large air-hydrogen diffusion flame. Besides phosphorus and sulfur compounds, they recorded emission spectra of compounds containing nitrogen, chlorine and carbon (158). At a later date, they separated the inorganic fluorides of arsenic, germanium, molybdenum, phosphorous, sulfur, antimony, selenium, silicon and tungsten by gas chromatography and detected their emission in an air/H₂ diffusion flame (159). They identified most of the emitters as fluorides, oxides and some homonuclear diatomic species. Fluorides were obtained by reaction of samples with ClF₃.

(b) Oxyhydrogen Flames: Thermal Emission

(1) Organoboron compounds

Sowinski and Suffet (160) applied a Melpar FPD to the

determination of boron hydrides. Good response was obtained only with a hot flame of near stoichiometric proportions of hydrogen and oxygen. The detector emits the "fluctuation bands of boric acid" (161), which are attributed to BO_2 . The detection limit for decaborane was quoted as less than one nanogram. Sowinski and Suffet also used their boron detector for the analysis of boron hydrides in rocket propellants (162).

(2) Chromium Chelates

Ross and Shafik (163) found that the early model of the Melpar FPD could be made to respond to chromium, and monitored the emission using a 425.4 nm filter. They suggested application of the detector to physiological fluids such as urine. Burgett and Green (79) used an improved model of the Melpar detector and monitored the emission at 520 nm. Their hot $\text{O}_2/\text{air}/\text{H}_2$ flame gave a detection limit of about 15 picograms for chromium (probably as the trifluoroacetylacetonate) and four orders of magnitude of selectivity versus hydrocarbons. The emitting species in chromium analysis has not been unequivocally established - Burgett and Green attributed it to atomic Cr but gave no supporting data.

(c) Sensitized Flames

(1) The Beilstein Detector

The well-known Beilstein effect has been used to produce a copper-sensitized FPD (164-166). Hydrogen and the column effluent pass through a copper screen and burn in oxygen admitted above it. The detector responds expon-

entially to organochlorine, bromine and iodine compounds and linearly to all other compounds. The emission is mostly CuOH bands with some emission from the copper halides. The reason for exponential response has not been established.

(2) Indium-Sensitized Flames

Gilbert (167) used a modified Van der Smits burner to obtain indium chloride emission from GC effluents containing chlorine. The burner produces a separated flame: the first flame decomposes the chromatographic eluates, which then can react with an indium-coated copper tube placed above the burner tip. The second flame, burning above this tube, produces the desired emission. The detector also works well for bromine and iodine but not fluorine-containing compounds. Because of its sensitivity, selectivity, and ample linearity, a lot of work has been done with indium-sensitized flames (168-176). Moseman and Aue (169), doped a normal FID with indium and obtained good results for both ionization and photometric measurements. Versino and Rossi (170) used a dual-flame detector in which they monitored sulfur and phosphorous compounds (as S_2 and HPO) in the first flame and organochlorine compounds (as $InCl$) in the second one.

(3) Sodium-sensitized Flames

Novak and Malmstadt (177) modified a sodium thermionic detector to respond to halogen-containing compounds in the sub-nanogram range. In this detector, the 589 nm

sodium "D" line is enhanced by the presence of halogens in a linear manner. An electrically heated, Na_2SO_4 -coated platinum spiral is used as a sodium source.

Aue and Moseman (178) looked at the photometric output of a normal alkali-flame ionization detector. They found both positive and negative responses for compounds containing chlorine, bromine, iodine and phosphorous (depending on detector conditions), and concluded that it had potential for qualitative analysis.

1.6 Choice of Species to Investigate

1.6.1 General Discussion

For many years mankind has used (to some extent, had to use) the natural environment as a convenient disposal ground for unwanted chemicals. Furthermore, man has used chemical warfare against that part of nature which challenged his right to mold the environment to suit his needs, e.g. some types of insects, plants, etc. (The use of chemistry to fight competition is of course not limited to the environmental arena - thiophosphate pesticides, for instance, were first developed for use on humans.) Only recently has mankind been made aware of some of the after effects of its careless treatment of Mother Nature; it is necessary for instance only to think of the disastrous after-effect on wildlife, especially birds, of the indiscriminate and widespread use of the insecticide DDT.

A lot of attention has recently been focussed on the effects of various metals and their organic derivatives on

the environment. The toxicity of organic derivatives has been found to be often much higher than that of the metals themselves. Organic derivatives can sometimes pass through membranes in living systems with ease and, because of their organic nature, (lipophilicity), can accumulate in fatty tissues. Biosynthesis of organometallics from metals (e.g. methylmercury from mercury) is a well-established process. The study of the metabolic pathways of these metals and their derivatives in the environment is of great concern to scientists, medical authorities and political bodies alike.

Hence one comes to realize that it is important to determine not only what metals or heteroatoms are involved, but also in which form they are present in a sample, i.e. their speciation. Chromatography, as a separation technique, can provide answers to the question of speciation, and selective detectors can give qualitative and quantitative information on the type and amount of species involved.

Our interest in the cool air-hydrogen flame as a sensitive and selective detector led us to investigate its potential for the analysis of a few selected compounds containing heteroatoms. Our primary interest was the determination of organotin and organo-selenium compounds. Both of these are important in today's society because of their many uses and their potentially harmful effects. To a lesser extent, organic compounds of germanium and tellurium were to be investigated as a corollary to the studies on tin and selenium.

The response of a number of heteroorganic compounds in a Melpar flame photometric detector, operating without a filter, was shortly investigated by Aue and Hastings (93). They used a pure survey approach, and no attempt was made to optimize the detector for individual elements or to establish the emitting species. Organotin compounds were shown to elicit the largest responses in this detector, the MDA (minimum detectable amount) of tetraethyltin being 30 picograms. Selenium showed a square-law response, but an MDA of only 10 ng for piasselenole. Based on these facts and the author's conviction of the potential usefulness of the FPD for organotin and organoselenium analysis, an investigation of the matter was undertaken in a thorough and systematic fashion. It was the good fortune of the author(s) to obtain a Shimadzu dual-channel FPD on (permanent) loan and all experiments were carried out with the instrument.

1.6.2 Tin Compounds

(a) Uses and Environmental Concerns

The annual world production of tin metal is of the order of 200,000 tons (179). It finds uses in tinfoil, solders, bearing metals, copper-tin alloys and in the production of inorganic and organic tin compounds. Organotin compounds have been produced in large amounts - estimate for 1975: 25,000 tons (180) - for a wide variety of uses.

Organotins are used in plastics and polymers, particularly to stabilize vinyl resins and to prevent the degra-

dation of oxygen-containing polymers and polyamides due to heat and/or U.V. light. The compounds used are of the type R_2SnX_2 , e.g. dioctyltin dilaurate. Tin compounds are also used as antioxidants and anticracking agents in rubber products and paints, as activators and catalysts for polymerization of olefins, and scavengers of HCl for corrosion resistance in transformer, capacitor and cable parts.

Compounds of the type R_3SnX possess marked biocidal properties. Tributyltin compounds such as tributyltin oxide (TBO) are particularly useful as timber preservatives and as active agents in anti-fouling paints. Triaryltin compounds are generally less toxic than trialkyl types, although they do possess strong fungicidal properties, making them suitable for agricultural use. Triphenyltin compounds are used to combat fungal attack on crops such as potatoes, sugar beets, coffee and bananas. Tricyclohexyltin hydroxide (Plictran) is used as a miticide on fruit trees and glass-house crops.

The toxicity of tin is almost entirely due to its organic compounds (179,181) and most particularly to its alkyl derivatives. Compared to other organometallics, e.g. some of the mercurials and arsenicals, they are replacing, tin compounds are relatively innocuous. The fact that the metal will eventually end up in a harmless form (SnO_2) - in contrast to residues containing mercury or arsenic - has done much to promote the use of organotins.

Accumulated knowledge of the toxicity of some organotin compounds and the uncertainty about the fate of these compounds in the environment, has led to a more conscientious attitude in their use. Better analytical methods for organotin compounds have been the concern of WHO and IUPAC committees for some time. An \$800,000. Batelle/EPA study included organotins in a list of 10 toxic substances, whose effect on human physiology and the environment were to be scrutinized (182). Organotins are on a "black list" (as opposed to a "grey list") of substances to be eliminated from the Mediterranean (183).

Direct incidents of poisoning by organotin compounds are few. An exception was the "Stalino" affair of 1954 when about 100 people died in France. Occasional poisonings still occur from careless use of, for example, marine paints containing TBTO. The lower alkyl derivatives, especially triethyltin, have been found to have a specific effect on the central nervous system, producing cerebral edema. A good deal of research into the toxicity of organotins has been carried out on rats and dogs (184). In general, they have been found to produce lesions on different parts of the body, atrophy of testicular tissue, and interference in some of the important biochemical pathways. Another important consideration is the possible biosynthesis of methylated tin in the environment (185). Model reactions with various types of bacteria have shown tin to be methylated. By fixing methyl groups from compounds like

methyl cobalamin (vitamin B₁₂) on metals, bacteria render them less polar and thus more soluble in the cell's organic phase. Furthermore, concern has been expressed about the leaking of tin-containing polymer stabilizers into food or medical infusions (186). On the surface it appears that there is no need to worry about organotins in the environment other than taking a few precautions with the use of the highly toxic ones. However, new evidence has shown that tin may be accumulating in the organic food chain and become a possible health hazard (185).

(b) Analytical Methodology

Inorganic tin can be determined by the common analytical methods: colorimetry, compleximetric titrations, spectrophotometry, gravimetric methods (SnO₂), polarography, fluorimetry, X-ray fluorescence and atomic spectroscopy. Organic tin compounds can be determined as total tin by the methods listed above and this area has been well reviewed (187,188).

A number of colorimetric and fluorimetric methods are popular because of their good sensitivity. Dithiol formation leads to a sensitivity of 0.01 ppm tin (IV). The reaction of tin (IV) with pyrocatechol violet, sensitized by cetyltrimethyl ammonium bromide, is faster and more selective than the dithiol methods. A number of fluorimetric reagents are available for tin, the most sensitive being 3,4,7-trihydroxyflavone (189). The most sensitive of the

atomic spectroscopy methods is atomic fluorescence in both flame and non-flame modes (190). An interesting method reported by Dagnall et al. (191) used the "SnH" band emission at 609.5 nm emitted in an air-hydrogen diffusion flame.

Organotins have been separated by paper and thin-layer chromatography and determined by colorimetry or by extraction of the separated compounds followed by the usual analytical techniques (187). Electron-spin resonance has been used to determine di- and triorganotin compounds by reaction with o-aminophenols to form stable paramagnetic complexes (192).

1.6.3 Selenium Compounds

(a) Uses and Environmental Concerns

The free world refinery production of selenium from 1964 through 1973 averaged 2.3 million pounds annually. Its industrial uses are in the electronics industry (amorphous selenium forms the basis of vidicon tubes), metallurgy (as a degassifier in stainless steels), the glass and ceramic industry (e.g. when added to glass melts, selenium produces a ruby-red glass used in traffic and signal lights), in pigments and the pharmaceutical industry (e.g. dandruff control on human scalp) (193). Selenium has been used in agriculture to ensure the health of livestock by preventing certain diseases resulting from selenium deficiency. This can involve the feeding of forage crops and feed that naturally contain protective (but non-toxic)

levels of this element. Otherwise selenium is introduced to livestock in several ways: 1) by direct injection; 2) as a feed additive; 3) as an additive to soil, and 4) as a foliar spray to forage crops. The latter two methods are aimed at producing plants with sufficiently high levels of selenium to be fed to animals (193).

The introduction of selenium into the environment is due to both man and nature and but few quantitative data are available on its cycles or sinks (193). Selenium perhaps best exemplifies a not uncommon ambivalence: it is toxic and essential, it both causes and prevents certain diseases. The literature on selenium and its various effects is extensive (for some reviews, see references 193 to 196). The nutritional and toxic levels for selenium are low and not too far apart, (0.1-0.3 and 2-10 mg/kg, respectively). This means that analysis of selenium must be both precise and accurate.

Selenium can be metabolized by the body and interferes in sulfur metabolism. In certain plants it is heavily accumulated but in others it can be injurious to seed germination and growth. Biosynthetic reactions involving selenium have been shown to produce seleno-amino acids (produced by microorganisms) and methylated selenium, i.e. dimethylselenium (produced by molds). An interesting effect is the lessening of the toxicity of mercury and cadmium in the presence of selenium.

(b) Analytical Methodology

Inorganic selenium can be determined by the usual analytical techniques. Analysis of selenium compounds has been almost exclusively restricted to that of total selenium (see reference 197 for a review and references 4, 5, 7, 8, 15, 53, and 198-203 for some newer papers, several involving hydride formation) as opposed to an analysis for various selenium species (9).

Selenium can be determined spectrophotometrically, or by EC detection after reaction with o-phenylenediamine or some of its analogues (198, 199, 202-204). Atomic absorption using low temperature flames and electrodeless discharge lamps is combined with hydride generation to gain sensitivity. Catalytic techniques forming highly absorptive azo-dyes are more sensitive than the usual spectrophotometric techniques (200). Proton-induced X-ray emission has been used in the determination of Se(IV) in blood serum (201).

1.6.4 Germanium Compounds

(a) Uses and Environmental Concerns

Germanium has a variety of uses (205), by far the most important of which is in the electronics industry where it is used as a transistor element in thousands of applications. Germanium and germanium oxide are transparent to the infrared and are used in infrared spectrometers and other optical equipment including highly sensi-

tive infrared detectors. The high index of refraction and dispersion of germanium oxide has made it useful as a component of glasses used in wide angle lenses and microscope objectives.

At present, germanium is not thought to be of great environmental concern. Some organogermanium compounds have low mammalian toxicity but display marked activity against certain bacteria. The toxicities of organogermanium compounds are generally similar to those of tin (206), hence the cheaper tin compounds dominate the market. Greater use of germanium compounds in the future would mean that a closer look at their effect on the environment would be needed.

(b) Analytical Methodology

Analytical methods for determining germanium are few. Atomic emission spectroscopy, X-ray fluorescence and gravimetric determination of germanium oxide have been used. Atomic absorption can also be used but it lacks sensitivity. Germanium hydride has been determined in the picogram range by mass spectroscopy (207). Sutton et al. (208) found a detection limit of 0.1 ppb GeH_4 using "Metastable Transfer Emission Spectrometry" (MTES)

1.6.5 Tellurium Compounds

(a) Uses and Environmental Concerns

Tellurium is used in industry to improve the machinability of copper and stainless steel. It also finds use in electronics as a p-type semiconductor. Bismuth tellur-

ide is used in thermoelectric devices (209).

Tellurium and its compounds are toxic and should be handled with care. Animals and humans exposed to tellurium develop "tellurium breath" due to exhalation of dimethyltellurium. Biosynthesis of the methyl derivatives of tellurium has been documented (181). Organotellurium compounds are less stable towards oxygen than their selenium or sulfur analogues, and degrade easily to tellurium metal. Because of its inherent toxicity, though, tellurium may become an environmental problem following an increase in its usage.

(b) Analytical Methodology

The general analytical chemistry of tellurium has been reviewed by Masson (210). There are several sensitive spectrophotometric methods based on the reaction of tellurium with thiourea, rhodamine dyes and others. Tellurium has also been determined by neutron activation, atomic absorption, emission spectrometry and gravimetry, the latter after reduction to the element.

1.7 Gas Chromatography of Compounds of Tin, Selenium, Germanium and Tellurium.

1.7.1 Tin

A number of factors must be taken into account when discussing the gas chromatography of organotin compounds:

- 1) the stability of the compound with respect to temperature, oxygen level in the carrier gas, surface activity of the chromatographic support, etc., and
- 2) the sensi-

tivity of the detector used. Many of the environmentally important organotin compounds do not chromatograph well. A detector such as the FID, which is of moderate sensitivity, may indicate good chromatography without decomposition at relatively high amounts of compound injected, while the same compounds may chromatograph poorly if at all at true trace levels. It is evident that derivatization is necessary to convert these compounds into more volatile and more stable analytes.

A detailed presentation concerning the chromatography of organotin compounds is given by Crompton (187) and Guiochon and Pommier (211). Basically, tetraorganostannanes chromatograph well, although some of the early work was hampered by an on-column decomposition. Improved column performance due to better technical know-how has rectified the situation. The retention indices on non-polar phases such as Apiezon L show linear variation with boiling point. In contrast, on polar phases such as Carbowax 1500, the unsaturated compounds differ clearly from the saturated ones: at equal boiling points their retention indices are much higher.

Organotin hydrides have been found to chromatograph well at high concentrations on Apiezon L, silicone SE-301 and dinonyl phthalate. At Dalhousie, problems associated with the chromatography of these compounds have been found only at trace levels. Organotin hydrides are reactive and have been extensively used to synthesize other organotin com-

pounds (212,213), or to reduce a variety of oxygenated compounds; hence the difficulty of chromatographing them.

A lot of work has gone into the chromatography of organotin chlorides and bromides (214-216). Decomposition problems occur because the tin-halogen bonds are weak. Disproportionation is a major problem. Reasonable chromatography at the nanogram level can be obtained by first saturating the GC system with the compound or by using a silylating reagent, e.g. dimethylchlorosilane, to cover the active sites of the support or the column wall (216). Good chromatography at trace (sub-nanogram) levels has not been achieved. Organotin oxides, hydroxides and acids do not pass through GC columns and must be derivatized.

In order to test the chromatography of tin compounds at trace levels, sensitive detectors are needed. Mass spectrometry, sometimes with selective ion monitoring, has found considerable use (217). A potentially helpful detector for tin is the hydrogen-atmosphere flame ionization detector (218), which has a minimum detectable limit of 20 picograms of tetraethyltin. The author was encouraged to undertake the investigation of the Shimadzu FPD as a sensitive and selective detector for tin because of the promise shown by the work of Aue and Hastings with a Melpar FPD (93).

There are several possible derivatization procedures that can be used. The most obvious would be to replace the problematic functional group by an alkyl group in a

Grignard reaction. Figge et al. (219) used ethyl magnesium bromide to convert n-octyltintri-, di-n-octyltindi- and tri-n-octyltinmono- 2-ethylhexyl thioglycolate to their respective tetraalkyltins. Organotin chlorides have been found to react with sodium borohydride in ethylene (or diethylene) glycol dimethylether to produce the corresponding hydrides quantitatively for most compounds (220). Organotin oxides, alkoxides and acyloxides have been reduced to the corresponding organotin hydrides by reaction with organosilicon hydrides (221). Itoi (222) reported a reaction of organotin alkoxides with a polymethylhydrosiloxane giving a high yield of organotin hydrides. Lithium aluminum hydride has been used to reduce bis(tributyltin) oxide to tributyltin hydride in 88% yield (223). Gauer et al. (216) converted tricyclohexyltin hydroxide and its degradation products with 48% hydrobromic acid to the corresponding bromides. After GC separation these were determined with a Coulson electrolytic conductivity detector.

Inorganic or total tin can be determined by hydride formation. The chromatographic separation and detection of metal hydrides (e.g. by AAS, mass spectrometry, etc.) has attracted a great deal of attention (53, 207, 224 and 225). In a similar fashion, volatile methylated species have been separated by gas chromatography and detected by atomic absorption (15).

1.7.2 Selenium

Evans and Johnson (226) have studied the gas chromatography of a range of organoselenium compounds including dialkylselenides and ethyl selenocyanate. Separation of these compounds was performed easily on Carbowax 20M, silicone oil 550 and polymethylphenylether. Chromatography of piasselenole derivatives has been adequate on SE-30 and OV-225.

Derivatization of inorganic selenium for chromatography can be done by formation of the hydride (8,53), alkylation (15), or reaction with compounds such as 1,2-diaminobenzene and its derivatives (198,202,203). Electron capture is used with those piasselenole derivatives that have halogens or nitro groups attached to the molecule for this purpose.

1.7.3 Germanium

The chromatography of germanium hydrides and organogermanes is usually studied along with that of analogous compounds of silicon as well as with compounds of mixed composition. Guiochon and Pommier (227) have put together a summary of these studies. The liquid phases used most frequently for chromatographic analysis are the silicone oils. The silane and germane retentions follow the same laws as those of the alkanes. The chromatography of organogermanes (227) exhibits behaviour entirely analogous to that of the mixed hydrides of silicon and germanium, with the same relations between retention and structure.

The chromatography of the chloro derivatives is very difficult as expected from their reactivity. A study of the separation of alkylchlorogermanes and the analogous silanes has been done by a team of Russian investigators. (228).

1.7.4 Tellurium

At present, there has been no study of the chromatography of tellurium compounds cited in the chemical literature because of the instability of such compounds. The author's experience has been limited to dibutyltelluride which is air-sensitive. Its chromatography on the 5% PEGA on Chromosorb W column, 100/120 mesh, indicated little or no decomposition on the column. It is expected that the chromatography of organotellurium compounds would be similar to (if somewhat more difficult than) the chromatography of their selenium and sulfur analogues.

2. Experimental

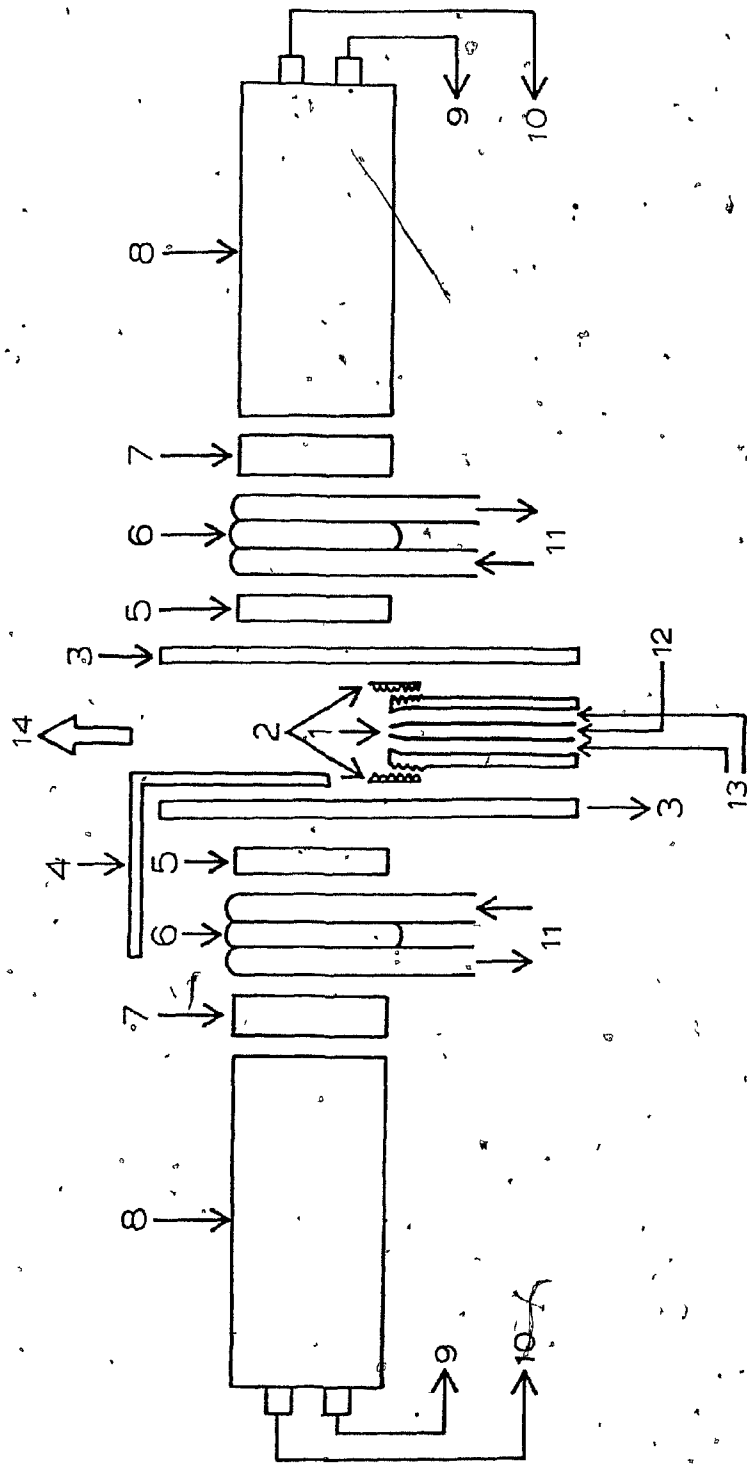
2.1 Shimadzu FPD: Construction and Operation

This detector (which is not available in North America on a commercial basis) has been used, with appropriate modifications, for all of the author's work. Figure 3 shows a detailed diagram of the detector. The burner consists of two concentric stainless steel tubes. Air or oxygen (sometimes both) flow through the inner tube while hydrogen, mixed with the column effluent, flows through the outer tube. The flame is normally hydrogen-rich as opposed to that of a flame ionization detector, which is air-rich. A stainless steel flame shield screws on top of the burner head, permitting simple adjustment of its shield height. Its purpose is to protect the photomultiplier tubes from the light of the luminous primary zone of the flame. A cylindrical quartz or pyrex tube surrounds the burner and serves to define the emission region of the detector. Modifications of the geometry of this enclosure are discussed later in Chapter 2. On either side of the cylindrical enclosure is a quartz window. Between the quartz window and the photomultiplier tube, filters and masks can be placed for optical and geometric selectivity if desired. A variety of interference and cut-off filters were used. The photomultiplier tubes were of the low-noise, high-gain type necessary to make optimum use of the low light levels of the detector. The most commonly used PM tube was the Hamamatsu R-268, S-11 response end-on

Figure 3

Schematic of the Shimadzu FPD

1. = Burner nozzle
2. = Adjustable flame shield
3. = Quartz or pyrex flame enclosure
4. = FID electrode
5. = Quartz windows
6. = Copper cooling coils
7. = Filters (interference, cut-off, etc.)
8. = Photomultiplier tubes
9. = To power supply
10. = To electrometer
11. = To cold water
12. = Air and/or oxygen
13. = Hydrogen and column effluent
14. = To exhaust



type. Its spectral response reaches from about 300 nm to 650 nm with a maximum at 420 nm. A Hamamatsu R-1104 high anode-sensitivity tube with a spectral response from 185 nm to 850 nm (maximum at 420 nm) was also used to give good spectral response for emissions above 600 nm (e.g. SnH and GeH). The electronic signal from each PM tube was amplified by an electrometer and displayed on a dual-pen recorder (Linear Instruments).

Water-cooled copper coils allow the detector to be operated in excess of 250°C while maintaining the optics at a safe temperature (i.e. below 50°C). An electrode for ion collection is also attached and polarized with 67.5 volts. The ion current flows between this electrode and the burner nozzle which is on ground. This ionization detector is, of course, inferior to a normal FID because of improper flame conditions. It is useful only as a monitor of large amounts of organic effluents.

A safety switch is provided which automatically turns off the voltage to the PM tube if the specially-designed cover of the detector is removed. Voltage is supplied to the PM tube at two levels: a setting of 300 volts is used as a check voltage high enough to detect light leaks but low enough to prevent damage to the PM tubes. The operating voltage of 700 volts cannot be applied without first applying the check voltage.

Separate mass-flow controllers are used for hydrogen, oxygen and air to ensure a smooth, stable flow of gases to

the detector. The detector and associated transfer block are heated separately from the injection port to ensure the absence of condensation.

2.2 Reagents and Gases

All standard compounds used were of 95% or better purity. Most of the compounds tested were obtained from the "mini-stockroom" of Chem-Service, West Chester, Pa.; from the regular stock as well as the Alfred Bader Library of Rare Chemicals, Aldrich Chemical Company, Milwaukee, Wis.; from Pfaltz and Bauer Inc., Stamford, Conn.; ICN Pharmaceuticals Inc., Plainview, N.Y.; PCR Research Chemicals Inc., Gainesville, Fla.; Applied Science Laboratories Inc., State College, Penn.; Research Organic and Inorganic Corp., Belleville, N.J.; Strem Chemicals Inc., Newburyport, Ma., and Ventron Alpha Products, Danvers, Ma. All solvents were of ACS certified grade. Chromatographic materials such as Chromosorb W, silanized glass wool and various liquid phases were purchased from Chromatographic Specialties Ltd., Brockville, Ontario.

The carrier gas was high purity nitrogen (Linde specialty gas, minimum purity 99.997%, maximum moisture and oxygen content, 10 ppm each). Before entering the chromatograph this carrier gas was passed through a trap containing activated charcoal, molecular sieve Linde 5A and Silica gel (Guild Corporation, Bethel Park, Pa.) and a high-capacity purifier (Supelco carrier gas purifier, Supelco Inc., Bellefonte, Pa.) to remove oxygen and water.

The combustion gases for the FPD were prepurified hydrogen (Linde specialty grade) and, for most of the work, compressed laboratory air (air compressor, Pneumatic, Monroe, La.). The compressed air was passed through an oil filter (Watts Regulator Company, Lawrence, Ma.). For some of the work the air used was Linde extra dry air (maximum moisture 10 ppm). Supplementary oxygen was Linde extra dry grade (minimum purity 99.6%, maximum moisture 10 ppm). Methane used as a doping gas was ultra high purity grade (Linde specialty gas). The silane used for the tin detector study was from Matheson and of semiconductor purity. 0.5% silane in ultra-high purity nitrogen, used in the generation of organotin hydrides, was also supplied by Matheson.

2.3. Detector Design Modifications: Flame Enclosure Geometry and the Use of Masks

2.3.1 Modified Flame Enclosures for Tin Detection

A number of quartz (or pyrex) flame enclosures were made which had different shape in the region to be viewed by the photomultiplier tube. The purpose of doing this was to determine whether or not any of these tubes would give "geometric selectivity" for any of the known emitting species of the FPD against the others.

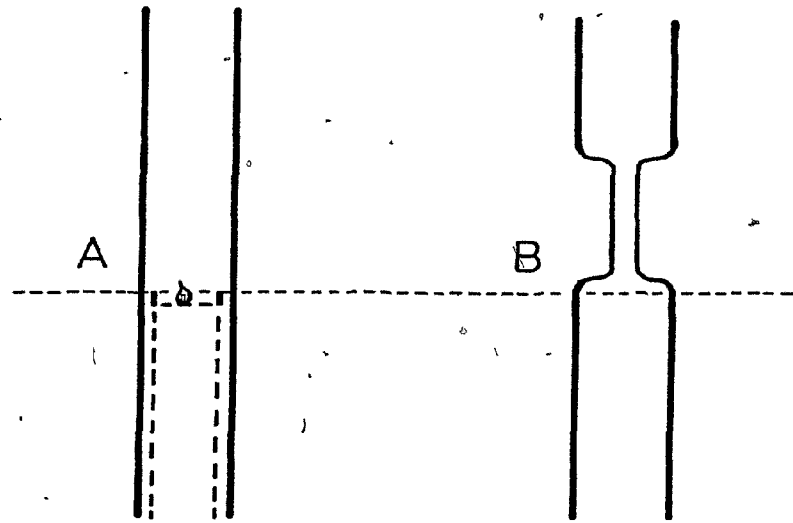
Figure 4 shows sketches of several modified flame enclosures which give enhanced tin response. Enclosure B was developed as a part of the preliminary study on organotin response. This tube was made by collapsing a

Figure 4

Modified Flame Enclosures for Tin Detection.

NORMAL

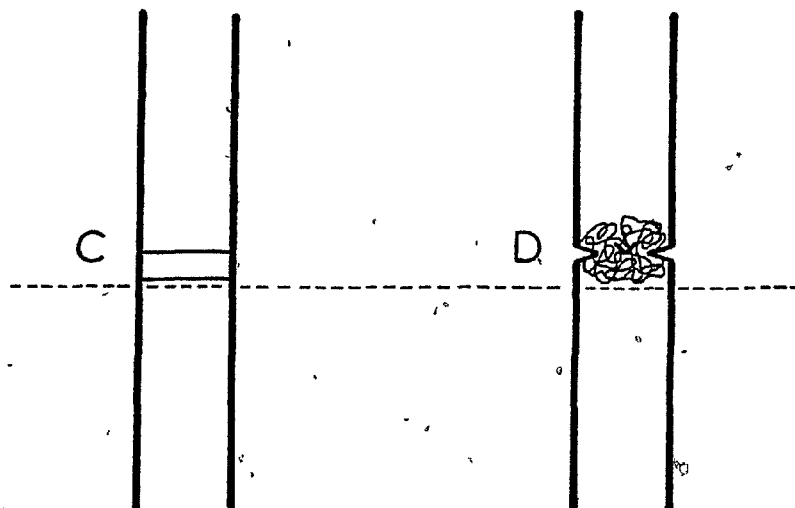
CONSTRICTED



0 1 2 cm

BISECTED

QUARTZ WOOL



normal cylindrical enclosure to a smaller diameter in the region of view of the PM tube. The effect of the diameter of the collapsed region on tin response was determined by making several tubes with constrictions of varying diameters. Enclosure C was developed to test the hypothesis that tin emission is a surface luminescence phenomenon. A normal flame enclosure was bisected with a much smaller diameter quartz tube (3.5 mm OD) so that the horizontal bisecting tube was positioned directly over the flame. Enclosure D was a pyrex cylindrical flame enclosure with three symmetrical indentations designed to hold a wad of quartz wool of low but even density just over the burner nozzle.

2.3.2 Masks for Bisected Flame Enclosures

A number of masks were made from aluminum foil, designed to fit the outside of the bisected flame enclosure. Sketches of these masks are shown in Figure 5. Their purpose was to obtain numerical data to support the surface luminescence theory of tin response. It was possible to view either the entire length of the bisecting tube ("side-on" view) or just one end of it ("end-on" view). Two pairs of masks were designed, one for each of these views of the bisecting tube. One mask was made to monitor the emission on or close to the quartz surface and nothing else; and the other, to monitor the emission in the gas phase excluding any emission on or near the bisecting tube. As much aluminum foil as possible was cut away from the mask

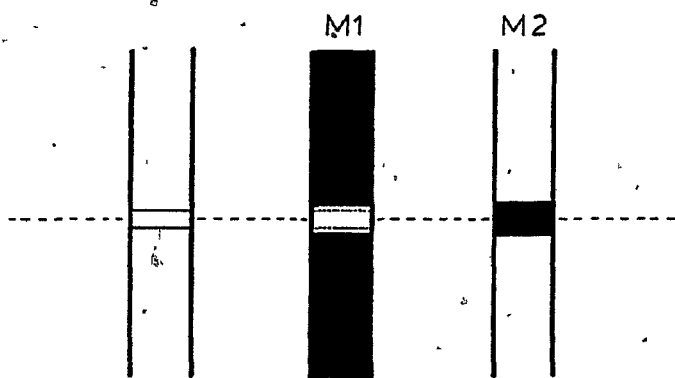
54

Figure 5

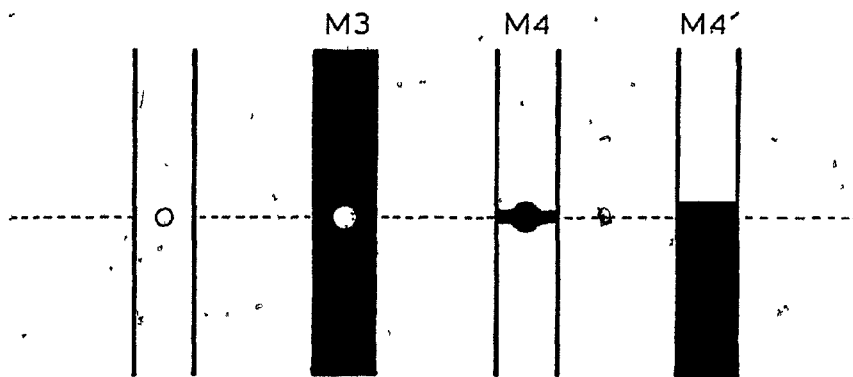
Masks for Bisected Flame Enclosure

MASKS FOR BIASECTED TUBE

"SIDE ON" VIEW



"END ON" VIEW



on the side opposite to one being viewed to reduce reflection problems.

Aluminum foil masks were not ideal because of their fragility and the reflection off their shiny surfaces. An improvement was made by painting the outside surface of a bisected flame enclosure with China black ink. Masks M3 and M4, used with the "end-on" view of the bisected flame enclosure, were combined on the same tube for dual-channel operation. This tube was designed to indicate whether response of the detector was due to gas-phase or surface-induced luminescence, by obtaining the ratio of the peaks recorded on each channel. The mask design, M4, was modified (shown in Figure 5 as mask M4') to ensure that little of the surface emission could be picked up on that channel.

2.3.3 Masks for Geometric Selectivity

Based on visual observation of the various emissions in the FPD, a number of masks were made to selectively view different areas of emission. Sketches of these masks are shown in Figure 6. Each was designed to friction-fit just behind the quartz windows. They were tested by comparing the responses of standard compounds of the elements of interest with and without the masks in place.

2.4 Optimization of Detector Parameters

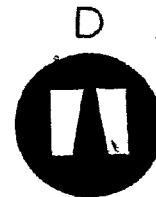
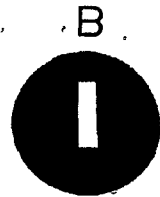
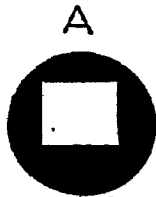
For many analytical problems, it is necessary, and in general it is desirable, to operate at optimum detector conditions. The most important parameter is the flow rate

56

Figure 6

Masks for Geometric Selectivity

MASKS FOR SELECTIVE VIEWING
OF EMISSION REGION



of the combustion gases, air and hydrogen. To optimize the flow rates, one makes a series of signal-to-noise ratio determinations by injecting a constant amount of the species to be determined in the working range (preferably close to the detection limit) at different flow rates. The procedure normally followed is to hold the air flow rate constant and vary the hydrogen flow rate. One curve is thus obtained for each chosen flow rate of air.

The optimization of flow rates can be done in filterless mode and/or using an interference filter. The optimum flow rates may be different for these two cases if the overall emission of a particular element is due to more than one emitting species.

A filter is usually chosen for selectivity purposes based on the emission spectrum of the element (or its compounds) in the detector. If the spectrum contains sharp bands, a filter with a narrow wavelength bandpass is chosen. If not, a broad-band filter or perhaps a cut-off filter may be preferred. The signal-to-noise ratio for an element may be much better in filterless mode if the emission is broad and featureless. The detector is always kept at a temperature at least 50°C higher than the highest column temperature used, to prevent condensation of column bleed or eluted compounds.

2.5 A Simple Method for Determination of a "Spectrum" Using a Flame Photometric Detector

The experimental set-up used for producing a spectrum

for any strongly emitting compound in the Shimadzu FPD was unusual. It was based on the idea that the measurements should be conducted on a typical, fully operational and optimized FPD, rather than on a simulated system involving a (spectroscopically more convenient) larger flame. The experimental set-up was as follows: A $\frac{1}{4}$ meter Jarrel-Ash monochromator was connected to the Shimadzu FPD by a stainless-steel, light-proof adaptor, replacing one of the PM tubes. This replaced tube was then connected to the exit of the monochromator by another stainless steel, light-proof adaptor. The PM tube was connected to an electrometer and recorder in the usual way. The other PM tube was left directly attached in its normal place on the detector. Since the monochromator was not equipped with a wavelength drive, and continuous introduction of the analyte was not considered typical of regular FPD operation, spectra were not recorded as a continuous changing signal. Instead, a constant amount of compound containing the element of interest was injected repetitively into the gas chromatograph, with the monochromator set at various wavelengths. By changing the entrance and exit slits of the monochromator, a "rough" spectrum can be obtained by making injections every ten nanometers (using an 8 nm bandpass) or a "high resolution" spectrum by making injections every two nanometers (using a 2 nm bandpass). It should be noted that this method also avoids the problem of continuously and constantly introducing rather toxic and volatile compounds

into the detector in high amounts. Using this method, a relatively non-volatile compound can be chromatographed to produce a spectrum. The other channel of the FPD records a normal peak for each injection, which is used to standardize all responses from the monochromator channel.

2.6 Doping Arrangements

2.6.1 Carbon Disulfide (Sulfur) Doping

There were two sources of sulfur doping that used the general scheme shown in Figure 7. A few microliters of CS_2 were injected into a one-liter stainless steel tank flushed out with nitrogen. The tank was then pressurized to 140 psi with high purity nitrogen. An in-line pressure regulator (Matheson) was used to reduce the pressure to about one psi. The doping gas was then added to the hydrogen or the air lines after the flow controller. The one-liter stainless steel cylinder was later replaced by a T-tank (1.54 ft.³) to which about 2 ml of CS_2 had been added and which had been pressurized to 500 psi with nitrogen from another tank. This tank was manually rolled before use and an IR lamp was used to heat the centre of the tank, as it lay on the floor of the lab, to promote mixing. This cylinder of CS_2 in nitrogen was used for most of the doping studies.

2.6.2 Hydrogen Chloride and Hydrogen Bromide Doping

These two strong acids in gaseous form were added to the nitrogen stream to condition the GC system for the chromatography of organotin halides and the on-column and/or

Figure 7**Flow Schematic for CS₂ Doping**

l. = To detector

PR. = Pressure regulator

S. = Shut-off valve

F. = Fine valve

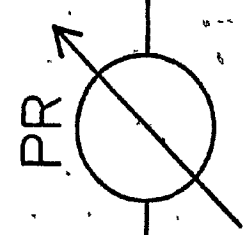
Air or H₂



F



S



CS₂
(in N₂)



injection port derivatization of organotin oxides, hydroxides and acids. As seen in Figure 8 the HCl or HBr was added through a very fine restriction - made by pounding capillary stainless steel tubing with a hammer - to the nitrogen stream just before the injection port.

2.6.3 Methane Doping

Methane was added to the carrier gas (as seen in Figure 9) to determine the effect of hydrocarbon quenching on various FPD emissions. Ultra-high purity (Linde) methane was added through a fine valve (Nupro) to the carrier gas before the flow controller by way of a "flow diverter" (Alltech Associates). By a flip of a switch, the methane could be diverted to a soap bubble flow meter for measurement and a back flip would redirect the methane into the nitrogen stream. A pressure of 80 psi on the methane tank was used to overcome the carrier gas pressure of 40 psi and allow calculation of the true methane addition rates.

2.6.4 Silane Doping

Silane was used for two purposes. The first was to study the effect of silicon on the flame photometric detection of organotin compounds. Semiconductor-purity silane was used for this purpose and the set-up is shown in Figure 10.

A fine restriction was made by pounding 1/8 inch copper tubing with a hammer and testing the flow using high-purity nitrogen. Silane in the line before the restriction could be bled off to the atmosphere (fume hood)

Figure 8**Flow Schematic for HCl or HBr Doping**

I. = To injection port and column

S. = Shut-off valve

R. = Restriction

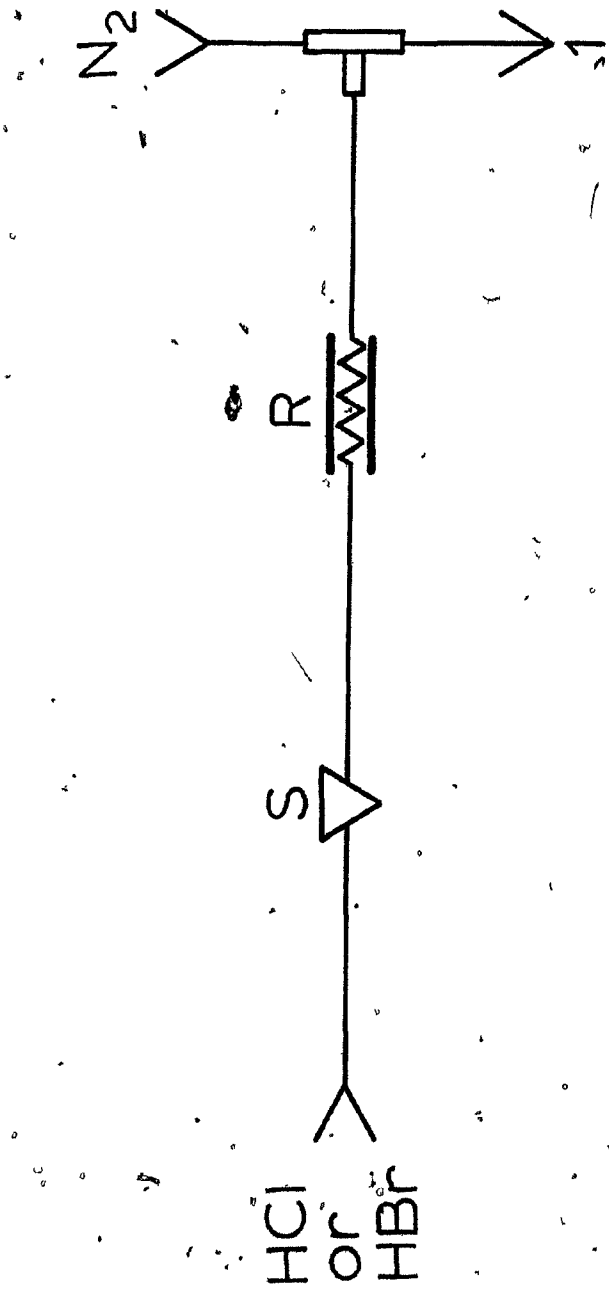


Figure 9

Flow Schematic for CH_4 Doping

- 1. = To flow rate measuring device
- 2. = To injection port and column
- S. = Shut-off valve
- F. = Fine valve
- FD. = Flow diverter

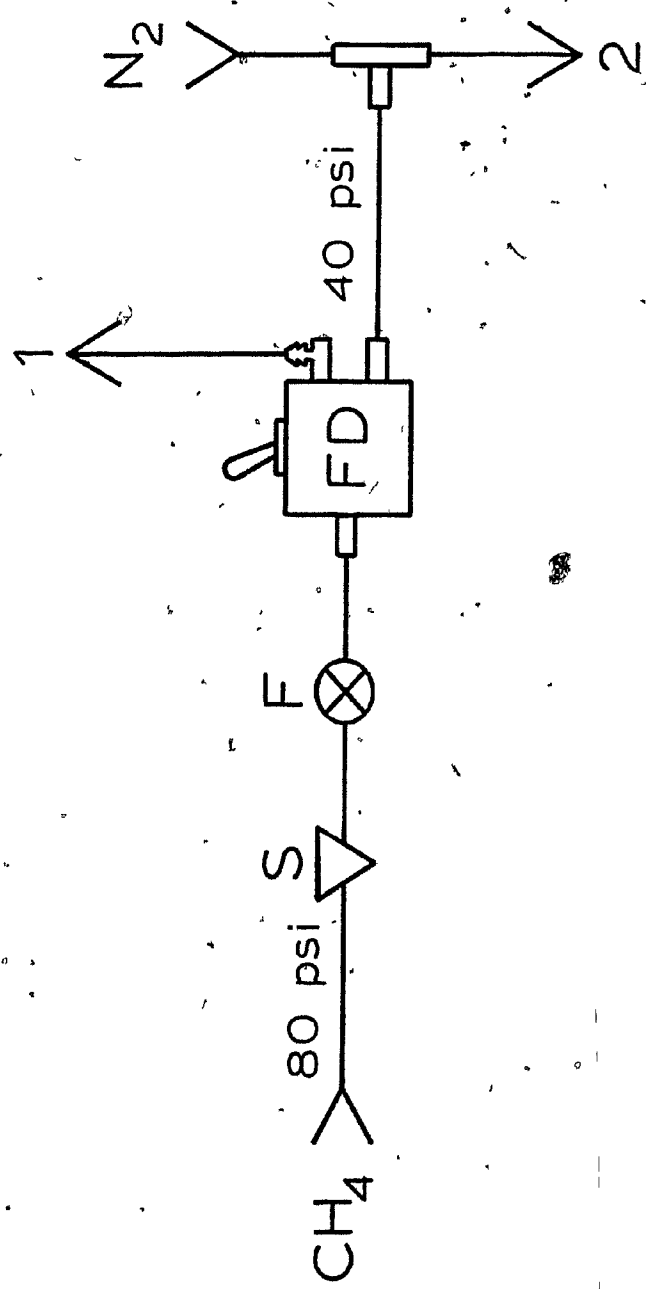
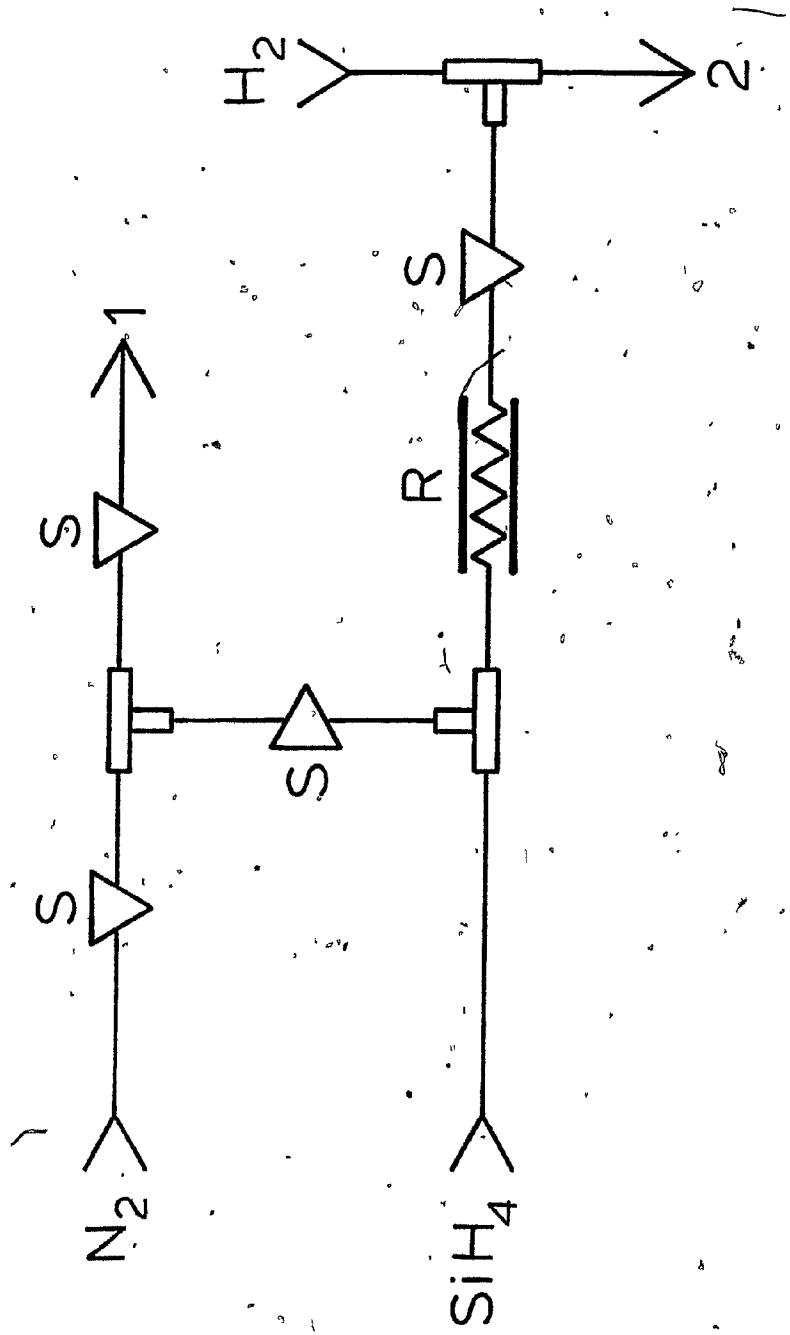


Figure 10

Flow Schematic for SiH_4 Doping

- 1. = To exhaust
- 2. = To detector
- S. = Shut-off valve
- R. = Restriction



through a Nupro shut-off valve. The line could also be flushed overnight with high-purity nitrogen.

2.7 Hydride Generation

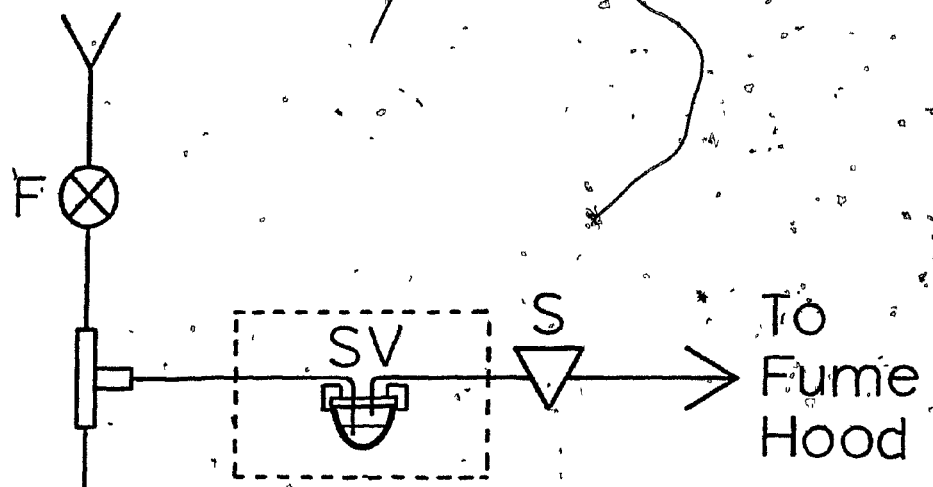
The second use of silane was for the derivatization of organotin halides, oxides, hydroxides and acids to their corresponding hydrides. This was accomplished by bubbling 0.5% silane in nitrogen through a methanolic or ethanolic solution containing the organotin compounds for 20-30 minutes using the set-up shown in Figure 11. Nitrogen was used to purge the solution of silane after the reaction. After nitrogen flushing, extraction of the hydrides into iso-octane or hexane was performed, aided by the addition of a little water to the two-phase system. A sample from the organic layer was injected directly into the GC. The reactions were carried out in silli-vials (Ohio Valley Specialty Chemical Inc.) which had a volume of about 0.5 ml and a screw cap with teflon-lined septum for easy addition or withdrawal of sample. The inlet and outlet tubing to the silli-vial was 1/16 inch stainless steel, firmly attached to the screw cap with epoxy resin. Teflon tubing in the line added mechanical flexibility. The gases leaving the silli-vial were routed to the fume-hood.

Figure 11

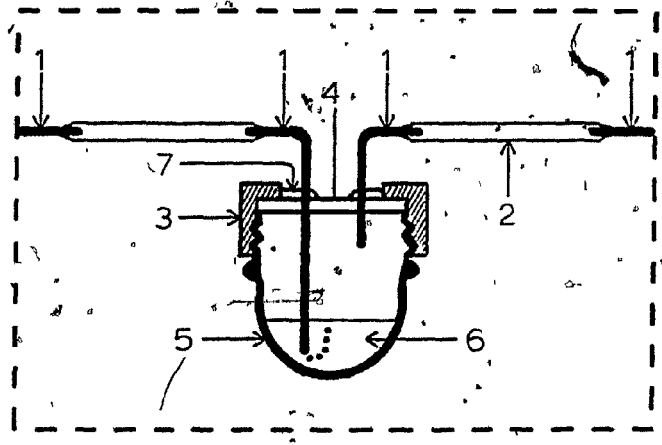
Flow Schematic for Organotin Reduction with Silane

1. = One-sixteenth inch stainless steel tubing
2. = Shrinkable teflon tubing
3. = Plastic cap
4. = Teflon coated septum
5. = Pyrex reaction vessel
6. = Methanolic or ethanolic solution containing compound(s) to be derivatized
7. = Epoxy cement
- S. = Shut-off valve
- F. = Fine valve
- SV. = Silli-vial

SiH_4 (in N_2)



N_2



3. Organotins: Detection, Derivatization and Application to Environmental Samples

3.1 Development of a Photometric Tin Detector: A Brief History.

Since the flame photometric detector had been shown to respond to organotin compounds during a general survey of organometallic response in a Tracor FPD (93), it seemed logical to follow up on this preliminary information and develop the Shimadzu FPD, which was at our disposal, for the analysis of organotin compounds.

Initial results of the investigation showed unexpectedly high sensitivity (in the picogram range). The only drawback was that the peaks were broad and tailed badly. However, things turned sour over the next few months as the tin response progressively and inexplicably declined. Interestingly, the peak shapes improved as the response declined.

It seemed logical at the time to suspect either a contamination or a decomposition problem. Therefore the burner nozzle parts and quartz flame enclosure were cleaned in an ultrasonic bath with methanol. When this did not help, the detector was dismantled and the injection port and transfer lines were cleaned with methanol. Still, there was no improvement. One could have also speculated that decomposition was occurring on column, so a number of other liquid phases were tested in place of the original column.

(5% OV-101 on Chrom W, 45-60 mesh, acid washed). Testing a few columns showed that no decomposition was occurring.

When one tries several avenues on "trial and error" in order to solve a problem with no readily apparent solution, the door is open for luck to come in and play a vital role.

Injection of a silylating reagent to improve column performance is common practice. It was just this common technique, using a commercial silylating mixture ("Silyl-8"), that gave the first hint of what was going on. The flame had been left on when the injections were made; as a result, the detector exhibited a high background emission and the response of a test organotin compound was restored to the high level initially shown by the detector.

Since column decomposition could be ruled out, this meant that high tin response depended on the presence of something in the detector which was a constituent or a reaction product of the silylating mixture. Compounds of silicon were the only obvious possibility. This guess seemed the more reasonable because the effect of silane on the response of organotin compounds in a hydrogen-rich flame ionization detector, the HAFID(218), is well known. While this correlation between an ionization and an optical emission detector seemed pure coincidence, it was still intriguing since the origins of both types of tin response had not been elucidated.

The link between tin response and silicon doping was

established by injections of neat tetramethylsilane. The high background and noise of the detector was found to be largely due to the deposition of a white solid, presumably SiO_2 , on the burner nozzle and the quartz flame enclosure. It was realized that neat injections of organosilicons was not the best way to optimize the detector for tin response.

Instead, silane gas was doped into the hydrogen line in very small amounts (1-10 microliters per minute) until the response of tin compounds leveled off. Once the silane doping was shut off, the tin response remained high and the poor peak shapes exhibited during doping got considerably better. Increasing the flow rate of silane hastened the increase in response for tin with time but did not affect its ultimate level.

At this point in time it seemed that the best sensitivity and general performance had been reached, but this turned out to be far from correct. A big improvement came about as the result of a side project. This project was designed to explore possible geometric selectivity, i.e. to favour certain species against others by distorting in various ways the quartz flame enclosure that surrounds the emission region. As it turned out, several of these tubes gave increased tin response while the response for the other emitting species, e.g. sulfur, decreased.

The design of the best performing of these tubes is shown in Figure 4; it has a restricted volume in the emission zone. A number of similar flame enclosures were

made in order to optimize the geometry. Surprisingly, these new tubes, which were very similar to the successful constricted design, did not yield a similar improvement of tin response.

A short while later, while attempting to clean the burner nozzle by injecting freon, it was found that tin response increased dramatically in one of the quartz flame enclosures that had originally shown disappointing performance. When other distorted enclosures were given the same "freon treatment", they also gave excellent tin response. In fact the best of these tubes (See Figure 4) gave higher sensitivity and better looking peaks than the silicon-doped detector. It appeared that the presence of a "freon-treated" quartz enclosure of the proper geometry converted the Shimadzu FPD into an extremely sensitive detector for tin. Using the best of the quartz flame enclosures, an investigation into the characteristics of the detector for organotin analysis was undertaken (229).

3.2 Characterization and Optimization of the Photometric Tin Detector

3.2.1 Spectral Characteristics

To know the emission spectrum of any FPD-active species is important for selectivity purposes (i.e. for choosing a proper interference filter). Insight into the mechanism of emission can often be gained by identifying the emitting species. The emission spectrum of tin in the

flame photometric detector is of considerable interest not only for analytical purposes but also for its own sake, because of the implications it carries in regard to the detection mechanism. This will be dealt with in more detail in this chapter.

Two different spectra were recorded. One was determined at the optimum conditions for sensitivity and the other, as a matter of interest, after the detector had been overloaded by receiving an amount of tetrabutyltin well beyond the linear range (one microgram). Figure 12 shows both spectra. The detector under "normal conditions" is dominated by a broad, featureless emission, with a maximum at 390 nm. Under "overloaded conditions", this emission disappears and two distinct emissions, a broad, featureless emission with maximum at 480 nm and a sharp band at 610 nm, show up. Dagnall et al. (191) reported on tin emission in a cool air-hydrogen diffusion flame. Their spectrum agreed closely with that of the "overloaded" detector. The sharp band at 610 nm, which was reported in Pearce and Gaydon (230), was attributed to SnH. Dagnall assumed the broad spectrum, maximum at 480 nm, to be in agreement with the SnO spectrum of Herrmann and Alkemade (231). However, the complexity of the emission at 480 nm prevents conclusive agreement that SnO is indeed the emitter. The best known, and most studied band systems of SnO lie in the violet and ultraviolet. Connolly (232) first reported SnO in a flame and produced a detailed analysis. More recently Joshi and

Figure 12

Tin Emission Spectra - 300 nm to 650 nm, in Both
"Normal" and "Overloaded" Conditions Using a
Constricted Quartz Flame Enclosure

8 nm bandpass

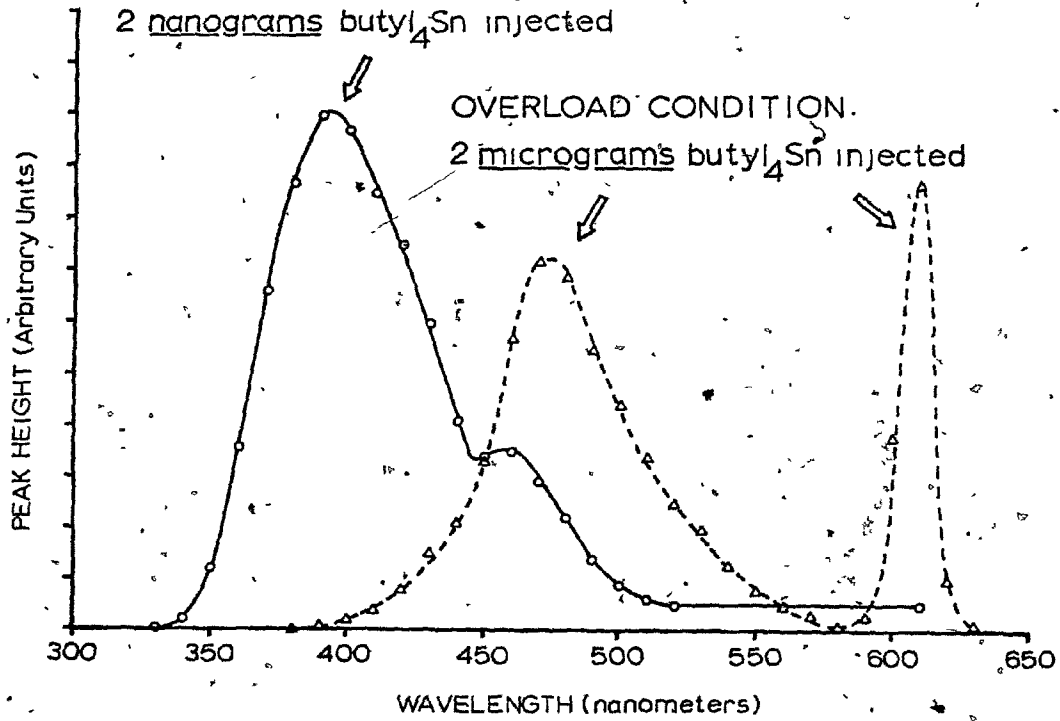
FPD RESPONSE vs. WAVELENGTH
FOR TWO DETECTOR CONDITIONS:

REGULAR CONDITION:

2 nanograms butyl₄Sn injected

OVERLOAD CONDITION:

2 micrograms butyl₄Sn injected



Yamdagni (233) provided a more complete analysis of SnO₂ emission. If the FPD "normal" detector spectrum is corrected for PM tube response, it closely resembles that of Joshi; however, the spectrum lacks structure, thus preventing positive identification. This lack of structure was confirmed by running a spectrum at higher resolution (2 nm bandpass instead of 8 nm bandpass).

3.2.2 Flow Rate Optimization

The conditions for optimum tin response were determined by varying the air and hydrogen flow rates. This was done both in an "open" or filterless mode, and by using 394 nm (conventionally used for sulfur) and 610 nm interference filters. The optimum conditions for sensitivity are the same for the "open" mode and the 394 nm filter mode. This is evident from the spectrum of the "normal" detector which is wholly dominated by the broad emission, maximum at 390 nm. The flow optimization is shown in Figure 13 for the 394 and 610 nm filters. The strong contrast between the two sets of data reinforces the idea that the two emissions are due to different tin species, possibly "SnO" for the 390 nm emission and likely "SnH" for the 610 nm emission. The excellent sensitivity of the detector is in part due to stronger emission at low air flows, which makes for low background emission and detector noise. Because the 390 nm emission spectrum is so broad, a loss in sensitivity by a factor of about four

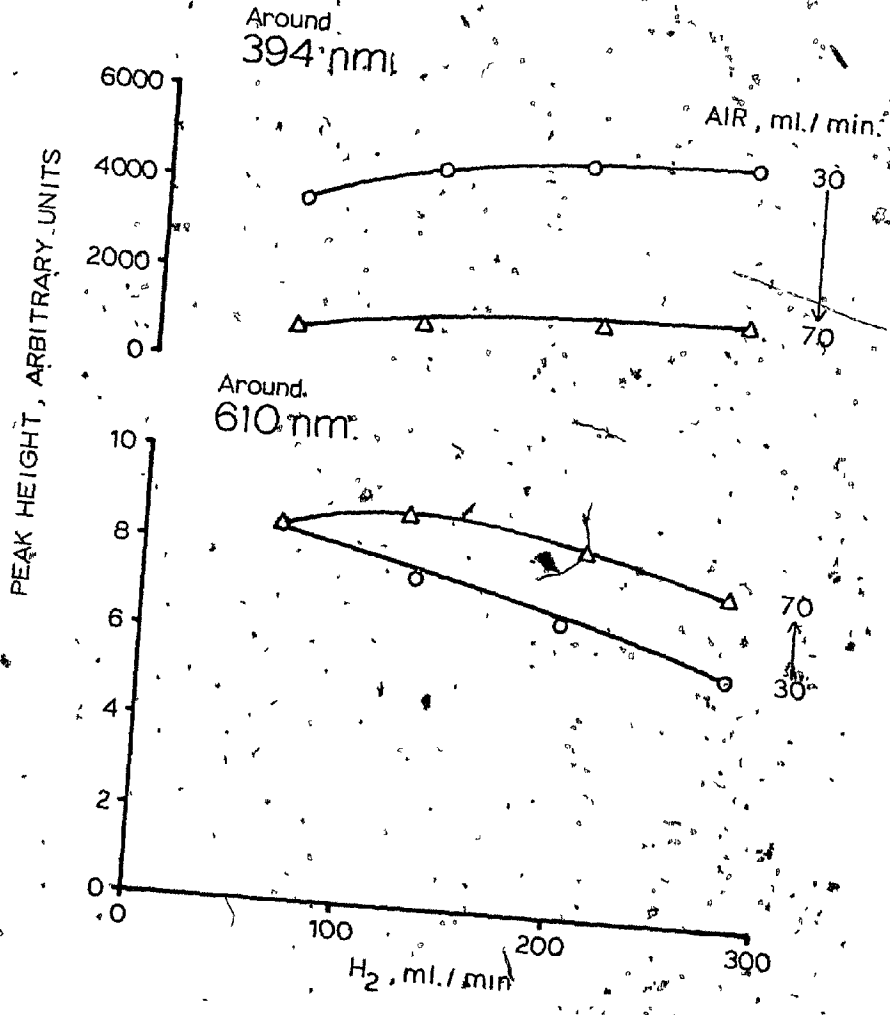
74

Figure 13

Sensitivity Versus Air and Hydrogen Flow Rates for
Two ¹¹⁹Tin Emissions

1 ng tetrabutyltin injected

TWO "TIN" EMISSIONS



occurs when the 394 nm filter is used in contrast to the filterless mode. Hence, the tin detector was characterized in the filterless mode.

3.2.3 Detector Performance

The general performance of the tin detector in terms of sensitivity and selectivity at optimum conditions is shown in Figure 14. Calibration curves of a standard mixture of five organotin compounds run in temperature-programmed mode and those of the compounds, most likely to interfere (run isothermally) are included to illustrate these important detector characteristics.

The response of tin compounds is precisely linear over more than two orders of magnitude and its magnitude, though not strictly proportional to tin content (possibly, because of experimental conditions) follows approximately the correct sequence $[(\text{CH}_3)_6\text{Sn}_2 > (\text{C}_3\text{H}_7)_4\text{Sn} > (\text{C}_4\text{H}_9)_4\text{Sn}]$. Above this range it becomes very slightly exponential (i.e. the slope is greater than one on a log-log plot). At the top of the tin calibration curves the detector obviously becomes saturated. Injections much beyond this amount will cause the detector to lose sensitivity.

The pure sulfur and phosphorous compounds show their expected exponential and linear behaviour; methyl parathion, which contains both elements, shows both types of behaviour in the upper and lower parts of its calibration curve, respectively. Stated very roughly, the detector is

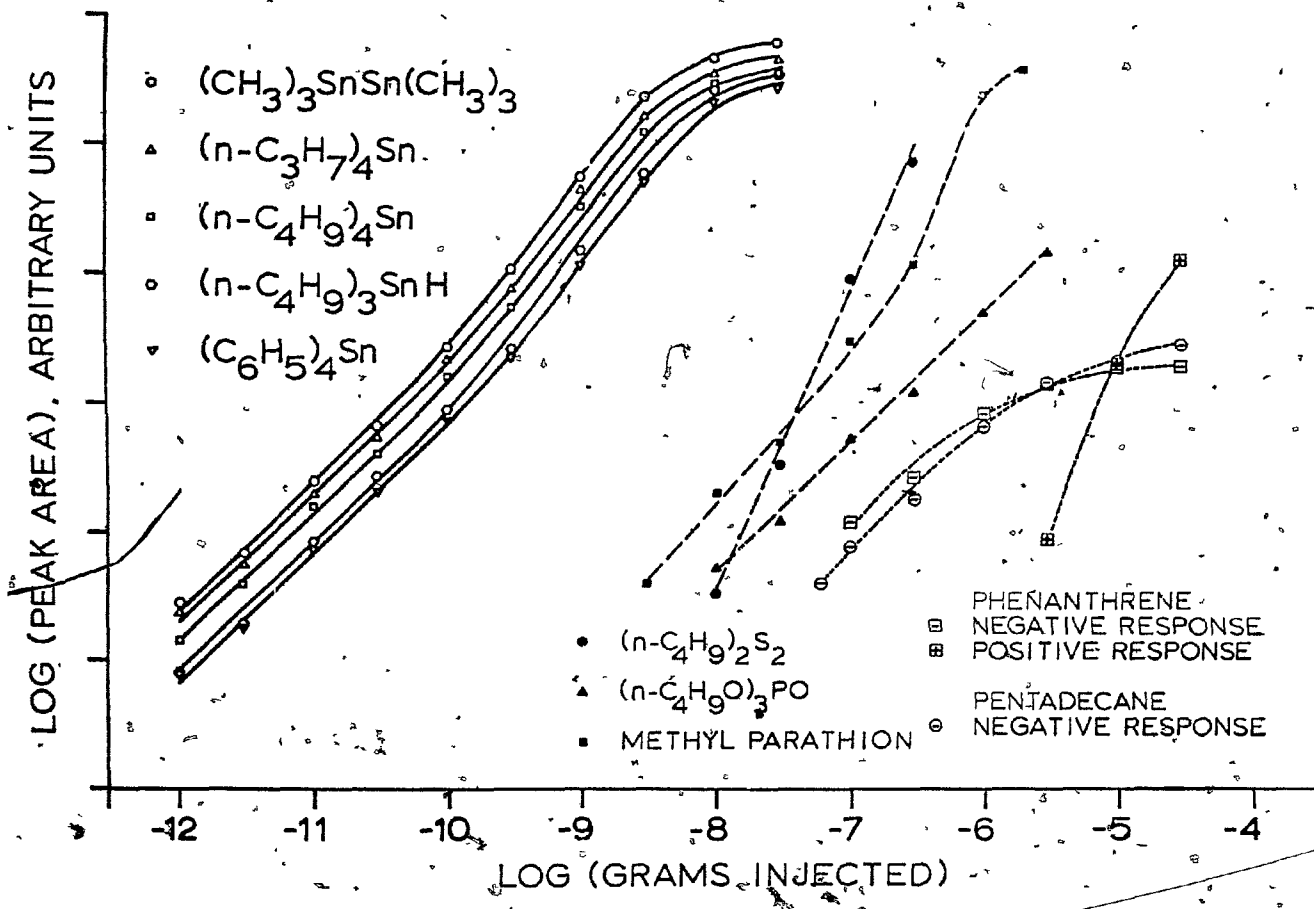
Figure 14

Tin Detector Performance - An Overall View

Calibration curves of various standard compounds, Tin compounds: temperature program as shown in Figure 15.

Other compounds isothermal: (t-C₄H₉)₂ S₂ 90°, (n-C₄H₉O)₃PO 160°, methyl parathion 175°, phenanthrene 165°, pentadecane 140°. No interference filter. Flows in ml/min: N₂ = 40, H₂ = 250, AIR = 30. 100 x 0.27 cm ID, borosilicate column, packed with 5% OV-101 on Chromosorb W, 45-60 mesh. Constricted Quartz Flame Enclosure.

Note: (n-C₄H₉)₃ SnH is really (n-C₄H₉)₃Sn₂ as identified by mass spectrometry; phenanthrene "positive response" is due to a sulfur containing impurity.



two to three orders of magnitude more sensitive to tin compounds than to sulfur and phosphorous compounds, although values outside this range can be easily found.

The selectivity of tin versus carbon compounds must be examined bearing in mind the well-known erratic response of hydrocarbons in the FPD. The calibration curves suggest that the detector is more sensitive to tin compounds than to carbon compounds by four to five orders of magnitude. However, a change in the nature or level of the background emission would lead to rather large changes in the negative peaks (i.e. reductions in background). Aliphatic and aromatic hydrocarbons give similar negative response. The positive response shown for phenanthrene was later traced to a sulfur-containing impurity, a not uncommon problem with polynuclear aromatics (234, 235).

It should also be remembered that these calibration curves were run without wavelength discrimination (excepting the spectral response of the PM tube) under the conditions of optimal tin response (i.e. at the maximum of the tin signal-to-noise profile) rather than under conditions of maximum discrimination against one or the other species. The latter approach would most likely have led to significantly different results.

The performance of the photometric tin detector is well suited for trace analysis, as can be seen in Table 1 from a comparison of minimum detectable amounts reported in this thesis and in the literature for compounds contain-

ing Cr, B, P, S, Se, Te, Ge and Sn; each of course under its own optimized conditions and using a particular instrument.

Table 1
Flame Photometric Detection Limits
1978
Minimum Detectable Amount

<u>X</u>	<u>Compound</u>	<u>g Compound</u>	<u>gX/sec</u>	<u>moles X/sec</u>
Sn	Pr ₄ Sn ⁴	4 x 10 ⁻¹⁴	5 x 10 ⁻¹⁶	5 x 10 ⁻¹⁸
Ge	Bu ₄ Ge	1 x 10 ⁻¹²	1 x 10 ⁻¹⁴	1 x 10 ⁻¹⁶
Cr	Cr(tfa) ₃	1 x 10 ⁻¹¹	8 x 10 ⁻¹⁴	2 x 10 ⁻¹⁵
P	C ₈ H ₁₀ NO ₅ PS	1 x 10 ⁻¹¹	1 x 10 ⁻¹³	4 x 10 ⁻¹⁵
S	φ ₂ S *	4 x 10 ⁻¹¹	7 x 10 ⁻¹³	2 x 10 ⁻¹⁴
Se	φ ₂ Se *	4 x 10 ⁻¹⁰	1 x 10 ⁻¹¹	2 x 10 ⁻¹³
Te	Bu ₂ Te *	1 x 10 ⁻⁹	6 x 10 ⁻¹¹	4 x 10 ⁻¹³
B	B ₁₀ H ₁₄	7 x 10 ⁻¹⁰	1 x 10 ⁻¹⁰	9 x 10 ⁻¹²

* on a sulfur background

Tin compounds are easily the most sensitive ones analysed by FPD. Initial work established a minimum detectable amount of 2 x 10⁻¹³ g tetrapropyltin. Figure 15 illustrates that situation by a temperature-programmed chromatography of a five-compound standard mixture at the ten and one picogram levels.

3.2.4 Hydrocarbon Interference: Methane Doping

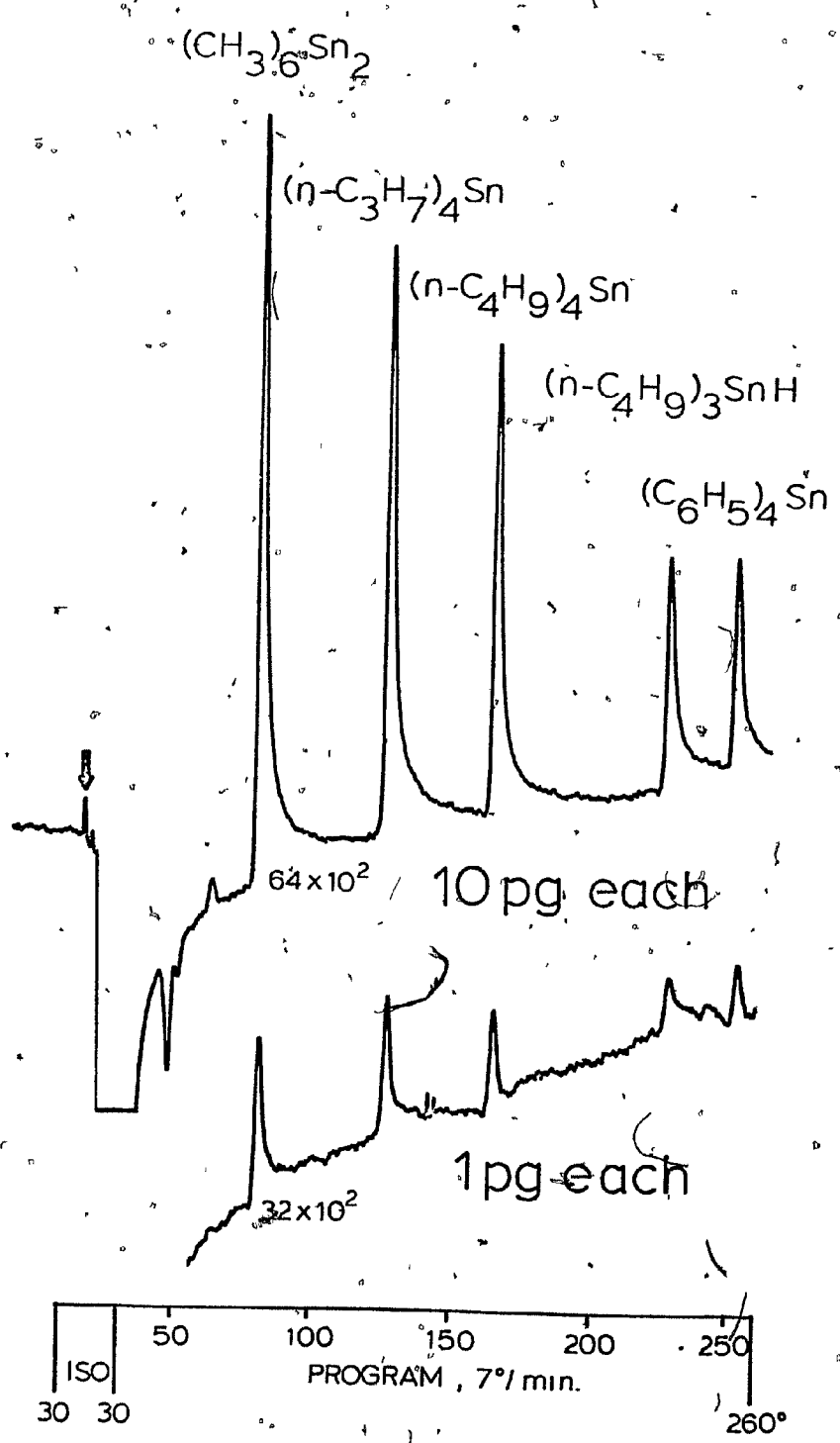
The depression of sulfur response in the FPD by carbon is well known. Therefore, it was deemed necessary

Figure 15

Detector Sensitivity - Temperature Programmed Chromatography of Five Organotin Compounds at the 10 pg and 1 pg Levels

Conditions as in Figure 14.

Note: $(n-C_4H_9)_3SnH$ is really $(n-C_4H_9)_6Sn_2$ as identified by mass spectrometry.



to investigate the effect of a co-eluting hydrocarbon on tin response by continuously adding methane to the carrier gas. Figure 16 shows the result of this experiment, which included a sulfur compound (at conditions optimized for tin) in more than a thousand-fold excess for comparison. It can be easily seen that the tin response decreased only marginally until the amount of methane was greater than 10% of the carrier gas. Further addition of methane caused the response to drop rapidly and the peak shape to deteriorate drastically. Taken from an analytical viewpoint, though, the interference of hydrocarbon compounds on tin response in the FPD should be minimal for normal applications.

3.2.5 Detector Poisoning

An unusual phenomenon, characteristic of the photometric tin detector, was that it could be poisoned, causing a "permanent" decrease in response. Tin, itself, could be the culprit if it was added to the detector in amounts well beyond the analytically useful range of the calibration curve (i.e. about 1 ug of compound injected). The results show a decrease of about three orders of magnitude in response and a radically different spectral output (see the "overloaded" detector spectrum in Figure 12). The poisoning effect was also exhibited by phosphorous-containing compounds and is illustrated clearly in Figure 17. It shows a drop in response by about a factor of three in the response of 200 picograms of tetrabutyltin

Figure 16

**Effect of Methane Doping on Tin Response, Using a
Constricted Quartz Flame Enclosure.**

**Methane flow as indicated, other conditions as in
Figure 14.**

METHANE - DOPED CARRIER GAS

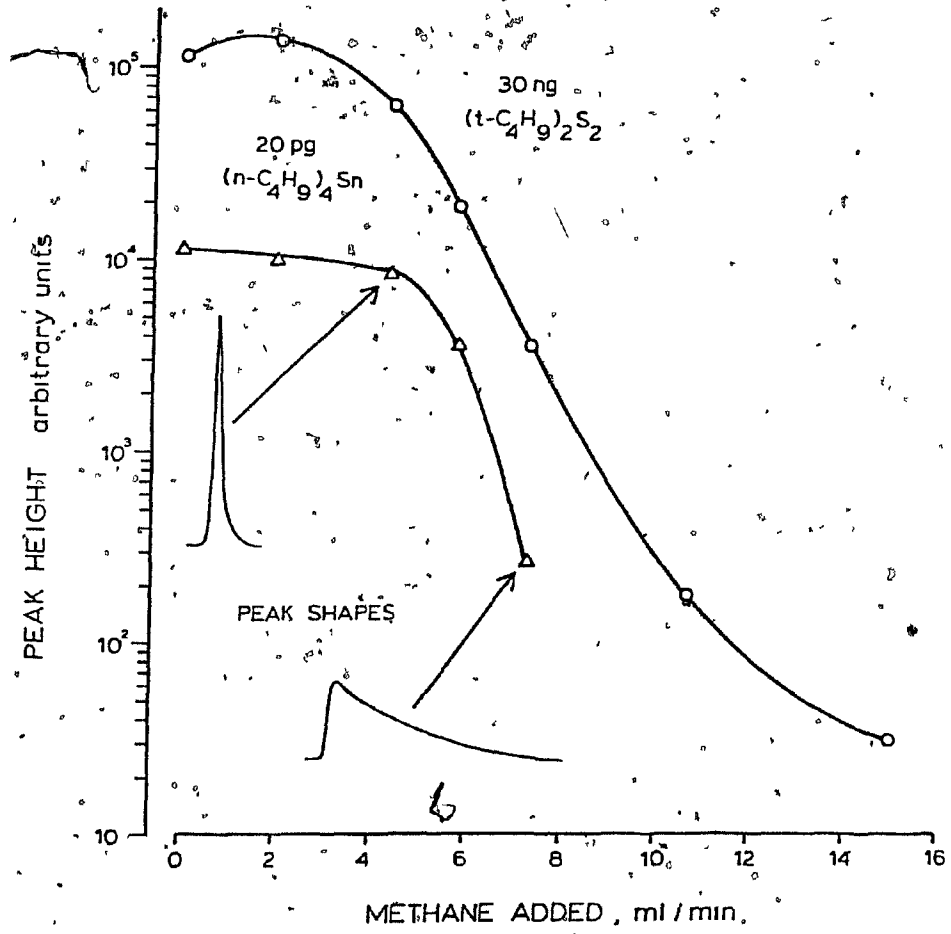
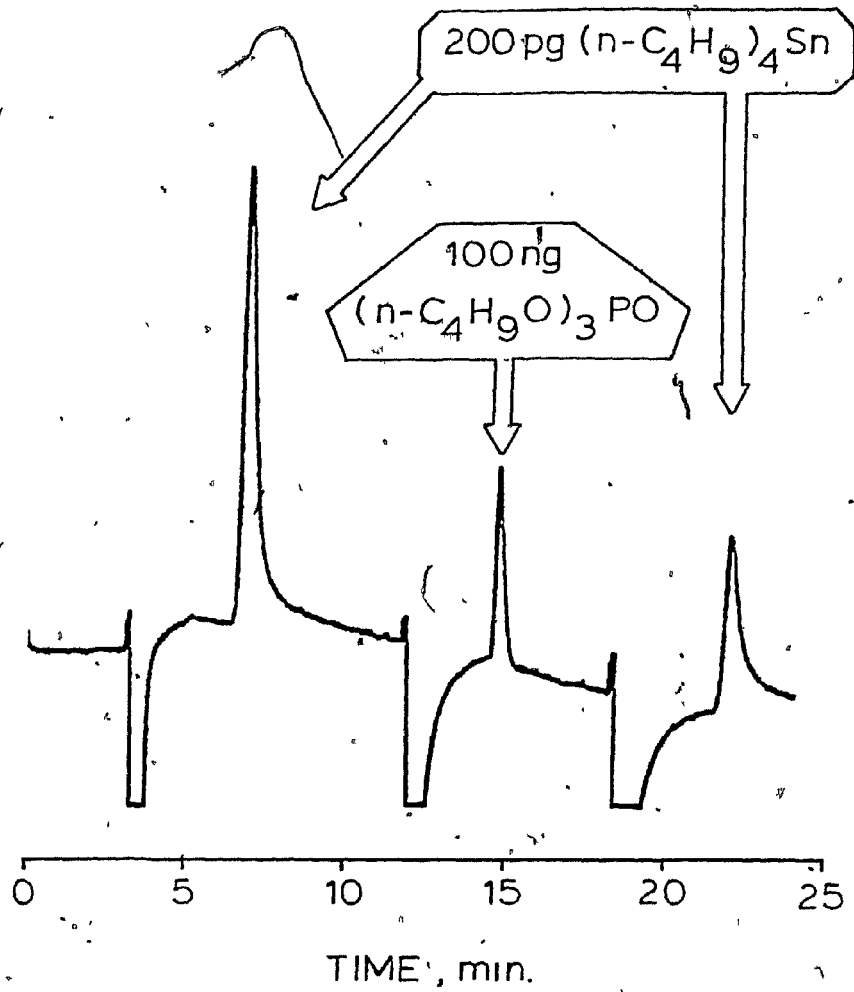


Figure 17

Detector Poisoning

Conditions as in Figure 14

DETECTOR POISONING



caused by the prior injection of 100 nanograms of tributylphosphate. Fortunately, good detector response for tin can be restored by the introduction of fluorocompounds into the operational FPD.

3.2.6 Effect of Quartz Flame Enclosure Geometry

The initial study of the effect of the geometry of the flame enclosure surrounding the burner indicated that a distorted chimney of the type shown in Figure 4 was best for tin response. This enclosure was radially constricted to a smaller volume in the region viewed by the PM tube. Several enclosures with different inner diameters of the restricted region, but of the same basic shape, were constructed and tested to further optimize the flame enclosure geometry. The most constricted enclosures showed somewhat greater response than those which were close to normal, and gave noticeably better peak shapes. Figure 18 shows a graph relating peak asymmetry to the inner diameter of the constricted region of the enclosure. The best of these had an inner diameter of 3 mm in the constricted region and it was used for the initial characterization of the photometric tin detector.

3.3 The Tin Emission Mechanism: Surface vs Gas-Phase Luminescence

During the experimentation leading up to the development of the photometric tin detector, a number of unusual effects became apparent; all of which suggested, though none proved, an involvement of the quartz surface surround-

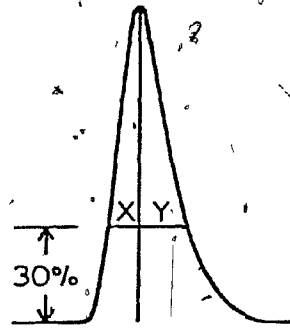


Figure 18

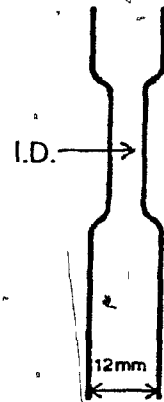
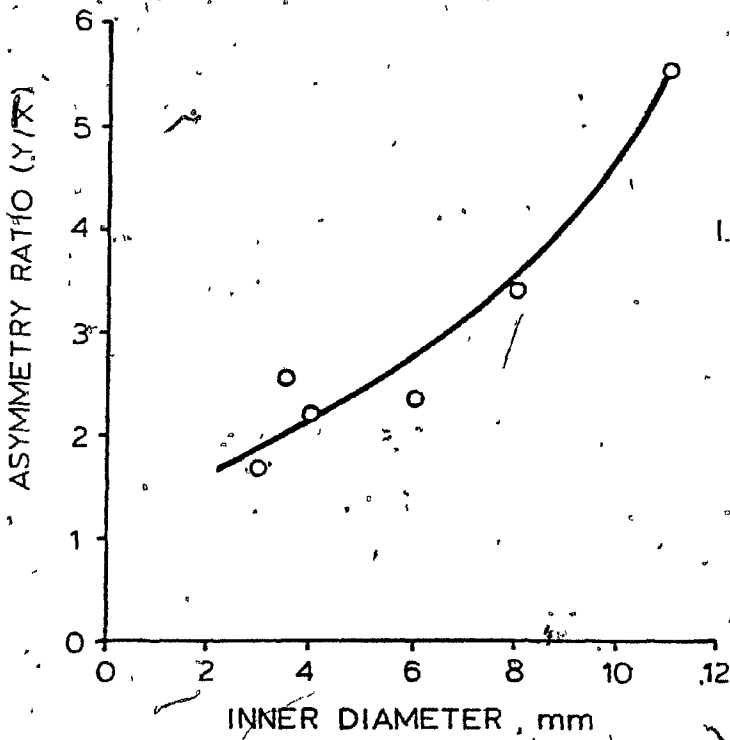
Dependence of Tin Compound Peak Shape on Quartz
Flame Enclosure Geometry

Measurement of peak asymmetry of tetrapropyltin,
chromatographed isothermally at 120° , correlated to
the inner diameter of the flame enclosure. Conditions
as in Figure 14.

PEAK ASYMMETRY vs. TUBE DIAMETER



ASYMMETRY RATIO = Y/X



ing the hot flame gases in the emission mechanism.

These effects were:

1) The introduction of silicon-containing compounds into a conventional Shimadzu FPD greatly improved tin response and broadened peaks. (High amounts of these compounds deposit some SiO_2 on the quartz enclosure.)

2) Injection of fluorine-containing compounds into the detector, when using distorted quartz flame enclosures (see Figure 4), improved response dramatically for subsequently injected tin compounds (the fluorine-containing compounds form HF in the flame which cleans the quartz surface by formation of SiF_4).

Note: Effects 1 and 2 occur with tin compounds only; phosphorous and sulfur compounds are not affected.

3) Tailing can be reduced considerably by constricting the quartz enclosure just above the flame (from 11 mm ID to, typically, 3 mm ID) see Figure 18.

4) The constricted flame enclosure, which permits a lower volume to be observed by the PM tube, decreases response for compounds of phosphorous, sulfur and selenium, but increases response for tin compounds.

5) A similarly-shaped borosilicate flame enclosure shows increased response for tin compounds after being "treated" with freon, but less response than a similarly-shaped quartz enclosure.

6) The injection of large amounts of tin or phosphorous compounds depresses the response of subsequently-injected

tin compounds, up to three orders of magnitude. This is similar to the poisoning effect of certain compounds on catalytic surfaces in that it is a "permanent" effect. The former detector performance can be restored only by the injection of fluorine-containing compounds (chlorine-containing compounds, e.g. methylene chloride, work less well). The response of phosphorous and sulfur compounds, on the other hand, is not subject to such a poisoning effect.

7) The upper parts of the calibration curve of various tin compounds show saturation such that all peak heights attain the same value. This is illustrated in Figure 19. It shows temperature-programmed chromatography of a five-compound standard mixture at the 3 and 10 nanogram levels, which represents the calibration curve close to and in the saturation region.

8) When the detector has been poisoned with large amounts of tin or phosphorous compounds or when tin is injected into a conventional FPD, its spectral output is radically different from that which is characteristic of a highly sensitive, fluorine-treated detector.

9) When large amounts of methane are introduced into the detector, the peak shape of tin compounds dramatically changes for the worse, but the effect is not observed for sulfur compounds (see Figure 16).

All these observations would be consistent with a surface emission mechanism of tin response, but do not

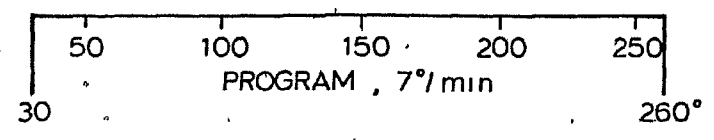
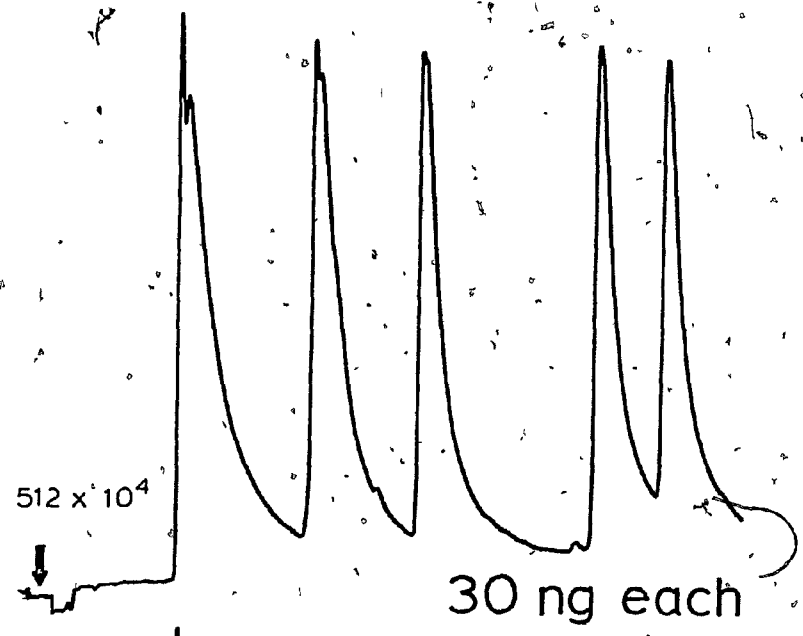
Figure 19

Chromatography in the Saturation Region of the
Calibration Curve of Standard Tin Compounds

Conditions as in Figure 14.

Note: $(C_4H_9)_3SnH$ is really $(C_4H_9)_6Sn_2$ as identified
by mass spectrometry.

DETECTOR SATURATION



really prove it. Therefore, it was decided to deliberately design some experiments to confirm the surface-emission hypothesis. These experiments were based on a special quartz flame enclosure as shown in Figure 4. This tube was a regular flame enclosure with a 3.5 mm OD quartz tube traversing through the centre, in a position one mm above the rim of the flame cup. The bisected quartz enclosure provides a quartz surface directly over the flame on which tin emission could take place. Normal quartz enclosures of 12 mm ID are not affected by freon to a large extent, hence any greatly improved emission would have to come from the tube crossing through the flame enclosure. "Freon treatment" of this tube did indeed produce a very sensitive photometric tin detector, thereby providing a positive test for the surface emission hypothesis. A series of experiments connected with this bisected enclosure are discussed below.

3.3.1 Visual Observation

On the assumption that a surface reaction is taking place, a bisected quartz enclosure provides an isolated quartz surface on which the emission occurs. In contrast, gas-phase emission like sulfur should spread throughout much of the viewing region. The act of viewing tin and sulfur peaks as they pass through the detector, should help to clarify the role of the bisecting quartz tube.

The bisected enclosure can be viewed from two basic directions. The first was an "end-on" view where the ob-

server's eye was in line with the bisecting tube axis. The second was a "side-on" view where the observer looked at the entire length of the bisecting tube, crossing perpendicular to his line of sight.

The results of visual observation (after some 30 minutes of dark adaptation) clearly indicate the importance of the bisecting tube in tin emission in contrast to sulfur emission. The "end-on" view is the most conclusive one; the tin peak produces a ring of blue on a dark background around the bisecting tube, while sulfur exhibits a large tongue of blue colour protruding from the mouth of the flame cup and filling most, if not all, of the quartz enclosure. Where the bisecting tube is located, a dark hole can be seen, indicating the quenching of the weak background emission from the tube itself. The "side-on" view is less clear but still good evidence; the tin peak produces a blue emission which shows up the entire surface of the bisecting tube but strongest on the bottom, while sulfur exhibits a large tongue of blue colour, intense above and below the bisecting tube and weak around it.

3.3.2 The Bisecting Enclosure and the Masks for Geometric Selectivity.

From visual observation it was clear that tin emission was occurring on or near the surface of the quartz. However, numerical proof would be more acceptable for anyone who had not seen it. Therefore, a number of masks were constructed from aluminum foil to alternately view

only the quartz surface or the rest of the emission region; one pair for each end-on and side-on viewing configurations. An illustration of the masks is shown in Figure 5; M1 and M3 are surface selective and M2 and M4 are gas-phase selective. The numerical results confirmed the visual observation and are presented in Table 2.

Table 2

(% of Relative Response in Unmasked Conditions)

<u>Compound</u>	<u>(Butyl)₄Sn</u>	<u>(Phenyl)₂S</u>
<u>Side-on View</u>		
M1, "surface"	118*	39
M2, "gas-phase"	16	106*
<u>End-on View</u>		
M3 "surface"	79	22
M4 "gas-phase"	43	116*

* Responses greater than 100% are due to reflection from the aluminum foil.

The masks, despite the problem of reflected light and the mechanical problem of fitting them in their intended place, gave numerical support to the surface-emission hypothesis for tin.

3.3.3 Effect of the Height of the Bisecting Tube Above the Flame on Tin and Sulfur, Using China Ink Masks.

The combination of a bisected flame enclosure and mask M3 seemed the logical choice for the greatest selec-

tivity for tin versus other emitting species. Because of the limitations of aluminum foils, it was decided to "paint" a bisected flame enclosure with China Ink so that the ends of the bisecting tube (for end-on viewing) were not covered. This ink was heat-resistant and eliminated the reflection problems associated with the aluminum foil. The effect of the height of the bisecting tube on tin and sulfur emission was investigated using this enclosure. A fluorinated-silicone rubber O-ring was friction-fit on the burner nozzle such that by adjusting its position the height of the bisected flame enclosure (and hence that of the bisecting tube) could be varied. The results, shown in Figure 20, indicate a sharp contrast between the behaviour of tin and sulfur emission. Tin emission is greatest when the bisecting tube is just over the flame and decreases dramatically as the tube is raised. Meanwhile sulfur response decreases both at short and long distances from the flame but much less compared to tin. This experiment does serve to illustrate the importance of the quartz surface once again.

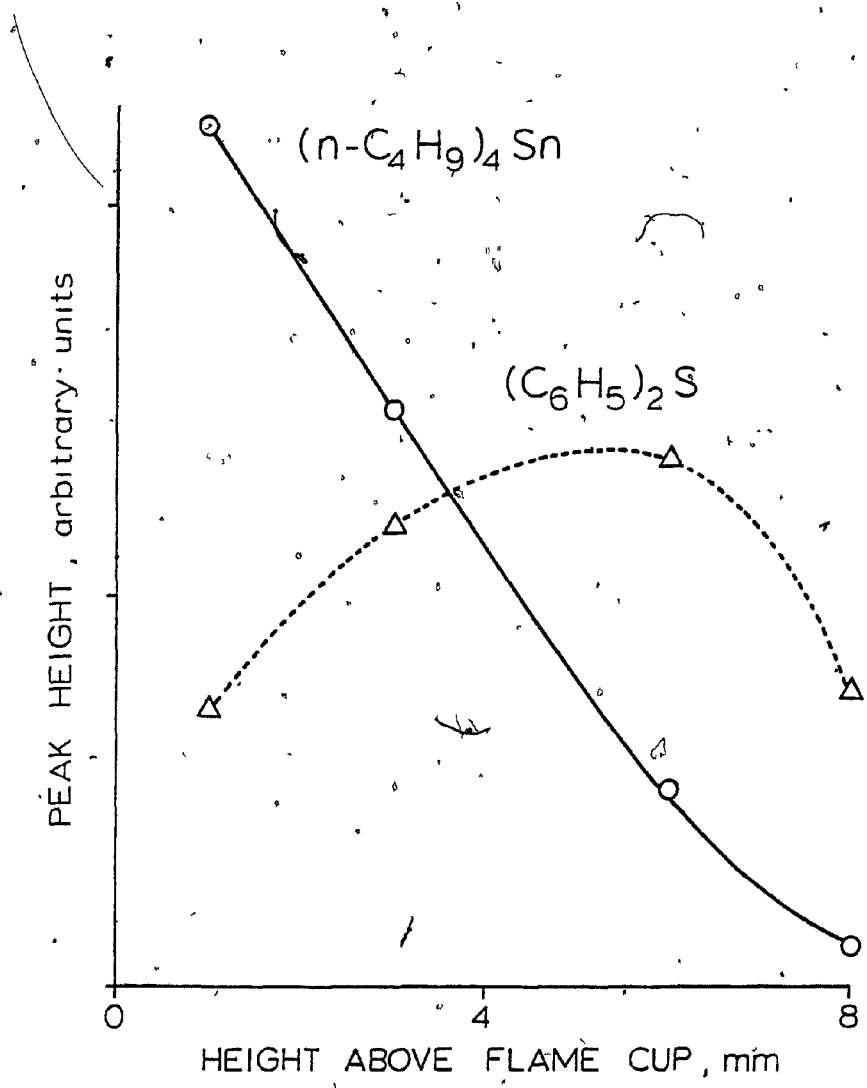
3.3.4 A Dual-Masked Bisected Quartz Flame-Enclosure for Geometrically Selective Monitoring of FPD Emissions.

The dual-channel capability of the Shimadzu FPD enabled the simultaneous monitoring of detector signals in both gas-phase-selective and surface-selective modes. This was accomplished by painting a bisected flame enclosure with China Ink so that it combined masks M3 and M4' as shown

Figure 20

Variation of Tin and Sulfur Response With the Height
of the Bisecting Tube Above the Flame Cup

Using dual-masked bisected quartz flame enclosure
(viewing mask M3 as shown in Figure 5). Compounds
run isothermally, $(n-C_4H_9)_4Sn$ 170°, $(C_6H_5)_2S$ 190°.)



in Figure 5. This dual-masked enclosure was placed in the position for "end-on" viewing. Thus, one channel monitored essentially the surface, the other the gas phase. The ratio of peaks appearing simultaneously in both channels would therefore indicate whether or not they originated in the gas phase or on the quartz surface. Calibration curves were run for tetrabutyltin, tetrabutyl germane (germanium compounds were also found to respond by surface emission, see Chapter 6) and t-butyl disulfide. For each injected amount giving peaks on both channels a ratio was calculated:

$$\text{ratio} = \frac{\text{"gas-phase" response}}{\text{"surface" response}}$$

A plot of log (ratio) versus log (amount injected) for each compound is shown in Figure 21. There are two to three orders of magnitude difference in ratio between those compounds that produce emission in the gas-phase and those that produce it on the surface of the quartz. Figure 22 shows temperature-programmed chromatograms of a mixture of t-butyl disulfide, tetrapropyltin, tetrabutylgermane and pentadecane on the surface-selective and gas-phase selective channels, respectively. A comparison of the two chromatograms shows the utility of the detector for reliable qualitative information.

3.3.5 Assessment

After looking at the facts presented, it would be very difficult to argue against the interaction of tin

Figure 21

**Ratio of "Gas-Phase" vs. "Surface" Emissions for Tin,
Germanium and Sulfur Response via a Dual-Masked
Bisected Quartz Flame Enclosure**

Masks as indicated, made with China Ink. Centre drawing
(without mask) for comparison only. Flow rates in ml/min:
Air = 60, H₂ = 240, N₂ = 30. 50 x 0.3 cm I.D. boro-
silicate column, packed with 5% Carbowax 20M on
Chromosorb W, 45/60 mesh.

DUAL-MASKED BIASECTED QUARTZ TUBE

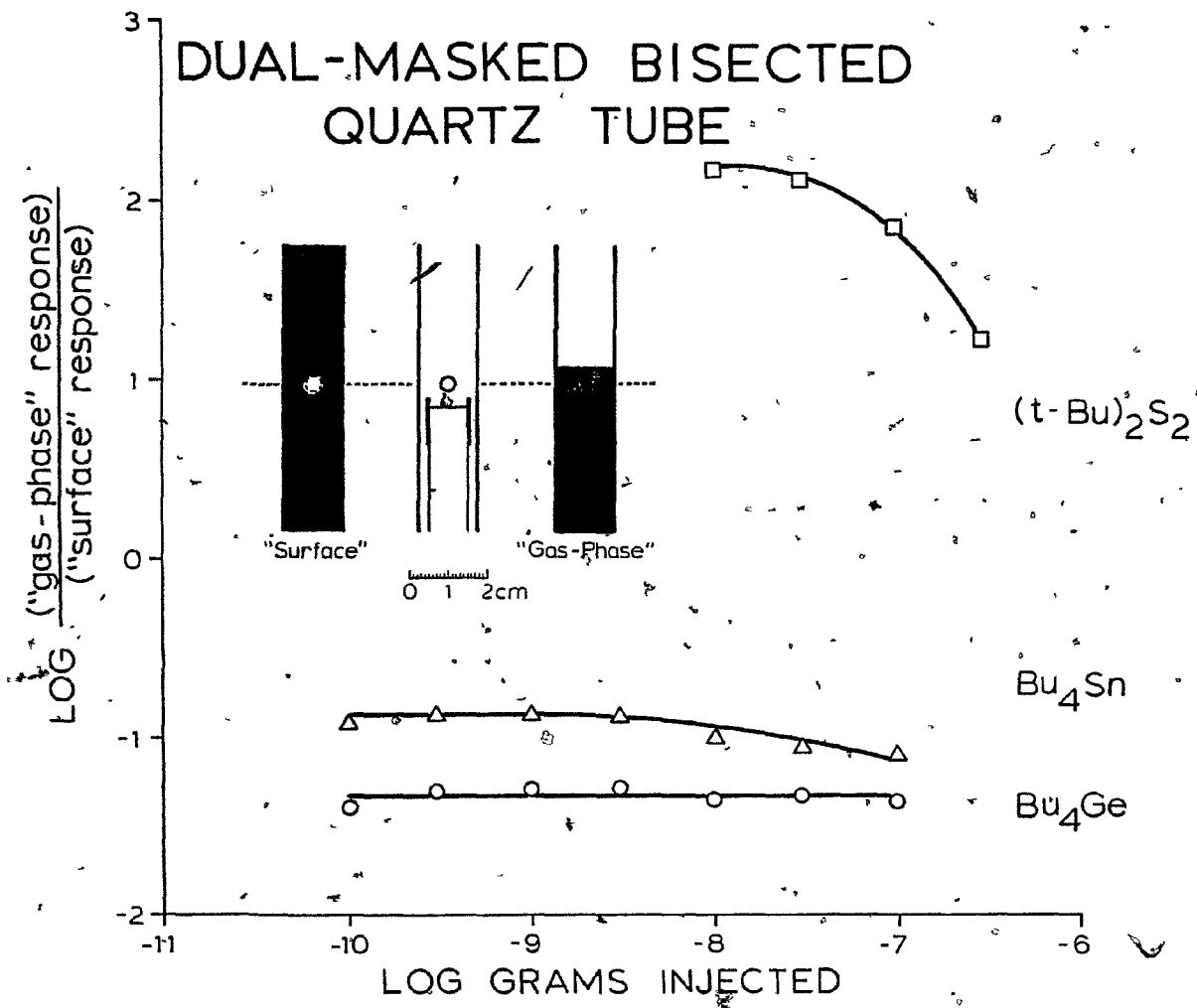


Figure 22

Temperature-Programmed Chromatography of a 4-Component Mixture with Detection on Both "Surface" and "Gas-Phase" Channels of a Dual-Masked Bisected Quartz Flame Enclosure

S = $(t\text{-C}_4\text{H}_9)_2\text{S}_2$, 3 ng injected

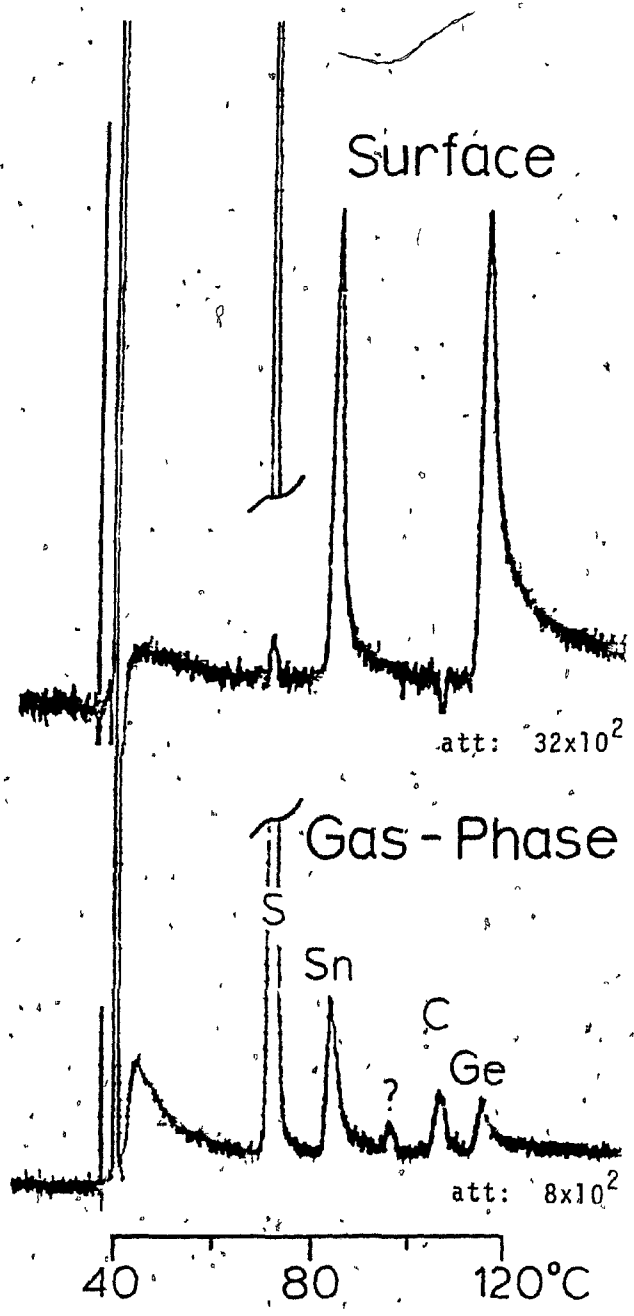
Sn = $(\text{C}_3\text{H}_7)_4\text{Sn}$, 100 pg injected

? = Impurity

C = Pentadecane, 5 μg injected

Ge = $(\text{C}_4\text{H}_9)_4\text{Ge}$, 100 pg injected

Conditions as in Figure 21



and a suitably prepared quartz surface to give chemiluminescent emission. Furthermore there is overwhelming evidence that the emission takes place on or near to the quartz surface. The one thing that has been proven is that tin emission in a flame photometric detector is a most interesting and potentially useful phenomenon.

3.4 The Quartz Wool Tin Detector (QWTD)

The sensitivity for tin of the FPD, using the modified quartz flame enclosures shown in Figure 4, was more than satisfactory; i.e. it was orders of magnitude better than that of any other species in the FPD. Consequently, further improvements in sensitivity were considered welcome but really not worth pursuing at the expense of other studies. However, without looking for it, increased sensitivity for tin was found in a new modification of the flame enclosure. This modification was a simple one, made by inserting a small amount of quartz wool in a normal, cylindrical quartz or borosilicate glass enclosure, such that it was positioned just over the flame. A later improvement (see Figure 4) had three symmetrical indentations in order to hold the wool in place. (Too much quartz wool caused problems with lighting the flame.) It was found that the quartz wool tin detector needed little or no "Freon treatment" to give high sensitivity for tin. Its low background emission helped in reducing the detection limit for tin by a factor of five. Table 3 expresses the detection limit for tin in various forms to illustrate its unusual sensitivity.

TABLE 3

Detection limit of Sn

$$\text{grams } (\text{C}_3\text{H}_7)_4\text{Sn} = 4.0 \times 10^{-14}$$

$$\text{grams } (\text{C}_3\text{H}_7)_4\text{Sn/sec.} = 1.3 \times 10^{-15}$$

$$\text{g. Sn/sec.} = 5.3 \times 10^{-16}$$

$$\text{moles Sn/sec.} = 4.5 \times 10^{-18}$$

$$\text{atoms Sn/sec.} = 2.7 \times 10^6$$

Calibration curves for tetrapropyltin were run with and without the quartz wool in a borosilicate glass flame enclosure and are shown in Figure 23. In addition to the increased sensitivity for tin compounds, the linearity of the QWTD is close to four orders of magnitude in contrast to the earlier photometric tin detector using a constricted flame enclosure, which was linear for just over two orders of magnitude before giving an as yet unexplained exponential response in the upper part of the calibration curve. Obviously this makes the QWTD more suitable for analytical applications. The surprisingly good sensitivity for tetrapropyltin in the normal FPD set-up is probably due to some contribution from surface emission due to silicon in the detector. Figure 24 shows the chromatography of 100 femtograms of tetrapropyltin using the Quartz Wool Tin Detector.

3.5 Derivatization of Labile Tin Compounds

3.5.1 Organotin Hydrides

The derivatization of organotin oxides, hydroxides,

Figure 23

Calibration Curves for Tetrapropyltin Using the Quartz Wool Tin Detector and a Normal Pyrex Flame Enclosure

Flow rates in ml/min: AIR = 20 H₂ = 240 N₂ = 30

50 x 0.3 cm ID borosilicate column, packed with Carbowax 20M deactivated Chromosorb W, 80/100 mesh

(252). Flow rates for the pyrex tube were AIR = 30 H₂ = 150 N₂ = 30; all other conditions were the same.

RESPONSE OF $n\text{-Pr}_4\text{Sn}$

(by two different mechanisms)

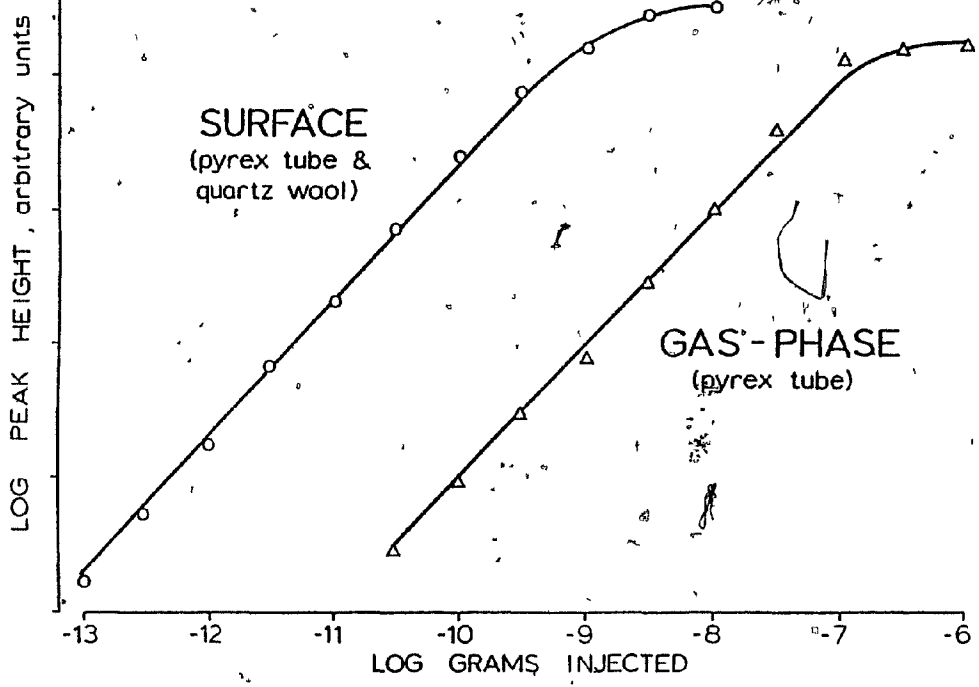


Figure 24

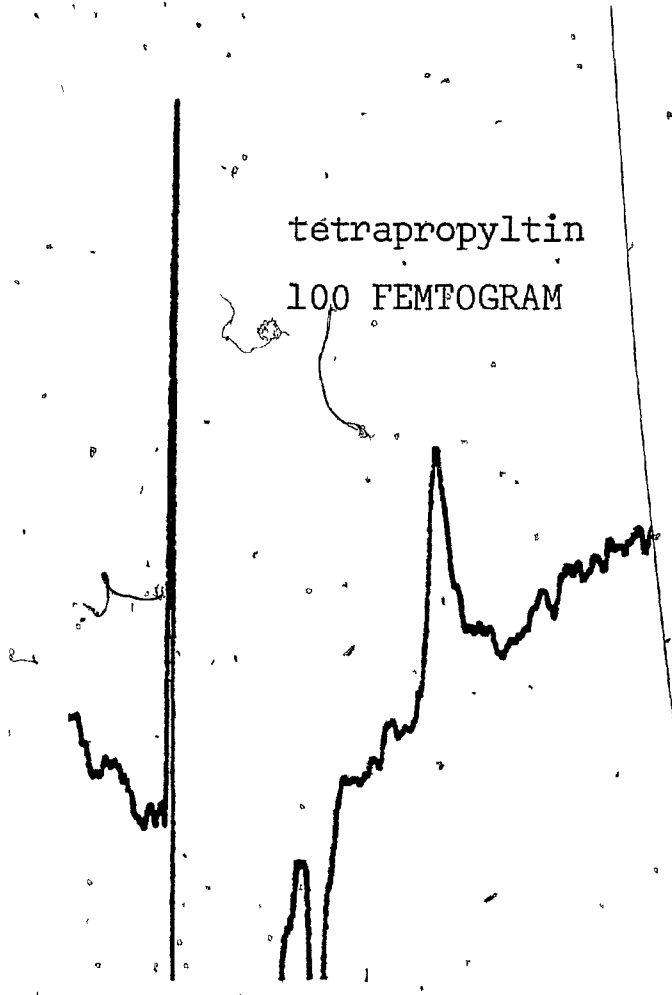
Chromatography of 100 Femtograms of Tetrapropyl Tin
Using the Quartz Wool Tin Detector

Spectrum Filter Setting = 0.01

Conditions as indicated in Figure 23.

tétrapropyltin

100 FEMTOGRAM



halides and acids by conversion to their corresponding hydrides, in combination with the very sensitive photometric tin detector and gas chromatography, was attempted at Dalhousie. A novel approach was taken, using a gas mixture of 0.5% silane in ultra-high purity nitrogen, as reagent.

A mild type of reducing agent was sought that ideally would reduce organotin compounds and not other, potentially interfering species (environmental samples could involve compounds containing other FPD responding elements such as P, S, Se and As). Polymethylhydrosiloxane (PMHS), a mild reducing agent, and silane, which is not used as a common reagent for the synthesis of hydrides (251) but obviously has reducing properties, were tested for the synthesis of organotin hydrides. PMHS showed initial success in producing organotin hydrides but was deemed unsuitable for trace analysis. This is because of poor conversion rates below 10 ng/ μ l concentrations of tin compounds and long reaction times (about 24 hours). It also failed to produce any hydride with triphenyltin hydroxide. It seemed surprising that silane had not been used as a common reducing agent; its pyrophoric nature was thought to be its biggest drawback in limiting its applicability. The present availability of silane diluted by inert gases such as nitrogen and argon have made this reagent considerably more easy to handle in a laboratory. Furthermore silane has several advantages over conventional reducing agents such as lith-

ium aluminum hydride and sodium borohydride. First of all, it is a gas. It can be effectively added by bubbling it through a solution of the compound to be derivatized. Unreacted silane can be purged from the system with an inert gas to a fume hood. Its likely end product is an inert solid, SiO_2 . In contrast, common reducing agents such as lithium aluminum hydride are very reactive and must be destroyed before injection into the GC system and separated from the desired reaction products. In short, silane appears to be promising reagent for the synthesis of organotin hydrides for analytical applications.

a) Reaction Conditions

At present, silane has been found to produce the corresponding hydrides for all of the di and triorganotin oxides, hydroxides and halides tested. A few of these compounds are trimethyltin hydroxide, tributyltin acetate, dicyclohexyltin dibromide, dioctyltin dichloride and triphenyltin hydroxide. Most of the work has been done with bis (tributyltin) oxide (TBTO) and triphenyltin chloride. Compounds such as butylstannic acid have proved unwilling to give the corresponding trihydride peak in the detector, either due to a failure in derivatization or chromatography. The method works at trace levels, i.e. in the picogram range, for the most carefully investigated compound, bis (tributyltin) oxide.

1) Importance of Solvent

A rather surprising feature of the reduction method using silane is that there is no conversion of the organotin compounds to their corresponding hydrides at trace levels unless methanol or ethanol is present. This seems unlikely to be a solubility effect since silane is non-polar and should dissolve better in non-polar solvents such as hexane. In fact a wide variety of solvents such as hexane, benzene, cyclohexane, diglyme, acetonitrile, tetralin, acetone, di-isopropyl ether and iso-octane, were tried. Aside from methanol and ethanol, only diglyme gave any hydride product with silane but yields were poor below the 10 ng/ μ l level.

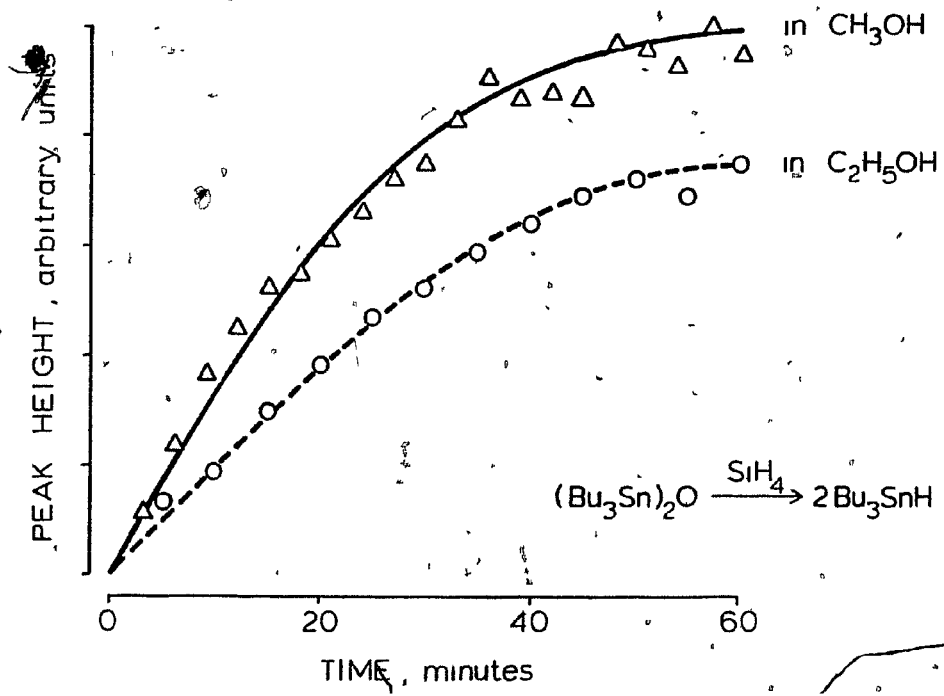
2) Reaction Rate

The reaction of TBTO in methanol or ethanol with silane was found to take about 30 minutes to go 80% to completion at the 1 ng/ μ l level. However, chromatographic decomposition makes these results rather uncertain. In order to minimize the effect of continuous evaporation of solvent, the experiment was carried out by saturating a methanol sample with silane and then adding enough TBTO to bring the concentration to about 1 ng/ μ l. One microliter samples were withdrawn from the "sillivial" every three minutes and injected into the gas chromatograph. The experiment was repeated with ethanol as the solvent and the results nearly paralleled those of methanol and they are shown in Figure 25.

Figure 25

"Yield" of Tributyltin Hydride versus Time of Reaction
for the Reduction of Tributyltin Oxide with Silane

A dual-masked bisected quartz flame enclosure is used.
Flow conditions in ml/min AIR = 30, H₂ = 240, N₂ = 30.
150 x 0.3 cm ID borosilicate column, packed with 5%
Carbowax 20M on Chromosorb W, 45/60 mesh.



3) Other Parameters

A number of important parameters were investigated such as temperature, silane bubbling rate and the presence of acid or base or certain additives like benzenesulphonic acid and disodium EDTA. Temperatures up to 65°C and down to near 0°C were tried with no apparent effect on the yield of reaction. Solutions of HCl and NaOH in methanol were made to test the effect of acid or base on the reaction, neither of which was significant. Very slow addition of silane to the solution containing the compound to be derivatized gave a slower conversion rate, probably due to lack of reagent. High bubbling rates did not help the reaction but only hastened the evaporation of the solvent. Additives such as benzenesulphonic acid depressed response to a small extent.

b) Chromatography

Because of the reactivity of organotin hydrides, it was expected that good chromatography for such compounds at trace levels would be difficult and so it was. Most of the work was done with the hydrides formed from TBTO and triphenyltin chloride. Tributyltin hydride, being more stable than triphenyltin hydride, gave fewer problems.

Basically, decomposition of the organotin hydrides can take place due to reaction with oxygen, especially at the relatively high temperatures required for GC. Solutions of tributyltin hydride, made up in solvents such as hexane, decomposed after a few days (and even after a few

hours if their concentration was low). Because of their reducing nature, they will react with "active sites" in the column or other parts of the GC system. Just how good the column is, in terms of deactivation of the support, is of prime importance. Throughout the experimental work on the hydrides, a number of columns were used:

- 1) 3% OV-101 on Carbowax 20M deactivated Chrom W, 45/60 mesh
- 2) 3% OV-101 on hydrogen-treated ($t = 900^{\circ}\text{C}$) Chrom W, 45/60 mesh
- 3) Carbowax 20M deactivated Chrom W, 80/100 mesh (252)
- 4) 5% Carbowax 20M on Chrom W, 45/60 mesh
- 5) 10% Carbowax 20M on Chrom W, 45/60 mesh
- 6) 10% OV-275 on Chrom W, 45/60 mesh
- 7) Carbowax 20M deactivated silica gel 62, 45/60 mesh
- 8) 20% OV-101 on Chrom P, 45/60 mesh

Columns 1, 2 and 4 gave good chromatography for the hydrides (in relative terms) but column 4 induced more triphenyltin hydride decomposition than 1 or 2. Column 3 was mediocre but columns 5 and 6 were poor. Columns 7 and 8 were tested only with trimethyltin hydride and dimethyltin dihydride because of their high retention ability but proved less than satisfactory. The temperature of the injection port played an unexpected role. Decomposition in the chromatographic system was up to three times less when the injection port was 300°C than when it was 200°C . This was not a rule but occurred when decomposition was bad.

The use of an efficient oxygen scavenger (Supelco carrier gas purifier, Supelco Inc., Bellefonte, Pa.) in the carrier gas line showed little effect. 100 ppm of hydrogen in nitrogen was used as carrier gas but made little difference on decomposition as well. The most effective method for reducing decomposition was to use very high carrier gas flow rates such as up to 80 ml/min of nitrogen or 240 ml/min of hydrogen. This effect was very noticeable for triphenyltin hydride which suffered considerably more decomposition than tributyltin hydride.

It is evident that more work must be done to reduce the decomposition of organotin hydrides in order for this method to be analytically useful. A clear understanding of the process of decomposition ought to lead the way to overcome this problem and allow this unique hydride generation method to achieve popularity.

3.5.2 Organotin Halides

The derivatization of organotin compounds such as TBFO, forming organotin halides, and their subsequent chromatographic separation and detection, was investigated as an alternative to hydride generation. Derivatization occurred "in situ" in the GC system in the injection port and/or the column itself. Halide was added to the GC system by injection of a methanolic solution of the acid or by doping of the carrier gas as shown in Figure 8, thus conditioning it for reaction and chromatography of the products. Conditions for the formation of the halide pro-

ducts of R_3SnX , R_2SnX_2 and R_1SnX_3 (where R = alkyl or aryl group and X = oxide, hydroxide, acetate, etc.) and their chromatographic behaviour were investigated.

a) R_3SnX

The conversion of compounds such as TETO, triphenyltin hydroxide and tricyclohexyltin hydroxide to the chlorides or bromides and subsequent chromatography, occurred simply by conditioning the GC system with injections of a few microliters of HCl or HBr in methanol (concentration in the 20ng/ μ l range). The method works well for tin compounds even in the low picogram range as can be seen in Figure 26. The remarkable sensitivity is gained using a Quartz Wool Tin Detector (QWTD), and chromatography is performed on Carbowax 20M deactivated Chromosorb W. (252).

b) R_2SnX_2 and $RSnX_3$

Compounds such as dibutyltin oxide and dimethyltin oxide do not dissolve in normal solvents such as acetone, benzene and hexane. However, they do dissolve in methanolic solutions of HCl. Similarly, compounds of the type $RSnX_3$ such as butylstannic acid must be dissolved in acid. Since HCl is necessary to dissolve these compounds, it is likely that they are present in the chloride form in solution (although other forms are likely to co-exist as well). If they are in the chloride form before injection into the GC system, then the ability of the system to convert them "in situ" to the chlorides cannot be measured. The appear-

Figure 26

Chromatography of Tripropyltin Oxide and Tributyltin Oxide as Chlorides at the 1 pg Level

The chromatograph was conditioned with HCl gas. High sensitivity was gained via the use of a quartz wool tin detector. Flow rates in ml/min: AIR = 20, H₂ = 160, N₂ = 10. 50 x 0.3 cm ID borosilicate column packed with Chromosorb W deactivated with Carbowax 20M, 80/100 mesh (252). Temperature programming: 100/10/150°C.

tripropyl- and
tributyltin oxides

ONE PICOGRAM EACH



HCl-doped GC

ance of the expected peak for such a compound indicates only the ability of the GC system to prevent decomposition of the chloride as it passes through. It was found that satisfactory chromatography of both types of compounds occurs only in a well-conditioned GC system under heavy HCl doping (i.e. with HCl doping into the carrier gas at about 10 μ l/min). This results from the fact that R_3SnX and R_2SnX_2 type compounds are more reactive than their R_3SnX counterparts and hence require a thoroughly conditioned system. Calibration curves for various compounds of all three types were run by monitoring gas-phase tin emission (in this case without wavelength discrimination) in the range of 100 picograms to 1 microgram of injected compound. Chromatography of compounds of R_2SnX_2 and R_3SnX below the 100 picogram level was not investigated. Figure 27 shows the chromatography of a mixture containing each type of tin compound as chlorides under HCl doped conditions. The chromatography of these compounds in the nanogram and sub-nanogram range thus appears to be at an analytically useful stage.

c) Important Considerations and Parameters

Both column temperature and elution time play an important role in this derivatization method. This proved especially true for methylated tin compounds, which are fairly volatile and hence elute from most columns at low temperatures. For the optimum reaction and chromatography, the column temperature must be kept reasonably high for

Figure 27

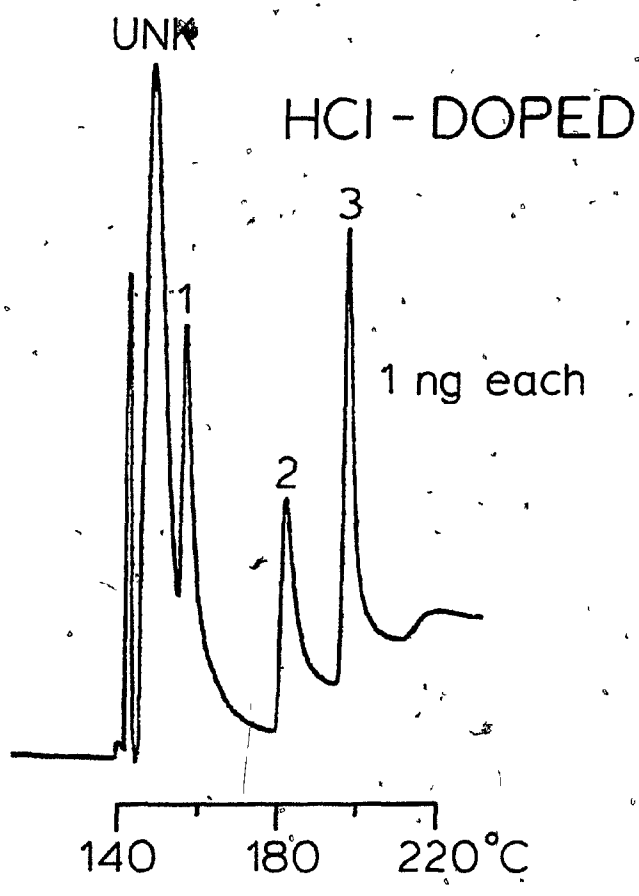
**Chromatography of Butylstannic Acid, Dibutyltin Oxide
and Tributyltin Acetate as Chlorides at the 1 ng Level**

HCl-doped GC, at approximately 10 μ l/min. Detector
operated in filterless mode with normal flame enclosure.

Flow rates in ml/min, air = 30, H₂ = 40, N₂ = 10.

100 x 0.3 cm ID borosilicate column, packed with 5%
OV-101 on Chromosorb W, 45/60 mesh.

UNK = Unknown peak which appears with solvent only.



each type of compound and this was accomplished by using a low carrier gas flow rate (e.g. 10 ml/min) and longer columns. For very heavy compounds such as triphenyltin chloride and dioctyltin dichloride, which elute very late off most columns, the effect of column temperature on reaction is not important. Shorter, faster columns are preferred to allow these compounds to elute at reasonable temperatures.

Slow temperature programs are not feasible because the organotin halides, especially the more reactive ones, tend to show broadened peaks and less than expected response, indicating some decomposition. Evidently, it is necessary to limit the time available for such compounds to react in a detrimental fashion.

Most notable for the case of compounds of the type R_2SnX_2 and R_4SnX_4 , is the situation where a certain percentage of the compound injected remains behind in the GC system, regardless of the amount injected (usually 5% or less). The compound left in the GC system can be eluted simply by injecting a solvent such as methanol and most of it will emerge from the column (so-called "ghost" peaks). The precise reason for this has not been investigated. This type of behaviour necessitates frequent checks by "blank" chromatograms (solvent only) to ensure the validity of the analytical data.

Decomposition of two types of compounds occurred in HCl-doped GC. Per-alkylated compounds, e.g. tetrabutyltin,

decomposed to a large extent to give tributyltin chloride. Tetrapropyltin, which elutes at a lower column temperature, decomposed to a much lesser extent under the same conditions.

Both triphenyltin hydroxide and tricyclohexyltin hydroxide react to give significant amounts of diphenyltin dichloride and dicyclohexyltin dichloride, respectively, under heavy HCl doping. The decomposition problem does not occur with the other derivatives (R_2SnX_2 and R_3SnX_3 types) and is not noticeable when the GC system is only lightly treated with HCl.

3.5.3 Application to Environmental Samples: Future Work

Both the hydride and halide generation methods for derivatization of labile organotin compounds were developed with environmental samples in mind. Samples from lobsters reared by the DFO (Department of Fisheries and Oceans) in TBTO-doped water, as well as "natural" lobsters, will be provided by Environment Canada in late summer of 1979. These samples will be analysed at Dalhousie for the possible presence of TBTO and its metabolites. A great deal of work must still be done to develop both derivatization approaches into routine analytical methods for organotins in the environment. The hydride generation method needs improved chromatography of the organotin hydrides formed. The halide derivatization method appears closer to readiness for analytical application. Samples

could be treated with acidic methanol to extract the organotin compounds as the chlorides. The extract could then be partitioned with hexane to remove fats leaving a cleaner sample for direct injection into the gas chromatograph. The success of the hexane treatment would depend on the distribution of the organotin halides between the acidic methanol and hexane layers. The hydride method could be used as a cross-check for the same sample following an extraction with an appropriate solvent. If possible this would be methanol or ethanol required for the subsequent silane treatment. Certainly, a great deal of work would be necessary to optimize the treatment of various types of samples and subsequent derivatization by either the hydride or halide method for future routine analysis.

4. Organoselenium Photometric Response

4.1 Development of a Selenium Photometric Detector

Aue and Hastings (93) first showed the possibility of organoselenium detection in a Tracor FPD in filterless mode. They recorded a detection limit of about 10 ng for piarselenole in an unoptimized detector. Since selenium is found below sulfur in the periodic table, it is not surprising that it too responds well in a flame photometric detector. Given the recent widespread interest in selenium and its organic compounds, it seemed worthwhile to pursue the early lead and develop the Shimadzu FPD, which was available for this study, into an analytically useful selenium detector (236).

4.2 Characterization and Optimization of the Selenium Photometric Detector

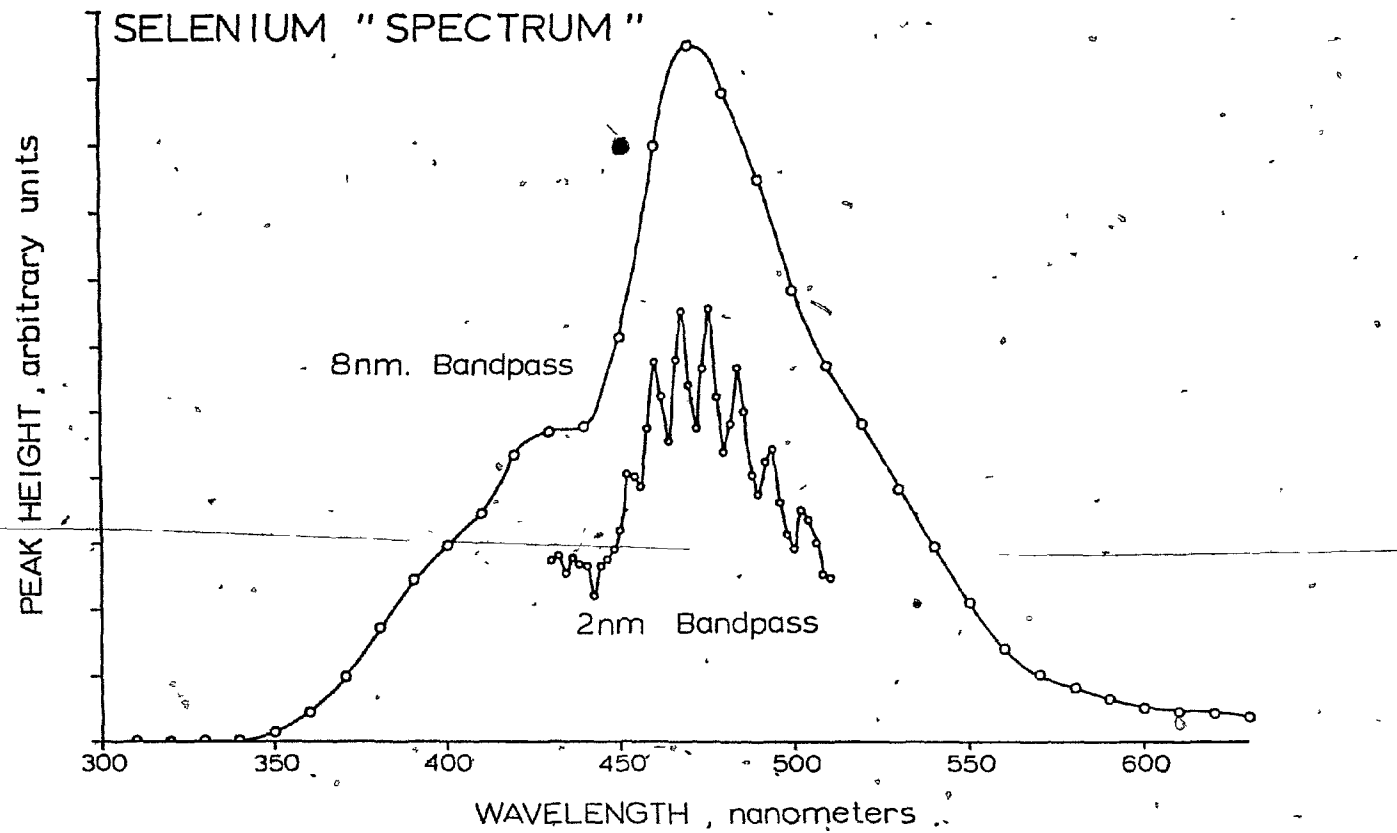
4.2.1 Spectral Characteristics

The FPD spectrum of selenium was determined as outlined in the experimental section, using chromatographic peak height measurements, uncorrected for the PM tube response profile. A "rough" spectrum of 8 nanometer bandpass was run from 300 to 630 nm. The region of greatest intensity, from 430 to 510 nm, was examined under a higher resolution of 2 nm bandpass. Both spectra are seen in Figure 28. Like the sulfur spectrum, the selenium spectrum is broad, the main emission lying in the region from 350 nm to 600 nm. The "high resolution" spectrum shows

Figure 28

Selenium "Spectrum" - 300 nm to 630 nm

Peak heights for piasselenole at different wavelengths,
using two sets of slits. The ordinate values are
different for the 8 nm and 2 nm tracings.



several distinct bands. They correspond to some of the bands noted by Salet (237) for selenium burning in air, by Emeléus and Riley (238) for a flame of alcohol burning in selenium dioxide vapour, and, presumably, by Mitscherlich, for selenium in a hydrogen diffusion flame (253). Emeléus and Riley thought, with some hesitation, that these bands were due to Se_2 . The approximately quadratic response of selenium in the FFD strongly supports their contention. The parallel behaviour of sulfur, i.e. quadratic response, is generally believed to be due to the recombination of two sulfur atoms (in the presence of a third body) to form excited diatomic sulfur. It is not at all far-fetched to assume that selenium could engage in an analogous mechanism of emission. The best sensitivity for selenium is found in filterless mode because of its very broad spectrum. The use of a 484 nm interference filter (one that was available, but does not necessarily represent the best choice of wavelength) caused an increase in selectivity (versus sulfur, phosphorous, etc.) but decreased sensitivity by a factor of three. A broad interference or band-pass filter, maximum around 475 nm, would likely be the best compromise between desired levels of sensitivity and selectivity. It is interesting to note that Gilbert pointed out the likely analytical utility of selenium band emission in the hydrogen-air flame in his excellent review on the subject (239).

4.2.2 Flow-Rate Optimization

The optimum flow rates for selenium sensitivity were determined as usual by varying the hydrogen and air flow rates and monitoring the change in signal-to-noise ratio of a selenium standard. For all practical purposes, selenium parallels sulfur in its behaviour towards flow rate changes. The optimum flow rates are 25 ml/min air and 40 ml/min hydrogen under normal conditions. Selenium was also determined in a constricted flame enclosure of the type shown in Figure 4. The optimum flow rates were somewhat different, about 20 ml/min of air and 35 ml/min of hydrogen.

4.2.3 Detector Performance

The best sensitivity, as already mentioned, is obtained by taking advantage of selenium's broad emission in a filterless mode. However, the sensitivity for the analogous sulfur compounds is much greater under the same conditions. Obviously, sulfur is the most serious interferent for selenium due to its high sensitivity and its similar behaviour, i.e. quadratic response. Furthermore, selenium compounds in biological or environmental samples are likely to be accompanied by similar sulfur compounds. Selectivity versus sulfur can be gained optically using a 484 nm interference filter, and geometrically using a constricted flame enclosure. The overall sensitivity decreases by a factor of about ten and still sulfur is a

more sensitive element. This can be seen in Figure 29, which shows calibration curves for piasselenole, t-butylsulfide, pentadecane and phenanthrene. The analytically useful range for selenium compounds is about two orders of magnitude under these conditions. The selectivity versus hydrocarbons, which give negative peaks, ranges from better than 1 to about 3 orders of magnitude, depending on concentration.

Figure 30 shows temperature-programmed chromatography of four selenium compounds at 1 and 10 nanogram levels in filterless mode with a normal flame enclosure. The peak for diethylselenide is partially quenched by solvent tailing and appears only as a trace at the 1 nanogram level. These data show that the detection of sub-nanogram amounts of common selenium compounds is definitely possible.

4.2.4 Hydrocarbon Interference: Methane Doping

Since sulfur response is well known to decrease when carbon compounds are present, an investigation into possibly similar effects on selenium was thought to be necessary. The matter of carbon-doping seemed of enough general interest to test other compounds along with organoseleniums, i.e. those containing sulfur, phosphorous and carbon. Methane was added to the FPD under conditions found best for selenium response, with no filter and a regular flame enclosure. The results are shown in Figure 31.

Figure 29

Calibration Curves for Piazselenole and Possible Interfering Species Using a 484 nm Interference Filter and a Constricted Quartz Flame Enclosure

Flow rates in ml/min, AIR = 20, H₂ = 40, N₂ = 30.
100 x 0.27 cm ID borosilicate column packed with 5% OV-101 on Chromosorb W, 45/60 mesh. Compounds chromatographed isothermally: Piazselenole 110°, (t-butyl)₂ S₂ 90°, pentadecane 140° and phenanthrene 165°C. Phenanthrene "positive response" is due to a sulfur containing impurity.

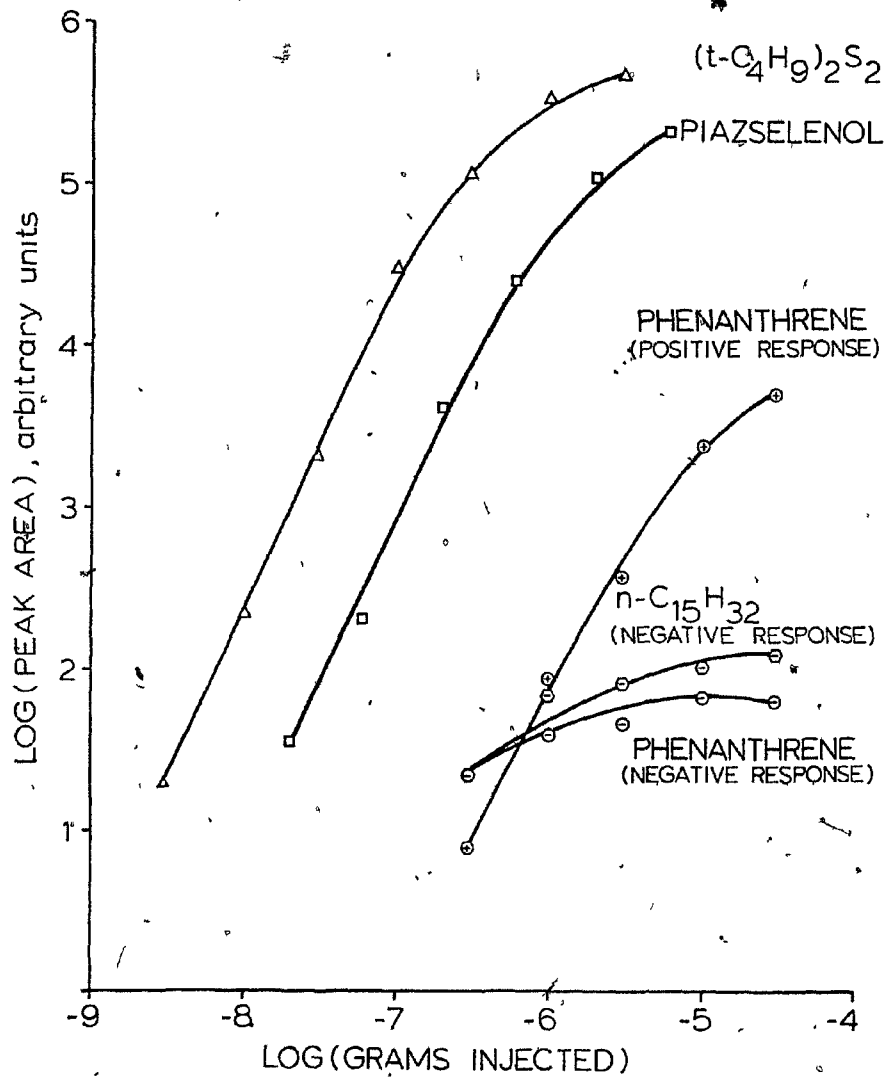


Figure 30

Temperature-Programmed Chromatography of Four Selenium Compounds at 1 and 10 ng Levels

Normal detector configuration, filterless mode. Flow rates in ml/min, AIR = 25, H₂ = 40, N₂ = 30. 150 x 0.3 cm ID borosilicate column packed with 5% PEGA on Chromosorb W, 100 120 mesh.

IMP = Impurity

The peak for diethylselenide is partially quenched by solvent tailing and appears only as a trace at the 1 ng level.

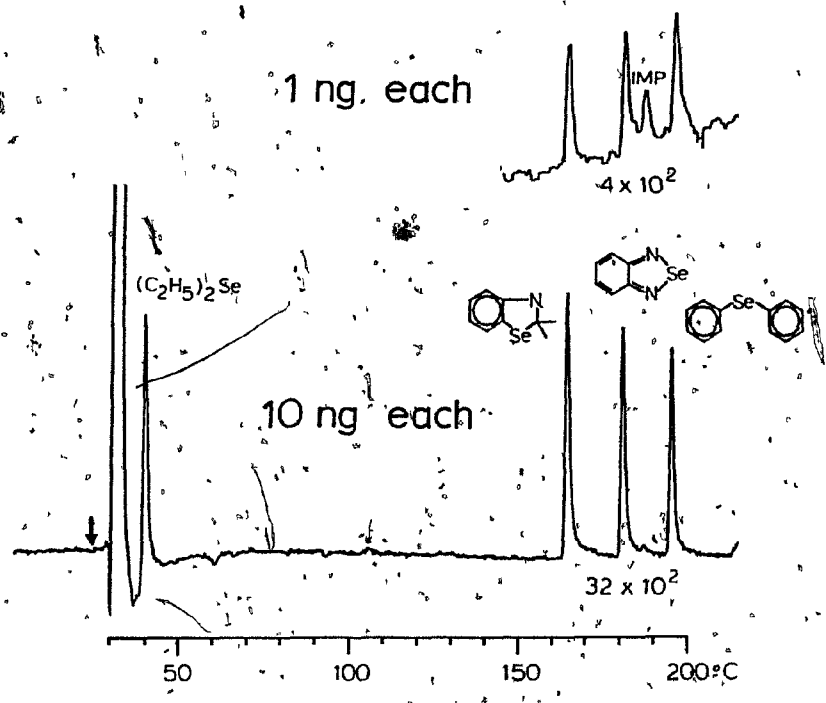


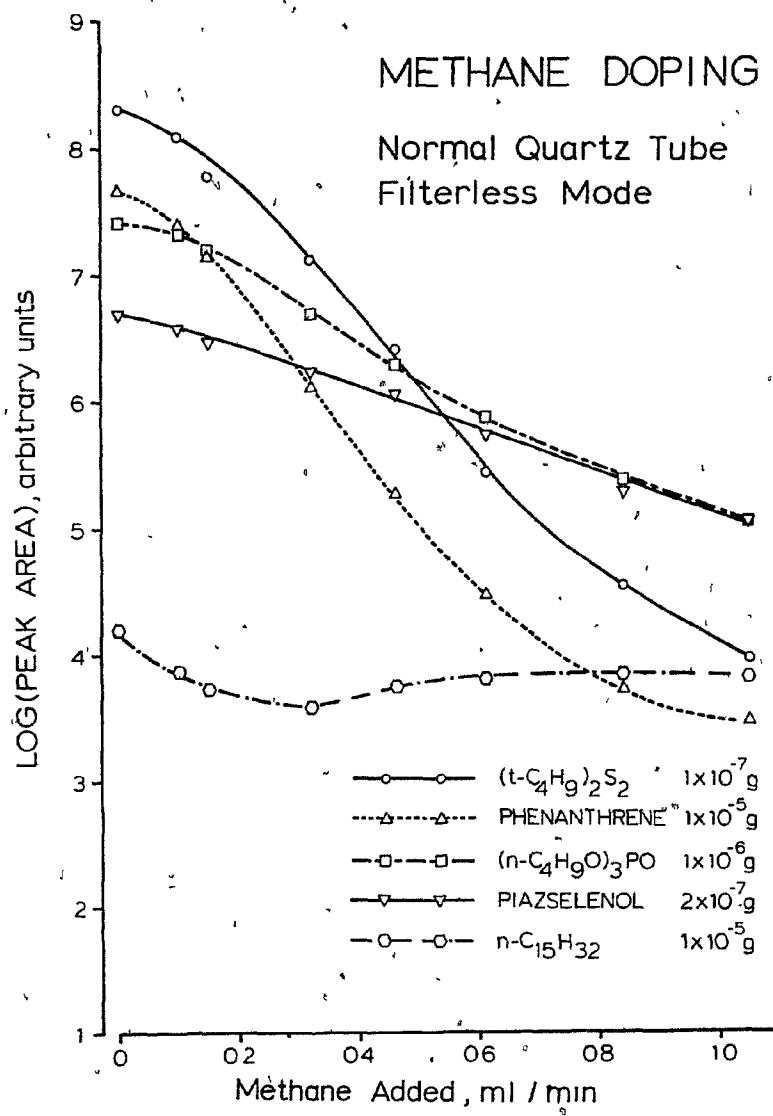
Figure 31

Response of Selected Compounds Versus Amount of Methane
Added to the Carrier Gas

Normal flame enclosure, filterless mode. Compounds
and injected amounts as indicated. $(n-C_4H_9O)_3 PO$,
isothermal: 165°C. Flow rates in ml/min, AIR = 25,
 $H_2 = 40$, $N_2 = 30$. Other conditions as indicated in
Figure 28. Phenanthrene response is due to a sulfur
containing impurity.

METHANE DOPING

Normal Quartz Tube
Filterless Mode



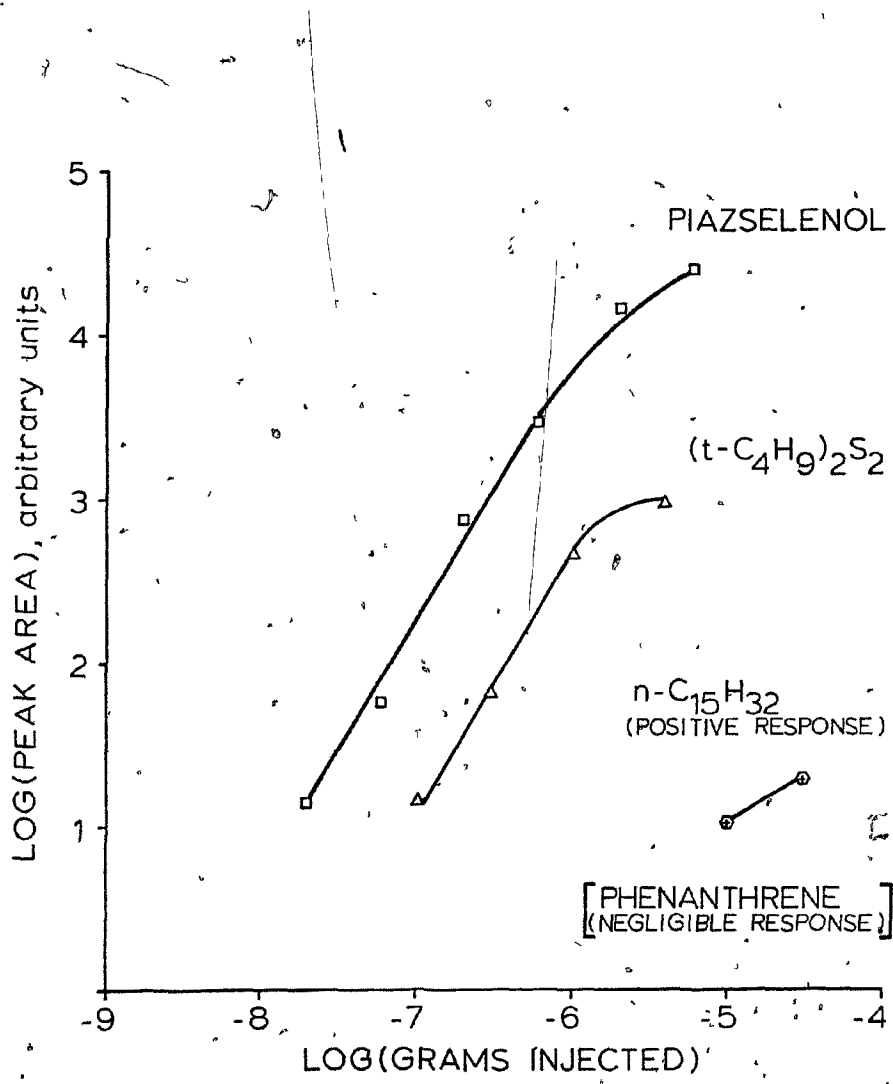
All hetero-organics decrease in response but to very different degrees. *t*-Butyldisulfide showed the strongest drop, over some four orders of magnitude. The phosphorous and selenium compounds drop much less, leading to increased selectivity (and decreased sensitivity) for them as the methane flow is increased. Equal amounts of methane produce stronger effects in a normal flame enclosure than in a constricted one, but the overall trends are the same. It should also be noted that the response of pentadecane and similar compounds is very small and subject to great variation with the history and operating conditions of the FPD.

It can be easily recognized that methane doping can be used to increase greatly the selectivity of selenium and phosphorous compounds against sulfur compounds, without a large drop in sensitivity. Figure 32 shows calibration curves for *t*-butyldisulfide, piaszelenole and pentadecane under conditions of high selectivity versus sulfur, optically using a 484 nm interference filter, geometrically using a constricted flame enclosure, and chemically using methane doping. By comparison with Figure 4, one can see a complete reversal in position of the sulfur and selenium calibration curves due to methane doping. A very small positive response for pentadecane was noted, indicating that carbon doping can also influence the selectivity of selenium versus carbon compounds.



Figure 32

Calibration Curves for Piazselenole and Possible Interfering Species Using a 484 nm Interference Filter, a Constricted Quartz Flame Enclosure and Methane Doping Conditions as indicated in Figure 29 except 1 ml/min of methane added to the carrier gas. Phenanthrene response interfered with by a sulfur containing impurity. *



5. The Interchalcogen Effect: S-Se-Te

5.1 Discovering the Interchalcogen Effect

The interchalcogen effect is essentially the ability of a supplementary background of any of the chalcogens, sulfur, selenium or tellurium, to enhance the response of any compound containing one of them. This background emission has also the ability to increase the response of any compound which quenches it, e.g. hydrocarbons give larger negative peaks.

The initial doping experiment involved selenium, not sulfur. Its purpose was to enhance the response of selenium compounds in preference to sulfur compounds to gain selectivity. In a fashion similar to sulfur doping, the second order reaction rate of the selenium emission was to be taken advantage of. It involved bubbling the FPD's hydrogen supply through diphenylselenide, the only liquid selenium compound available at that time. As was expected, diphenylselenide showed an increase in response with the doping. A sulfur compound was also tested and, surprisingly, showed a similar increase in response. Since selenium thus increases sulfur response, it seemed reasonable to assume that the reverse would also hold true. A few microliters of CS_2 were added to a one-liter stainless steel tank which was then filled with compressed nitrogen. The mixture was added to the detector as indicated in the experimental section. This proved to be a more convenient method of doping, besides being less haz-

ardous and obnoxious than the corresponding selenium doping. Preliminary investigations showed that both selenium and sulfur calibration curves could be linearized without a major loss in sensitivity. Equilibration of the FPD for a particular doping level was a rather lengthy process, however, and so a different method was attempted. About 2.5 milliliters of CS_2 was added to a large nitrogen cylinder (1.5 ft.³) that was then pressurized with nitrogen to 500 psi. This doping tank provided somewhat better performance and was placed in the hydrogen or air line as shown in Figure 7. In order to obtain adequate gas mixing, the cylinder was rolled manually for one hour. It was kept in a horizontal position with an infrared heat lamp trained on a narrow spot on its centre to keep the gas circulating inside. CS_2 doping in this set-up was used to determine that the interchalcogen effect also applied to tellurium as well as selenium. At this point, a careful quantitative investigation of the interchalcogen effect was undertaken.

5.2 Characteristics of CS_2 (Sulfur) Doping

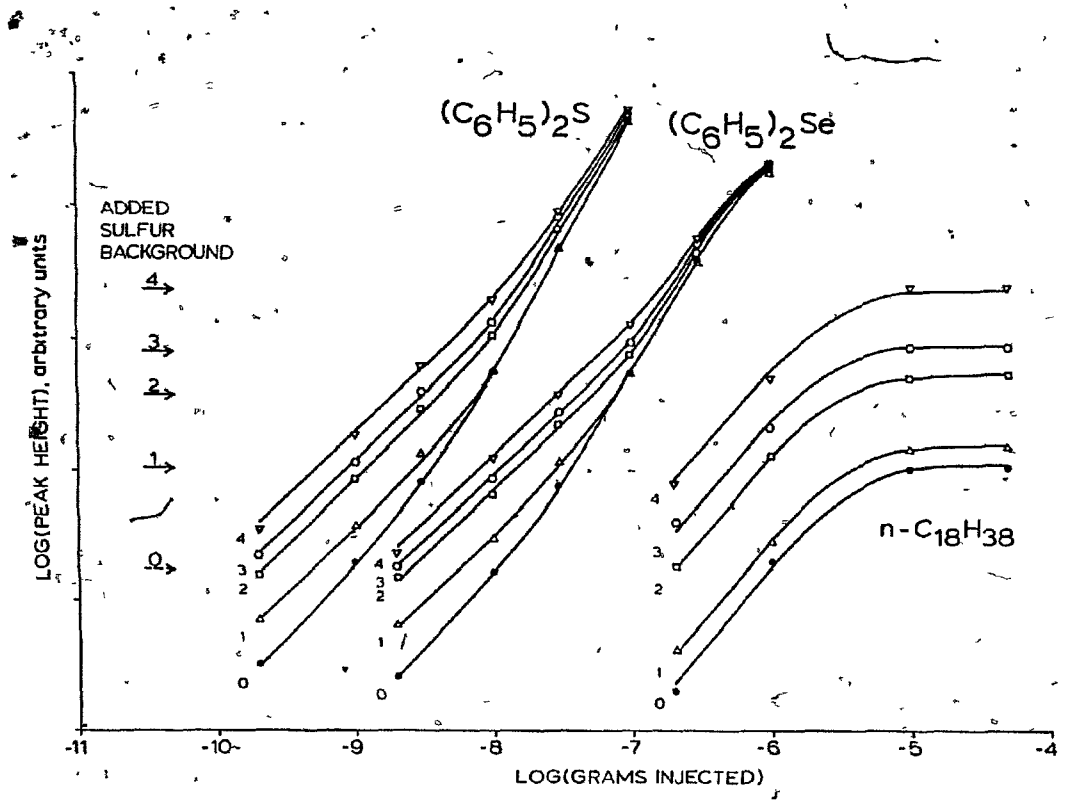
A detailed investigation of sulfur doping on sulfur, selenium, tellurium and carbon-containing compounds was undertaken. Calibration curves for all compounds were run first with no deliberately added sulfur. Then increasing amounts of sulfur were added to the FPD and calibration curves were run for each doping level. Figure 33 shows

Figure 33

The Effect of Different CS₂ Doping Levels on the Calibration Curves of Diphenylsulfide, Diphenylselenide and Octadecane

These compounds were chromatographed as part of a mixture containing triethylphosphate and phenanthrene and temperature programmed, 100/7/220°C. Flow rates in ml/min, Ar = 30, H₂ = 40, N₂ = 40. 150 x 0.3 cm ID.

borosilicate column packed with 5% PEGA on Chromosorb W, 100/120 mesh. Octadecane peaks are inverted. Detector operated in filterless mode.



calibration graphs for diphenylsulfide, diphenylselenide and octadecane on different sulfur backgrounds. The calibration curves for selenium and sulfur are very similar. When there is no deliberately added sulfur, both calibration curves show a great deal of deviation from quadratic response at low amounts injected, indicating a lot of sulfur already in the detector background. (The FPD air supply is laboratory air compressed to ca. 40 psi and apparently contains ca. $3-4$ ppb sulfur compounds.) The response increases with the amount of sulfur added, especially for low injected amounts. It is difficult not to notice the increased linearity of response as the sulfur in the background increases.

Octadecane, on the other hand, quenches the sulfur background, giving inverted peaks. The response increases linearly with the sulfur background; hence, the selectivity of selenium and sulfur compounds versus hydrocarbons deteriorates under sulfur doping at high levels (since Se and S response increase linearly with the square root of the sulfur background). The "0" level of added sulfur background corresponds to the amount of sulfur calculated to be in the non-doped detector background, as a direct application of the mathematical treatment of sulfur doping (as discussed in section 5.4.1).

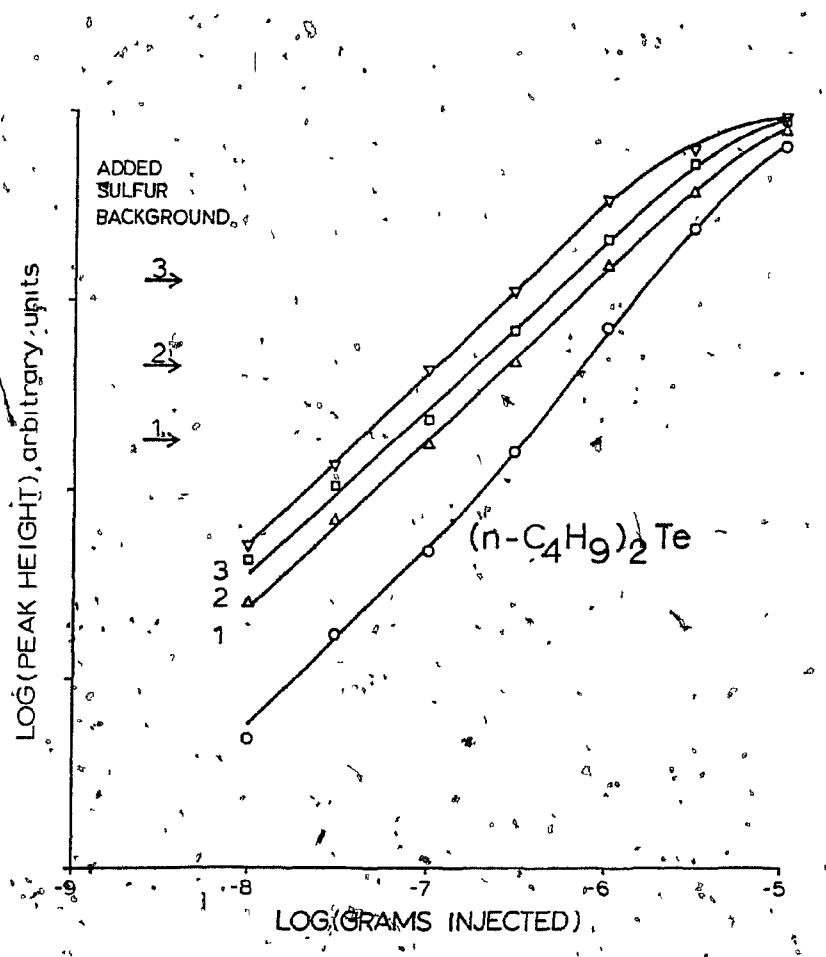
The study of the standard compound dibutyltellurium, which was marred by the need to prepare freshly diluted solutions prior to injection, is shown in Figure 34. Des-

Figure 34

The Effect of Different CS₂ doping Levels on the
Calibration Curve of Dibutyltellurium

Dibutyltellurium temperature programmed, 60/7/120°C.

Other conditions as indicated in Figure 33.



pite the greater variation in the data, it is clear that tellurium behaves similarly to selenium and sulfur in the increase and linearization of its response with increasing sulfur background levels. In fact, linearization appears to be achieved more easily than with the other two chalcogens. The non sulfur-doped calibration curve appears to be quadratic only in the upper part. It is not clear whether this is due to a different emitting species, e.g. TeO, or to the sulfur present in the background.

A closer examination of linearity under high sulfur-doping conditions is shown in Figure 35. Calibration curves for diphenylsulfide and diphenylselenide are given using 394 nm and 484 nm interference filters, respectively. For each, the linearity exceeds two orders of magnitude, good enough for most analytical work.

This means for practical application that a single chromatographic run (including an internal standard) would suffice to produce the desired analytical result. The internal standard method is the most convenient approach to correct for shifting sulfur background and detector sensitivity levels, provided that the sulfur background is high enough to keep all peaks within the linear range.

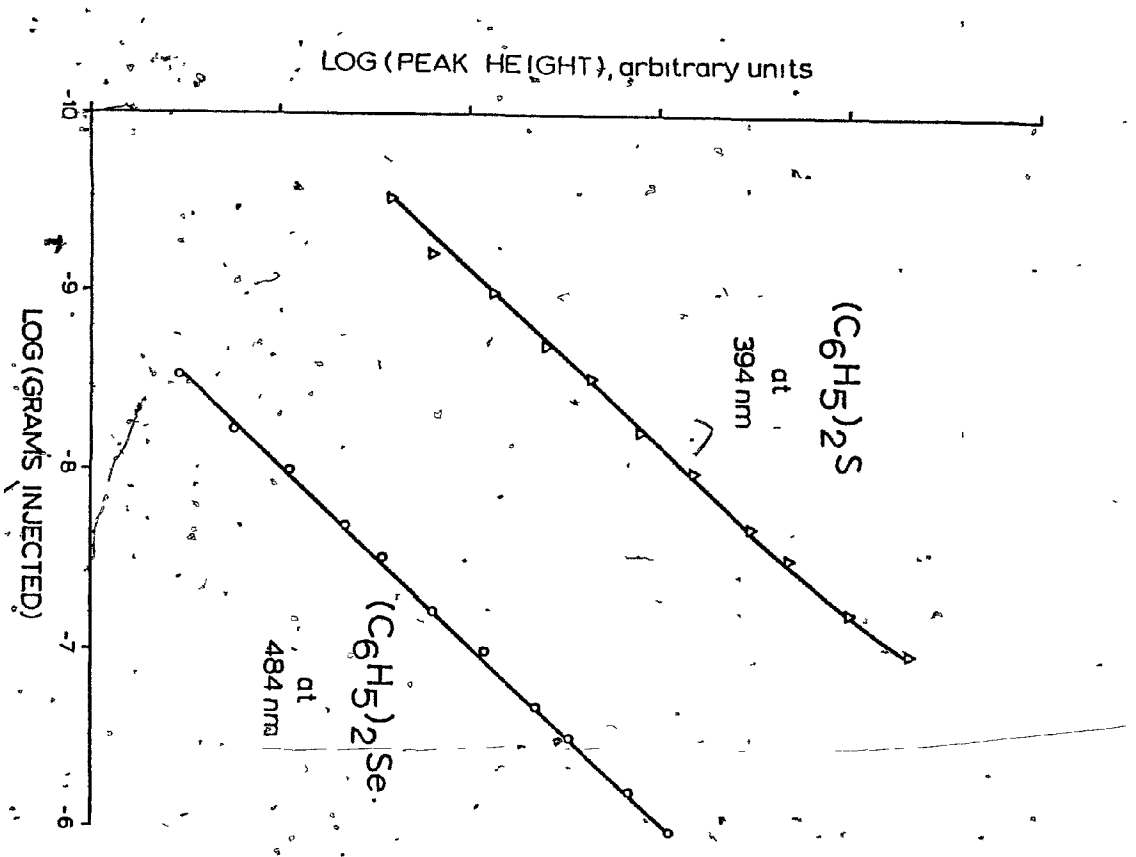
This was demonstrated by using three solutions containing 10 ng/ μ l of standard and 1, 10 and 100 ng/ μ l of analyte. These were injected repeatedly over the course of several weeks with different (but always relatively high) levels of sulfur. The amount of the "analyte" present in

Figure 35

**Linearization of Sulfur and Selenium Response Via CS₂
Doping**

Calibration curves run on a large sulfur background.

Interference filters as indicated. Diphenylsulfide
and diphenylselenide temperature programmed with phenan-
thene, 140/7/230°C. Other conditions as indicated in
Figure 33.



each solution was calculated using the equation:

$$W_A = \frac{R_A}{R_S} \cdot \frac{W_S}{RWR} \quad (1)$$

where W_A and W_S are the weights and R_A and R_S , the responses (peak heights) of the analyte and internal standard, respectively. RWR is the relative weight response, predetermined at the 10 ng level. Two typical runs are shown in Table 4.

TABLE 4

Typical Linear Calculations of Analyte Content By
the Internal Standard Technique

Internal Standard ¹ (ng) Added	Analyte ² (ng) Added	Analyte Found (ng)	
		1	2
10.0	1.00	0.94	1.05
10.0	10.0	9.8	10.2
10.0	100	102	100

1 - Internal standard: diphenylsulfide

2 - Analyte: t-butyl disulfide

The data confirms the usefulness of the internal standard technique in conjunction with sulfur doping for analysis of sulfur-containing compounds. The sulfur response is effectively linear in the 1 - 100 ng range.

In this context, a few things should be kept in mind. The sulfur background should be large enough (about double the size of the largest peak for less than a 10% deviation

from the true value) to ensure linearity; however, care must be taken not to reach a concentration range where saturation of the system begins to occur. The light level of the FPD is high under the circumstances, and it may be necessary to employ some means of reducing the light level to prevent damage to the photomultiplier tubes and to keep within readout capabilities. This may be accomplished by using filters with low transmission capability, an additional neutral density filter or masks to physically block out light from the emission zone. These tactics decrease sensitivity and may increase selectivity. For instance, the decrease in sensitivity found using a mask of the type shown in Figure 6 was not large; the drop in signal-to-noise ratio didn't exceed a factor of three.

As sulfur is added to the detector, the detection limit for injected sulfur compounds improves at first (up to a factor of about 8), reaches a maximum, and then depreciates as more and more sulfur enters the detector as background. Because the detector noise increases with total light emitted (i.e. background emission), it will linearly increase with the background emission produced by the quadratic response of added sulfur as dopant, i.e. it will show a quadratic dependence on background sulfur. The increase in analyte sulfur response, on the other hand, is a linear function of the amount of background sulfur. Hence the observed behaviour of the sulfur detec-

tion limit with increasing amounts of doped sulfur, comes as no surprise. In a high background system designed for maximum linear range, the poorer detection limit (versus non-doped conditions) is offset by the benefit of a long linear range.

Sulfur detection by FPD is not normally hampered by sensitivity; rather, the non-linearity of response has up to now given rise to great inaccuracies and prevented wider use of the FPD. A discussion of previous attempts to cope with sulfur's quadratic response is given in section 1.5.2(c). These methods, notably electronic linearization, have proved to be less than satisfactory (102). Chemical linearization through sulfur doping has been achieved with a clearly tolerable loss in sensitivity. The extent of linear range possible is shown in Figure 35 and the excellent reliability is reflected in the results of the standard addition experiment given in Table 3.

The study was, of course, designed to demonstrate a reasonable linear range (two decades) up to high concentrations; this may be excessive for practical samples, the chalcogen concentrations of which may be close to the minimum detectable limit, and for which, therefore, a lower sulfur background would result in better analytical data.

5.3 Development of Mathematical Models for Sulfur and Selenium Response under Sulfur Doping Conditions.

5.3.1 Sulfur

A mathematical model was developed to facilitate the calculation of the extent of linearization brought about by a particular level of sulfur doping. To do this, the response R_S (peak height at constant chromatographic conditions) of a sulfur analyte A is assumed to be a purely quadratic function of S_A , the amount of sulfur injected, i.e.

$$R_S = (k_S S_A)^2 \quad (2)$$

k_S being a constant characteristic of sulfur and the particular chromatographic system.

If a background B (measured in the same units as the peak height of the analyte) is produced by continuously adding the appropriate amount of sulfur, S_B , then

$$B = (k_S S_B)^2 \quad (3)$$

(Here it is assumed that the response is independent of structural differences between the sulfur-containing compounds, or that the analyte and the substance responsible for the background are identical. It is also assumed that S_2 is the only emitting sulfur species, that interference from carbon, selenium, tellurium, etc., is absent, and that possibly different methods of introduction for S_A and S_B are of no major consequence when background and analyte sulfur combine in the FPD.)

The total sulfur response R (analyte response, R_S , plus background, B) can be expressed by a simple binomial

$$\sqrt{R} = \sqrt{R_S} + \sqrt{B} \quad (4)$$

$$R = (k_S S_A + k_S S_B)^2 \quad (5)$$

$$R = k_S^2 S_A^2 + k_S^2 S_B^2 + 2k_S^2 S_A S_B$$

and, as $k_S S_B^2 = B$, we have

$$R_S = k_S^2 S_A^2 + 2k_S^2 S_A S_B \quad (6)$$

Thus, the analyte response becomes the sum of two terms, one quadratic and the other linear; representing, respectively, the peak height of the analyte without the sulfur background, and the additional increment in peak height brought about by the sulfur background. When a sulfur background is present, analyte peaks are increased by a factor $f = 1 + 2 S_B/S_A$. Furthermore, it is possible to calculate the sulfur background necessary to achieve linearity of response up to a certain limit.

If we define $X =$ deviation from linearity

$$\text{as } X = \frac{\text{quadratic response}}{\text{linear response}} \quad (7)$$

$$\text{then } X = \frac{k_S^2 S_A^2}{2k_S^2 S_A S_B} \quad (8)$$

$$S_A = 2S_B X \quad (9)$$

$$\frac{R_S}{B} = \frac{k_S^2 S_A^2 + 2k_S^2 S_A S_B}{k_S^2 S_B^2} \quad (10)$$

and substituting equation (9).

$$\frac{R_S}{B} = 4 X(X + 1) \quad (11)$$

e.g. for $X = 0.1$, $\frac{R_S}{B} = 0.44$

for $X = 0.025$, $\frac{R_S}{B} = 0.10$

Using equation 11, a simple calculation shows that in order to stay within a 10% deviation from linearity, the analyte peak must not be larger than about half (44%) of the sulfur-induced background. If the peak measures only 10% of the background, the deviation from linearity will be less than 2.5%, i.e. insignificant for any practical purposes. Similar considerations could be applied to selenium or tellurium analytes on selenium or tellurium backgrounds.

The constant k_S can be determined in several ways. Firstly, it is possible to select a clearly quadratic region of the calibration graph (S_A large, $S_B(\text{added}) = 0$) and to calculate k_S according to

$$R_S = k_S^2 S_A^2$$

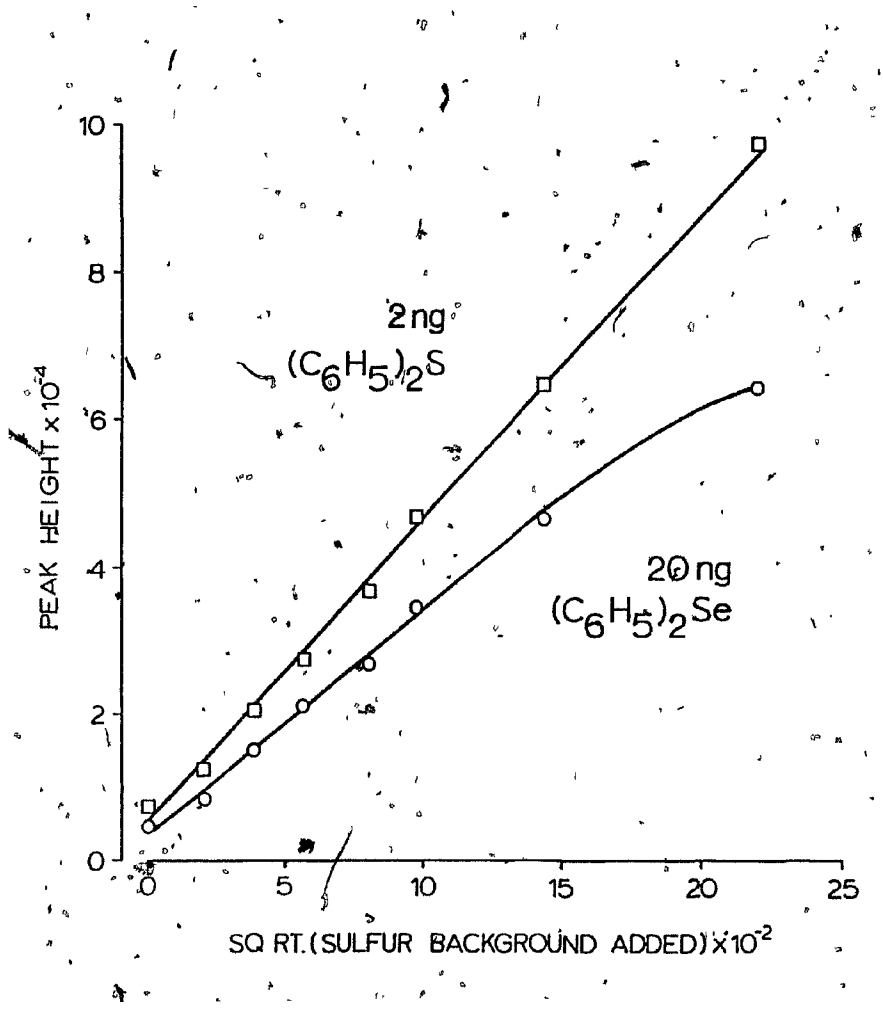
Secondly, the responses from a constant amount of analyte on different amounts of background sulfur can be measured. Figure 36 shows such measurements in a plot of R versus \sqrt{B} for sulfur and selenium analytes. Because

$$\sqrt{B} = k_S S_B \quad (12)$$

Figure 36

Effect of Sulfur Background on the Response of 2 ng of Diphenylsulfide and 20 ng of Diphenylselenide

Responses and background in cm at sensitivity (1 cm = 4×10^{-14} A). Both compounds chromatographed isothermally at 135°C. Conditions as indicated in Figure 33 except 50 x 0.3 cm ID borosilicate column packed with 3% OV-101 on Chromosorb W, deactivated with Carbowax 20M, 45/60 mesh.



a linear relationship is obtained for the sulfur analyte:

$$R_S = k_S S_A^2 + 2k_S S_A \sqrt{B} \quad (13)$$

and k_S can be determined from the slope $2k_S S_A$. The values found for k_S by the two methods, as expected, were practically identical.

The amount of sulfur in the background, S_B , could then be calculated using

$$S_B = k_S / \sqrt{B} \quad (14)$$

Having determined k_S and S_B values, calibration graphs were calculated for the sulfur analyte on the various sulfur backgrounds used. These curves are shown on the left-hand side of Figure 37 together with the experimentally determined data points (the "zero" curve is experimental only). The pattern is obviously well-reproduced by the calculation. To view the satisfactory degree of correlation between experimental and calculated data as proof of the correctness of the approach taken would involve a circular argument; however, the procedure appears to be reasonable.

5.3.2 Selenium

The development of a mathematical model to represent selenium response on a sulfur background became more difficult. After due consideration, it was thought best to attempt the simplest possible treatment of what was expected to be a rather complex reaction system. The shape of

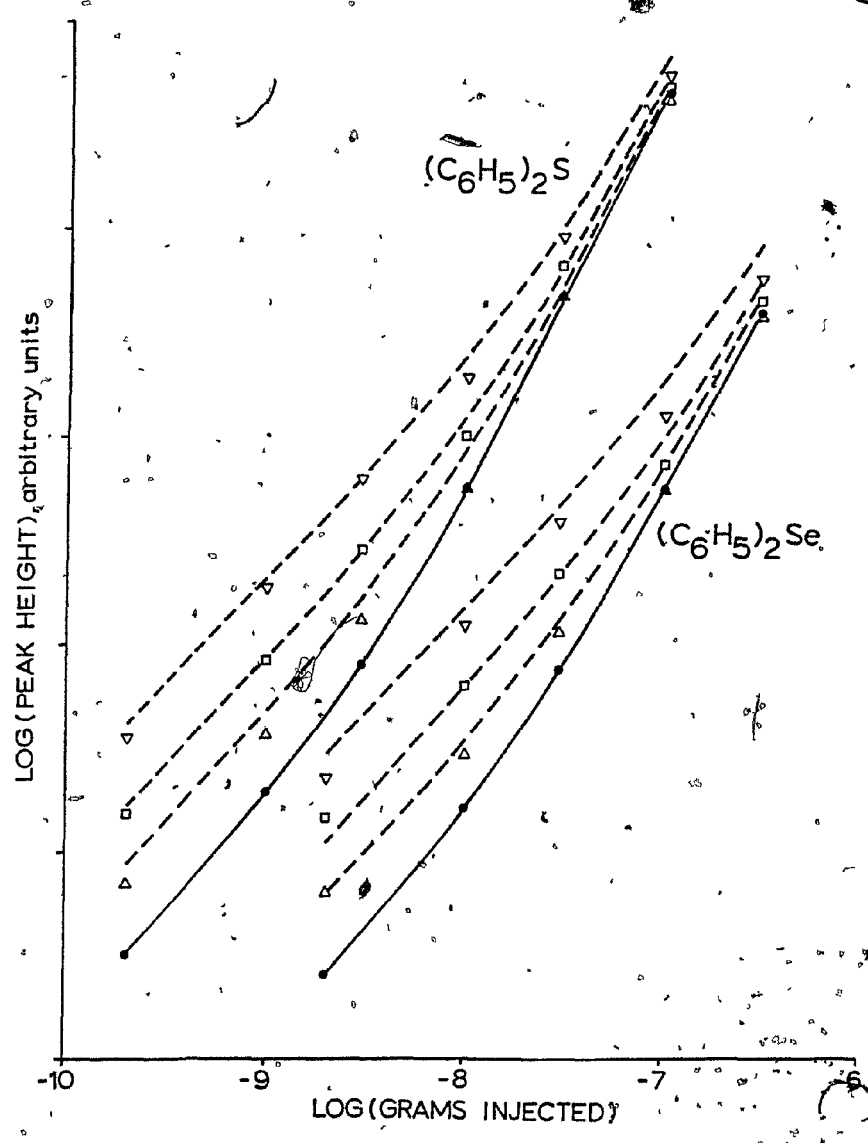
Figure 37

Comparison of Calculated and Experimental Calibration Curves for Diphenylsulfide and Diphenylselenide under Sulfur Doping

----Calculated Responses; see text for method.

____Experimental Curves, non-sulfur doped, as in Figure

33.



the calibration curves of selenium on sulfur was similar to that of sulfur on sulfur, suggesting a similar mathematical treatment. In a purely formal analogy, a binomial expression could be written,

$$\sqrt{R} = \sqrt{R_{Se}} + \sqrt{B} \quad (15)$$

$$R = (k_{Se} Se_A + k_S S_B)^2 \quad (16)$$

where R is the total response (selenium peak height, R_{Se} , plus sulfur background, B), k_{Se} is a constant typical of selenium and Se_A is the amount of analyte selenium injected.

By analogy with the mathematical treatment for sulfur on sulfur, we have on expansion of equation 16

$$R = k_{Se}^2 Se_A^2 + 2k_{Se} k_S Se_A S_B + k_S^2 S_B^2$$

and as $B = k_S^2 S_B^2$, we obtain

$$R_{Se} = k_{Se}^2 Se_A^2 + 2k_{Se} k_S Se_A S_B \quad (17)$$

i.e. the sum of a linear and a quadratic term, if the sulfur background is held constant. When a sulfur background is present, analyte peaks are increased by a factor $f = 1 + k_S S_B / Se_A$, where $k^1 = k_S / k_{Se}$.

The constant k_{Se} was determined from the quadratic portion of the calibration curve (Se_A large, S_B (added) = 0). This value was used, together with the previously calculated values for k_S and S_B (for each sulfur background level

used) to produce the desired calibration curves. When these calculated curves were compared with the actual experimental data, they were found to have the same general shape though with a significant, consistent bias. Such a bias came as no surprise; it is related to the physical meaning of the linear term $2k_S k_{Se} S_B S_{SeA}$, the analogue of $2k_S^2 S_B S_A$ in the pure sulfur system. Here as there, it represents the additional response generated by the sulfur background. While it was based on S_2 emission in the sulfur-sulfur system, its equivalent in the selenium-sulfur system had not been established. If the emitting species were assumed to be SeS^* , then it would have been surprising if the product of the constant for S_2 and Se_2 emission, $k_S k_{Se}$ were to equal a similar expression for SeS . In other words, k_{Se} in the quadratic term and k_{Se} in the linear term would not be identical, the former relating to Se_2 , the latter to SeS emission. Expressing the constants, therefore as k_{Se} and k'_{Se} , respectively, the formal approach was rewritten as

$$R = k_{Se}^2 S_{SeA} + 2k'_{Se} k_S S_{SeA} S_B \quad (18)$$

where the term $k'_{Se} k_S$ was considered to be characteristic of the kinetic and spectral properties of the assumed interchalcogen molecule SeS or of whatever process happened to linearize the analyte response.

The constant for the linear term, k'_{Se} , was determined experimentally by injecting a constant amount of a selenium compound on a varying sulfur background. Akin to the sulfur-sulfur system, equation 18 can be rewritten as

$$R_{Se} = k_{Se} Se_A^2 + 2k'_{Se} Se_A \sqrt{B} \quad (19)$$

A plot of R_{Se} versus \sqrt{B} , shown in Figure 36, gave a linear graph (deviating from linearity only a very high sulfur backgrounds) and the constant k'_{Se} was determined from the slope, $2k'_{Se} Se_A$. The value found was only a third (28%) smaller than that for k_{Se} , reflecting the similarity of the three assumed emitters, S_2 , Se_2 and SeS . Calibration graphs for a selenium analyte determined on different sulfur backgrounds were recalculated using equation 18 and compared to the experimentally determined curves. This is shown on the right hand side of Figure 37. This time the correlation between calculated and experimental data was found to be nearly as good as for the pure sulfur system.

The reasonably good correlation of the calculated and experimental data for the selenium-on-sulfur system lent a sense of self-consistency to the formal approach taken. As mentioned before, the actual situation must surely be more complex than that which is suggested by the simple equations. The response, as the photomultiplier tube sees it in a filterless mode, is due to at least two, probably three, and perhaps from even more, band systems.

The obvious ones are S_2 and Se_2 , the possible one SeS , and some contributions from oxide, hydride or carbide species are always a possibility.

5.4 Search for the Interchalcogens (SeS , TeS , $SeTe$)

5.4.1 What is the Cause of the "Interchalcogen Effect"?

The fact that there is an interchalcogen effect, where a background containing one of the chalcogens, sulfur, selenium or tellurium, enhances the emission of any compound containing one of these aforementioned elements, is almost a certainty (the combinations, Te , S or Se on Te , and Te on Se have not been attempted). The reason that such an effect takes place can most likely be traced to one of two possible sources. The first is the formation of interchalcogen compounds such as SeS , and the second is that the doping element changes the chemical environment of the emission zone in such a way that it leads to increased emission from the analyte element.

If a species such as SeS were formed, the S_2 bands from a sulfur background should decrease and less Se_2 (than in an undoped system) should be emitted. The SeS emission would then have made up for these losses and provided the additional increase in response. A further complicating effect which could be important for high amounts of injected compound is the depression of both S_2 and Se_2 species by carbon (although some C_2 emission may also be

present). As both dopant and analyte contain carbon, this effect must be operative. However, it was not accounted for in the mathematical model, since it was considered to be of minor importance.

It is interesting to consider what happens when a selenium analyte emerges from the column and then burns in a flame that also produces a constant sulfur background emission. Such a peak is schematically shown in Figure 38 (the drawing is speculative and not based on actual measurements). As the peak passes, the background S_2 bands decrease (due to reaction to form SeS and carbon quenching) and Se_2 and the assumed SeS bands appear. The latter two vary in their relative magnitude during the rise and fall of the peak, reflecting the respective quadratic and linear contributions. The "spectral" composition of a "peak" is therefore not constant with time as can be clearly recognized by considering the question of which wavelength it is best to select for an interference filter under these circumstances for "selenium" response. (Obviously there is no clear answer; the "best" wavelength would depend on the relative concentration of Se analyte and S background).

5.4.2 Search for Spectral Evidence

If the increased response is due to SeS emission for selenium compounds on a sulfur background,

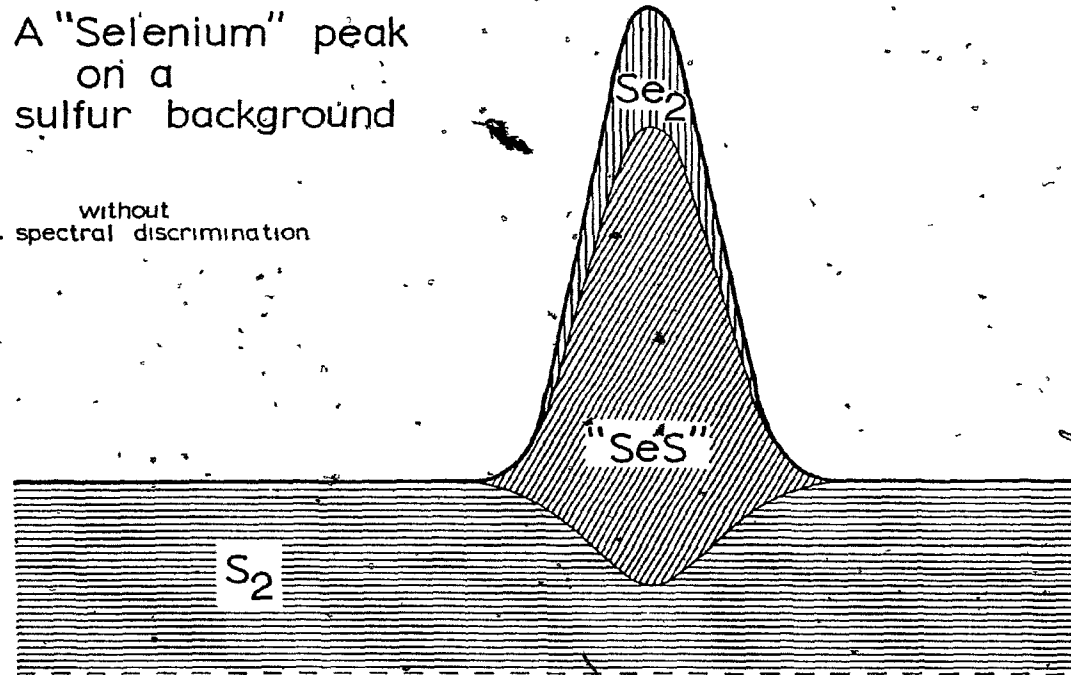
145

Figure 38

Representation of a Selenium Peak on a Sulfur Background

A "Selenium" peak
on a
sulfur background

without
spectral discrimination



then there should be spectroscopic evidence of new bands appearing in the spectral output of the detector. However, a number of complicating factors enter the picture, namely, the likely emission of the Se_2 spectrum, the background being made up of bands from the S_2 spectrum, and the effect of carbon quenching of the background S_2 bands. Furthermore, the amount of injected compound necessary to obtain a spectrum is large. This means a large sulfur background is needed to produce a sizeable portion of SeS emission and hence the increased likelihood of obscured bands because of carbon quenching. The spectrum would have to be obtained using a resolution at least high enough to resolve the individual bands for identification purposes. High resolution means a significantly lower light throughput of the monochromator, hence, more compound must be injected to compensate.

The electronic spectra of all three interchalcogen compounds, SeS , TeS and TeSe have been reported in the literature (241-245). Although the ultraviolet spectra of TeS and TeSe have been studied in 1961 by Mohan and Majumdar (241) and in 1967 by Joshi and Sharma (242), respectively, the visible spectra of the interchalcogens have been studied only recently. This was probably due to the interference from the homonuclear diatomic species, Se_2 , Te_2 and S_2 which emit (or absorb) throughout the visible region. Another problem is one of isotopes: selenium has two major

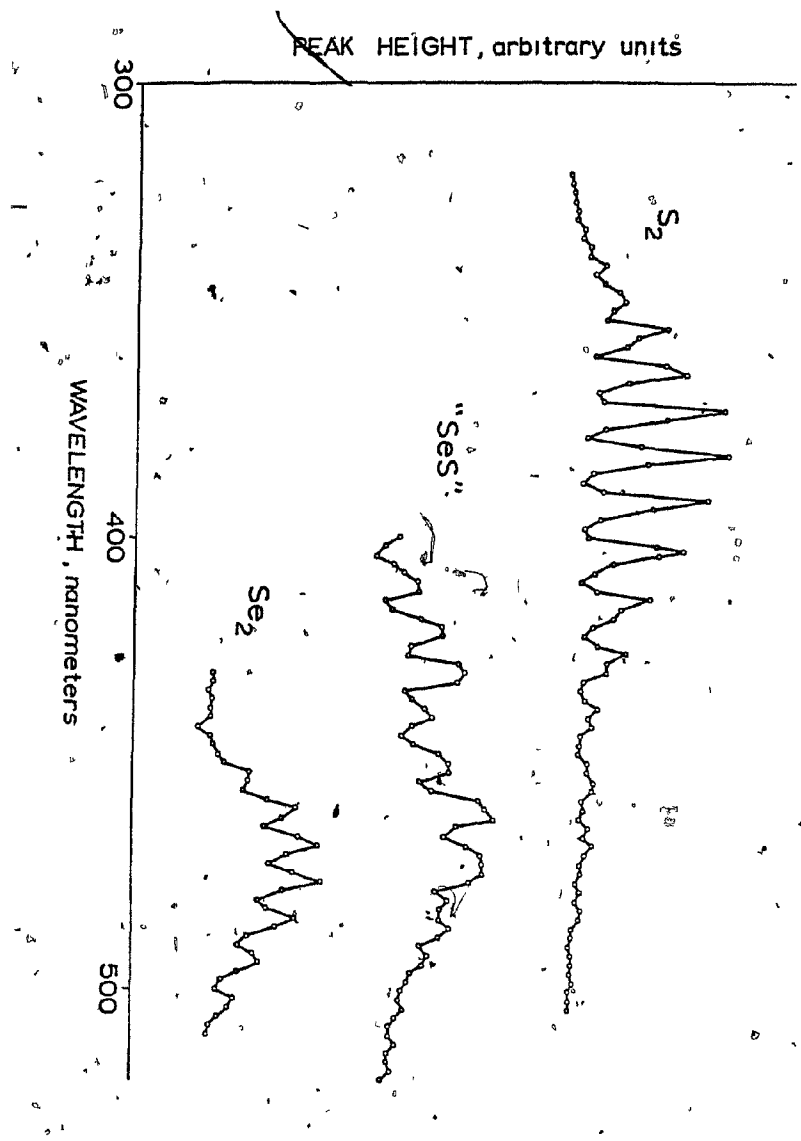
isotopes (Se^{78} and Se^{80}) and tellurium, three (Te^{126} , Te^{128} and Te^{130}) and both elements have a large number of minor isotopes as well. This means many overlapping bands if isotopic separation is not carried out and, hence, the spectra will appear very complex. A listing of the prominent bands was not given in these papers, except (244), nor were there reproductions of the spectra recorded. Despite the technical limitations mentioned, a detailed spectroscopic investigation of selenium and tellurium on a high sulfur back ground was still considered desirable. Although positive identification appeared unlikely due to lack of literature data, it was felt that such an investigation could be used as a check on the implications of the mathematical model for response of selenium on a sulfur background.

The results of this investigation, although not completely clear due to the complexity of the system, definitely show a new band spectrum. That it represents SeS is likely but still subject to verification. Figure 39 shows a spectrum of selenium on a sulfur background between an S_2 and an Se_2 spectrum. It has been corrected for the quenching of the background sulfur bands. To do this, it was assumed that the amount of quenching for every sulfur band was a constant fraction. Several sulfur bands around 360 nm (where there was likely to be little selenium emission) were monitored and the negative response measured. Approximately the same percentage quenching was

Figure 39

A Comparison of Detector Spectral Output: A Sulfur
"Spectrum", a Selenium "Spectrum" on a Large Sulfur
Background, and a Pure Selenium "Spectrum"

2 nm bandpass

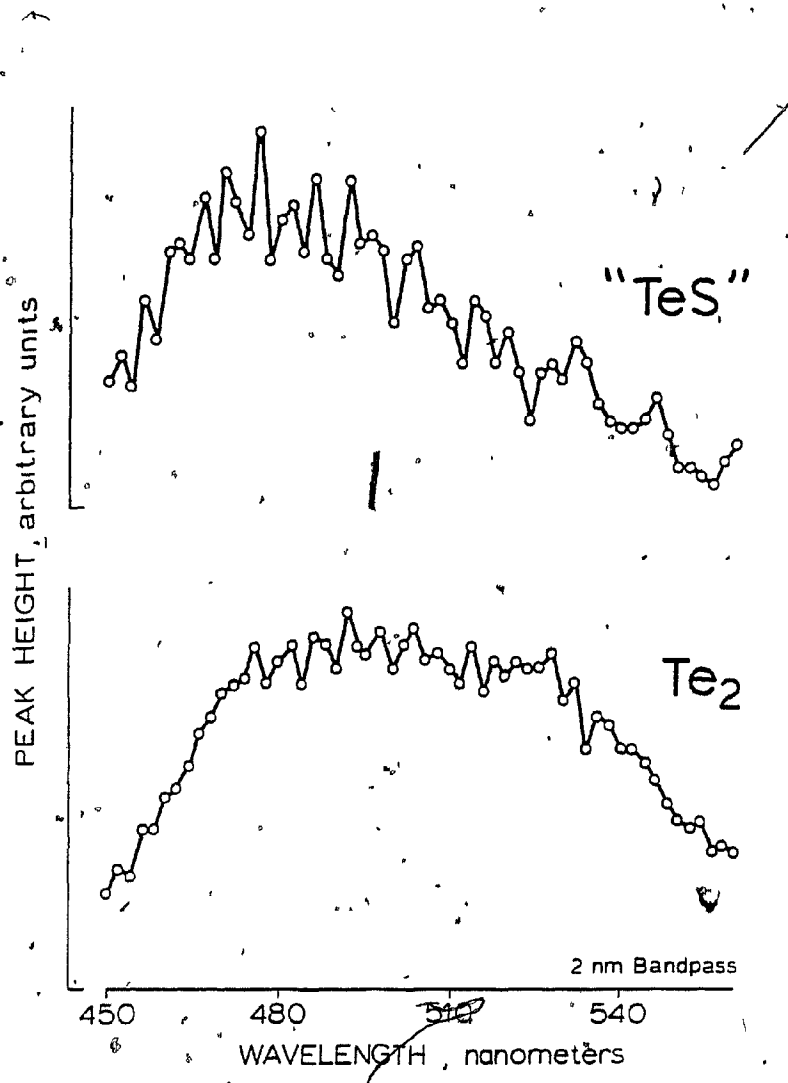


149

Figure 40

A Comparison of Detector Spectral Output: A Tellurium
"Spectrum" on a Large Sulfur Background and a Pure
Tellurium "Spectrum"

2 nm bandpass



noted. These values were averaged and the quenching factor was used to determine at every wavelength (and background level) the size of the negative peak due to quenching. This calculated negative peak was added to the response (positive or negative) recorded for each injection making up the spectrum of selenium on sulfur.

This corrected spectrum shows unmistakable bands that are definitely not present in either the S_2 or Se_2 spectra shown and which are proposed as the SeS spectrum. Only a careful spectroscopic investigation with much higher resolution and the proper tools of the trade could ultimately prove the existence of the molecule SeS and its emission spectrum.

Figure 40 shows tellurium spectra in an undoped and sulfur-doped detector. The spectrum in the sulfur-doped detector was not corrected for quenching because of the relatively low sulfur background in that spectral region. The undoped spectrum shows very little band structure even at a 2 nm bandpass. It can be attributed to Te_2 with a possible contribution from TeO . The calibration curve for dibutyltellurium in undoped mode, shown in Figure 34 indicates that Te_2 is the major emitting species, at least at high concentrations. The spectrum produced under sulfur doping conditions shows a lot more structure than the normal spectrum. There is a major shift of the major emission bands towards lower wavelengths which may be indicative of

an emitting species containing sulfur. The bands do not match with consistency any of the known tellurium molecular bands (Te_2 , TeO , etc.). To say they are due to the interchalcogen TeS is an interesting but yet to be proven statement.

6. Germanium Photometric Response

6.1 Surface-Induced Emission

6.1.1 Initial Investigation

When it became obvious that tin emission in a flame photometric detector equipped with a suitably modified quartz flame enclosure was strongly influenced by the surface of the quartz, the possibility that other species might behave similarly was duly noted as a point to be investigated at a later date. A general survey of organometallic compounds was undertaken using a dual-masked bisected quartz tube. Only the surface-selective channel was monitored. Various organometallic compounds and chelates of elements such as arsenic, bismuth, antimony, boron, manganese, chromium, lead, copper, nickel, iron, aluminum, tungsten and germanium were chromatographed. Only germanium showed a large response; arsenic, bismuth and antimony gave small positive responses and the others gave negative responses. All compounds were tested under two flame conditions; a cool flame (optimum for tin emission) from 30 ml/min of air and 200 ml/min hydrogen, and a relatively hot flame from about 60 ml/min of air and 40 ml/min hydrogen.

The fact that germanium interacted with the quartz surface was confirmed by testing it with a new bisected flame enclosure, prior to and then after a "freon treatment". Like tin, compounds containing germanium gave increased response after the cleaning action of freon in

the flame. The characterization of the detector for germanium response was of particular interest in light of the surface emission question of tin response. The fact that lead did not give any positive response, despite also being a Group 4b element like tin and germanium, rated as a surprise.

6.1.2 Spectral Characteristics

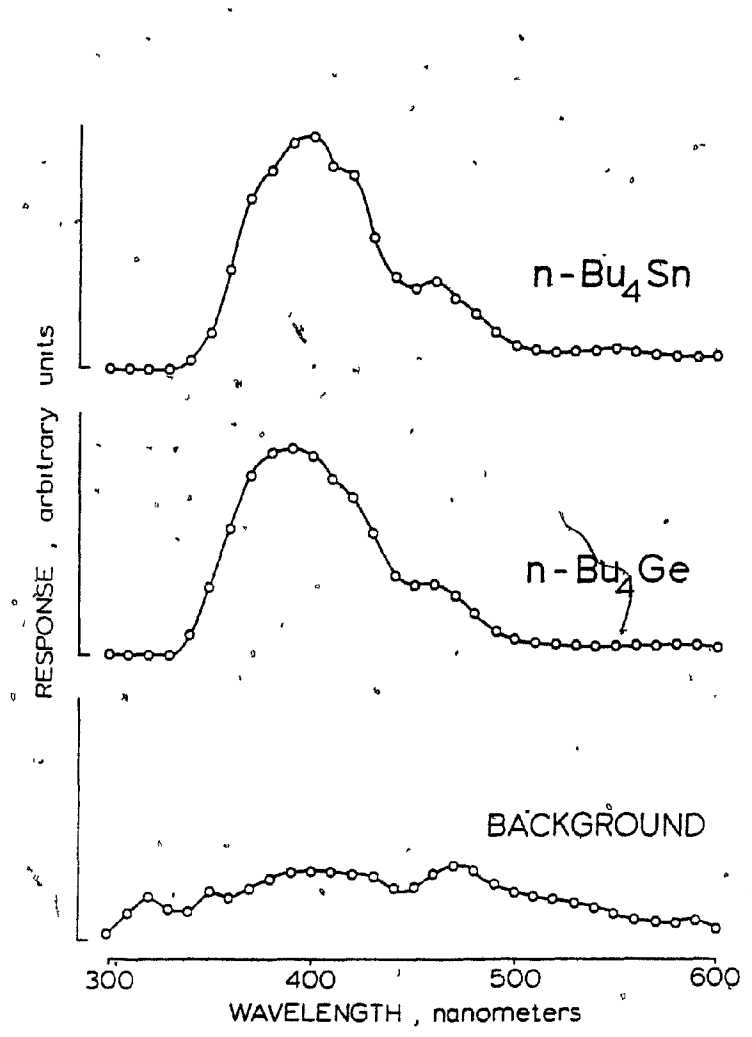
The spectrum of germanium in the FPD, in the presence of a suitably treated quartz surface (as in bisected flame enclosure), can be seen in Figure 41, along with the corresponding tin and background spectra recorded under the same detector conditions. It must be noted that the background spectrum was recorded before any tin or germanium was injected into the detector. This was done because the background emission of the detector was found to take on the exact appearance of the tin or germanium surface emission spectrum after repeated injections of either element. This was probably due to permanently adsorbed tin and germanium on the surface of the quartz. At first glance, the tin and germanium spectra look identical but on closer examination, the germanium spectra can be seen to be slightly shifted to lower wavelengths with respect to tin. Both spectra are broad and featureless and cannot be identified from the literature.

The two molecular species which seem most likely to be formed in the flame are GeO and GeH . The $a^3\pi - X^1\Sigma^+$ system of GeO reported by Sharma and Padur (247) and

Figure 41

**A. Comparison of Germanium, Tin and Background Spectra
Using a Bisected Quartz Flame Enclosure**

8 nm bandpass. Flow rates in ml/min, Germanium: Air = 50,
H₂ = 70, N₂ = 30, Tin: Air = 25, H₂ = 240, N₂ = 30.
Background: Air = 70, H₂ = 100, N₂ = 30.



Meyer et al. (248), which has numerous bands in the 300 to 500 nm region, could be responsible for the surface emission spectrum. The interaction of the quartz surface may sufficiently broaden the spectrum so as to make it unrecognizable. The violet system of GeH, $^2\Delta - X^2\Pi$ (249), reported to have a few strong bands around 400 nm, may also contribute to the total emission. The distinct lack of band structure could be taken to be evidence that the emission is due to an as yet unreported continuum. (Better spectral resolution may prove otherwise.)

6.1.3 Flow Rate Optimization

The determination of the optimum flow conditions for germanium response using a bisected quartz flame enclosure, i.e. the surface reaction, encountered several problems. The peak shape changed with flow conditions becoming broader and more asymmetrical in a cool low air flame as opposed to a hot high air flame. Basically, a new bisected flame enclosure gave lower sensitivity but fairly symmetrical peaks; however, at various times the sensitivity increased without readily apparent reason and, along with it, the tailing of the peaks. The detector had different optimum flow rates when the sensitivity was low than when it was high. The optimum flow rates for a detector with low sensitivity for germanium produced a hot flame (high air and low hydrogen flow); on the other hand, as it became more and more sensitive to germanium, the

detector required a cooler flame (similar to the optimum conditions for tin response). In order to reduce the tailing and increase the sharpness of peaks, the flame was run with higher than optimum air flow rates.

6.1.4 Detector Performance

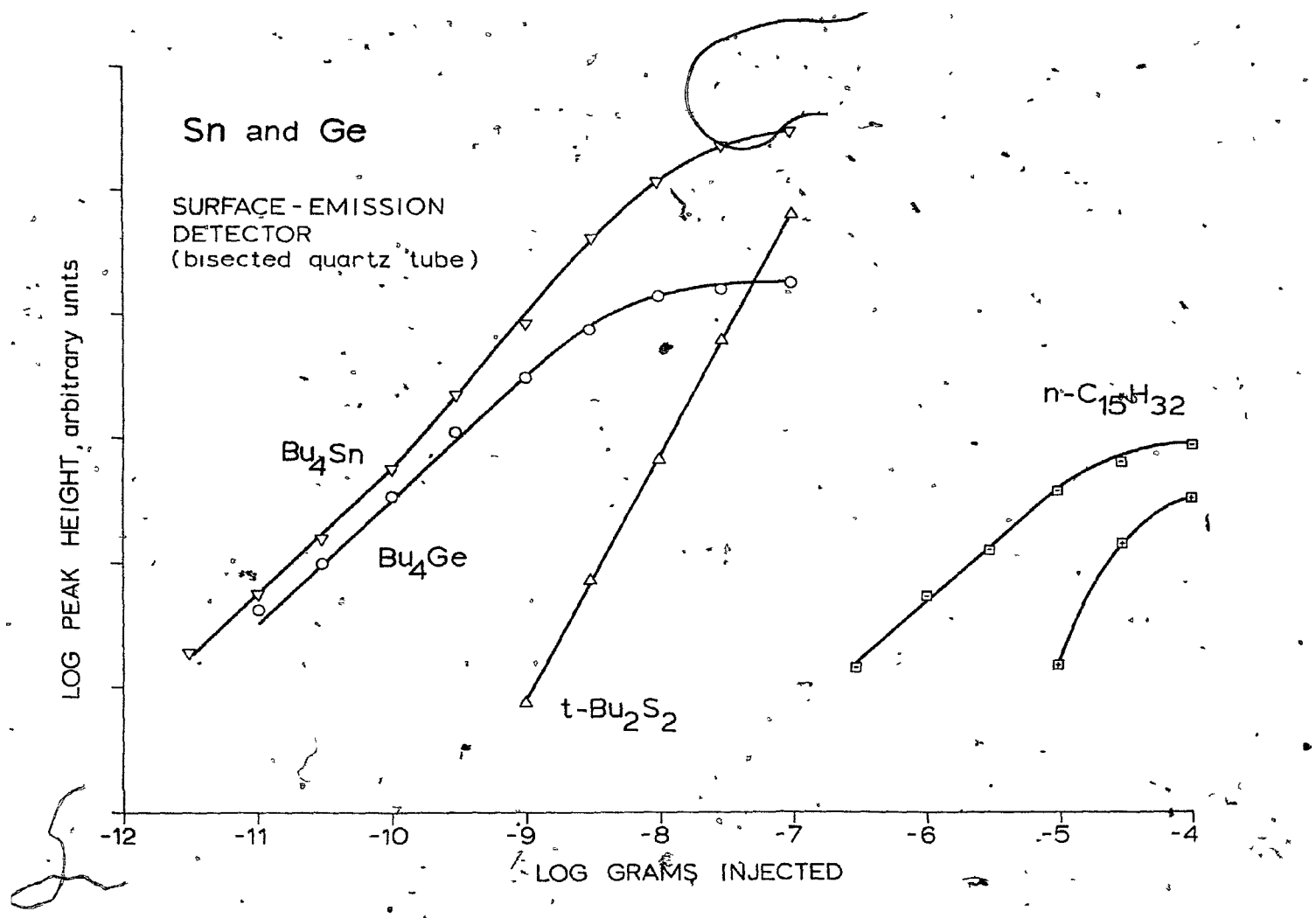
An overall view of the performance of the detector can be seen in Figure 42 which shows calibration curves for tetrabutylgermane and several possible interferences, namely t-butyl disulfide, tetrabutyltin and pentadecane. The data were taken with a bisected quartz enclosure in filterless mode, using a relatively hot flame with flow rates of air and hydrogen set at 60 and 240 mL/min, respectively.

By far the biggest potential problem in determining germanium compounds by surface luminescence is interference by tin compounds. As can be seen in Figure 42, tin response, even under less than optimum conditions for this element, is greater than germanium response. The tin calibration curve exhibited (slightly) non-linear response over a wide range of concentrations, the reason for which is not understood. Neither the use of masks nor filters can improve the selectivity of germanium versus tin because their emission spectra are practically identical and both arise from apparently similar interactions with the quartz surface of the bisecting tube. The selectivity of tin and germanium can be significantly

Figure 42*

Germanium Detector Performance: An Overall View

Bisected quartz flame enclosure, no mask and no filter.
All compounds temperature programmed, Bu_4Ge : 70/8/130°C,
 Bu_4Sn : 90/8/130°C, (t-Butyl) $_2\text{S}_2$: 50/8/110°C and penta-
decane: 70/8/120°C. Flow rates in ml/min, Air = 60,
 H_2 = 240, N_2 = 30. 50 x 0.3 cm ID borosilicate column
packed with 5% Carbowax 20M on Chromosorb W, 45/60 mesh.



increased towards compounds which emit via gas-phase mechanisms by using masks favouring emission that takes place on or near the surface of suitably-treated quartz, as has been demonstrated in the case of sulfur compounds (see Figure 21). This does not hold true for carbon compounds, which quench the background emission emanating from the surface of the bisecting tube. Still, the selectivity of germanium compounds versus sulfur compounds and hydrocarbons, using only a bisected quartz enclosure without wavelength discrimination, ranges from one to three and four to five orders of magnitude, respectively. The minimum detectable of tetrabutylgermane is about one picogram with the aid of a Spectrum electronic filter.

6.2 Gas-Phase Luminescence

Because of the difficulties associated with surface luminescence detection of germanium compounds such as broad, asymmetrical peaks and less-than-satisfactory reproducibility, its gas-phase luminescence was investigated to provide an alternate method of analysis.

6.2.1 Spectral Characteristics

Figure 43 shows a comparison between the surface-induced emission spectrum of germanium using a bisected quartz enclosure, and a spectrum taken under similar conditions but using a normal flame enclosure. The spectrum produced under normal FPD conditions was considered to be the result of emission in the gas phase of one or more

Figure 43

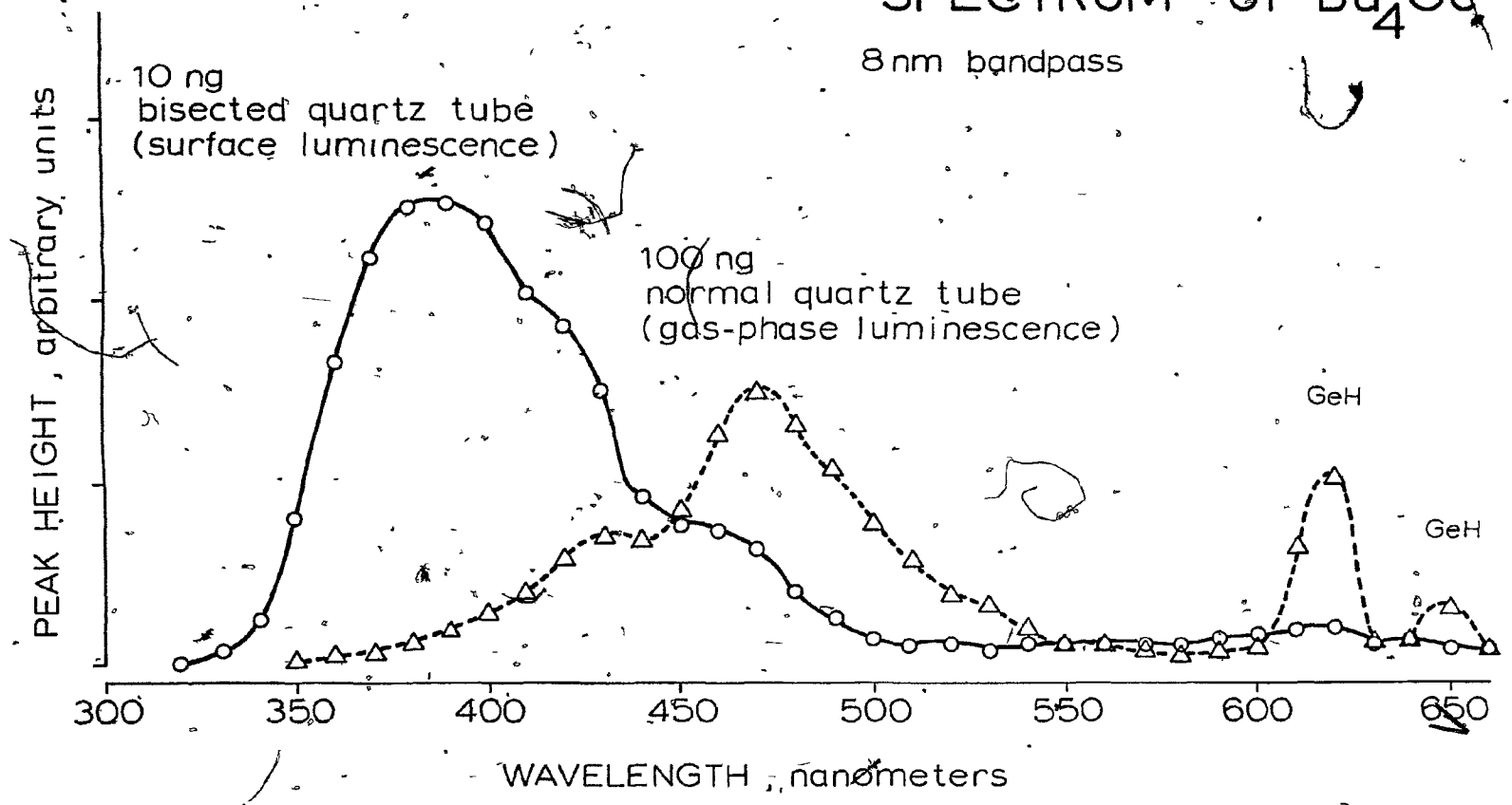
Comparison of Germanium "Spectra" in Surface-Induced
and Gas-Phase Emission Modes

—○—○— 10 ng injections, freon-cleaned bisected
quartz flame enclosure (no mask). Flow rates and column
as in Figure 42 except 40 ml/min H₂ flow.

--△--△-- 100 ng injections, regular flame enclosure.
Flow rates and column as in Figure 42 except 80 ml/min H₂
flow.

"SPECTRUM" of Bu_4Ge

8 nm bandpass



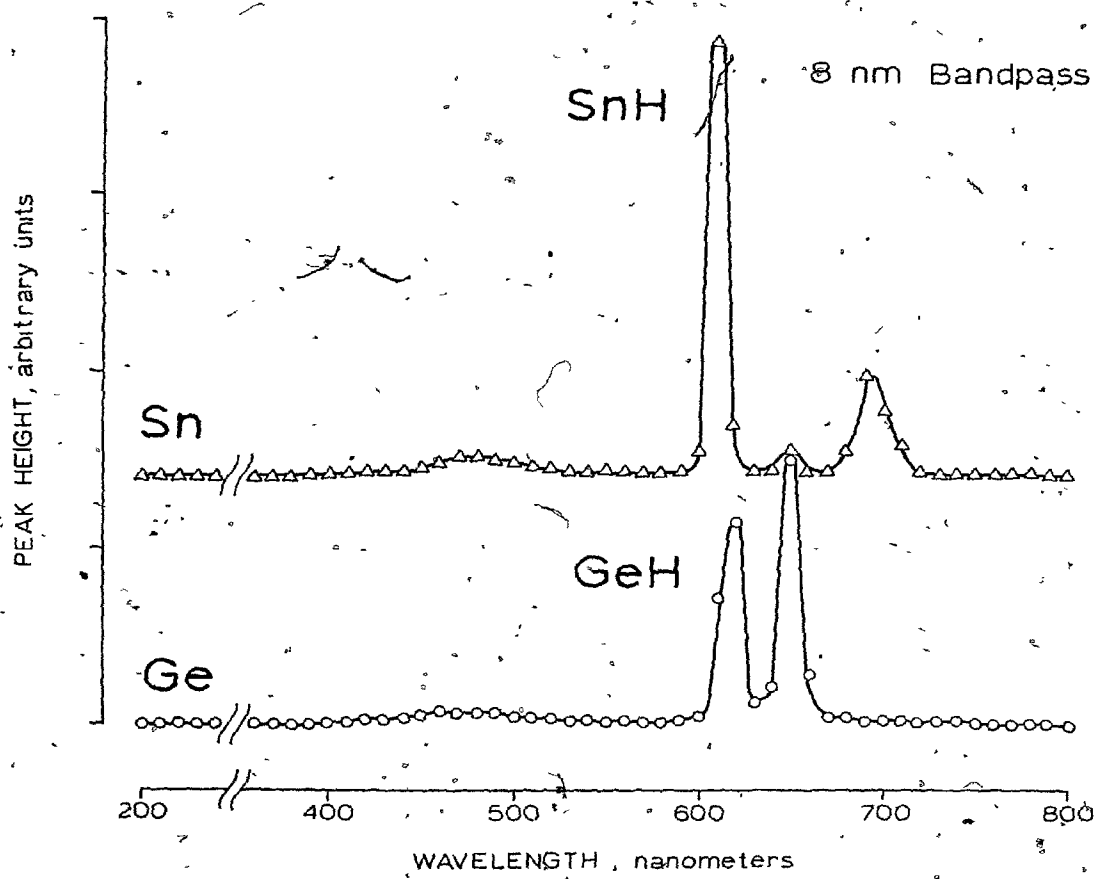
molecular species containing germanium. Like tin emission in the FPD, the gas-phase spectrum of germanium has two distinct regions. There is a broad emission stretching from about 360 nm to 560 nm with a maximum at 470 nm, and two additional bands in the red at 620 nm and 650 nm. The two bands lying in the red correspond well to those listed in Pearce and Gaydon for GeH (249). The species responsible for the emission with maximum at 470 nm is difficult to assign, first and foremost, because of the lack of band structure. The most likely possibility appears to be GeO. Two band systems, $B - X^1\Sigma^+$ reported by Tewari and Mohan (250) and a $3\pi - X^1\Sigma^+$ reported by Sharma and Padur (247) and Meyer *et al.* (248) may be responsible for this emission.

Up to this point, the photomultiplier tubes used in all the experimental work were R268, S-11 response type Hamamatsu tubes. Their spectral response was limited to the range of 300 nm to 650 nm. A Hamamatsu R1104 tube with a range from 185 to 850 nm was obtained and used to determine the spectral response of tin and germanium in a normal FPD from 200 nm to 800 nm. These spectra are shown in Figure 44, using an 8 nm bandpass. The response of germanium was optimized for its emission in the red and, using these conditions and the new R1104 PM tube, its spectrum and that of tin were obtained. The spectra clearly emphasize the bands appearing above 600 nm when compared to

Figure 44

Tin and Germanium "Spectra" in the Gas-Phase-200 nm to 800 nm, Optimized for "GeH" Emission

Using R-1104 PM tube instead of the usual R-268 PM tube.
8 nm bandpass. Flow rates in ml/min, Air = 40, H₂ = 70,
N₂ = 30. 50 x 0.3 cm ID borosilicate column packed with
Chromosorb W deactivated with Carbowax 20M (252), 100/120 mesh.



the spectra shown in Figures 12 and 43. For selectivity purposes, i.e. choice of an interference filter, spectra of tin and germanium above 600 nm were obtained using a 2 nm bandpass and are shown in Figure 45. The red germanium emission is easily recognized as the 650.4 nm and 615.4 nm GeH bands. For tin, there is emission at 690 nm which may have potential in terms of selectivity versus other emitting species, and a weak band at 650 nm (not reported in Pearce and Gaydon), in addition to the better known band at 610 nm. The strong GeH bands appear to be useful for analysis, especially the 650 nm band which overlaps only a weak band from the tin spectrum.

6.2.2 Flow Rate Optimization

The detector was easily optimized for the GeH bands using a 600 nm cut-off filter and varying the air and hydrogen flow rates in the usual way. The results of the optimization are presented in Figure 46. Generally, the response increases with increasing air flow - but so do the detector background and noise levels. A rough trend of response being optimum for each air flow rate at the same air-hydrogen ratio can be observed. The optimum flow rates chosen were 40 ml/min of air and 100 ml/min of hydrogen, although other flow rates could have been chosen without a significant difference in sensitivity.

6.2.3 Detector Performance

It was decided to evaluate the potential of gas-phase

Figure 45

Tin and Germanium "Spectra" above 600 nm - "High Resolution"

Same as Figure 44, but 2-nm bandpass and 100 ml/min H₂ flow.

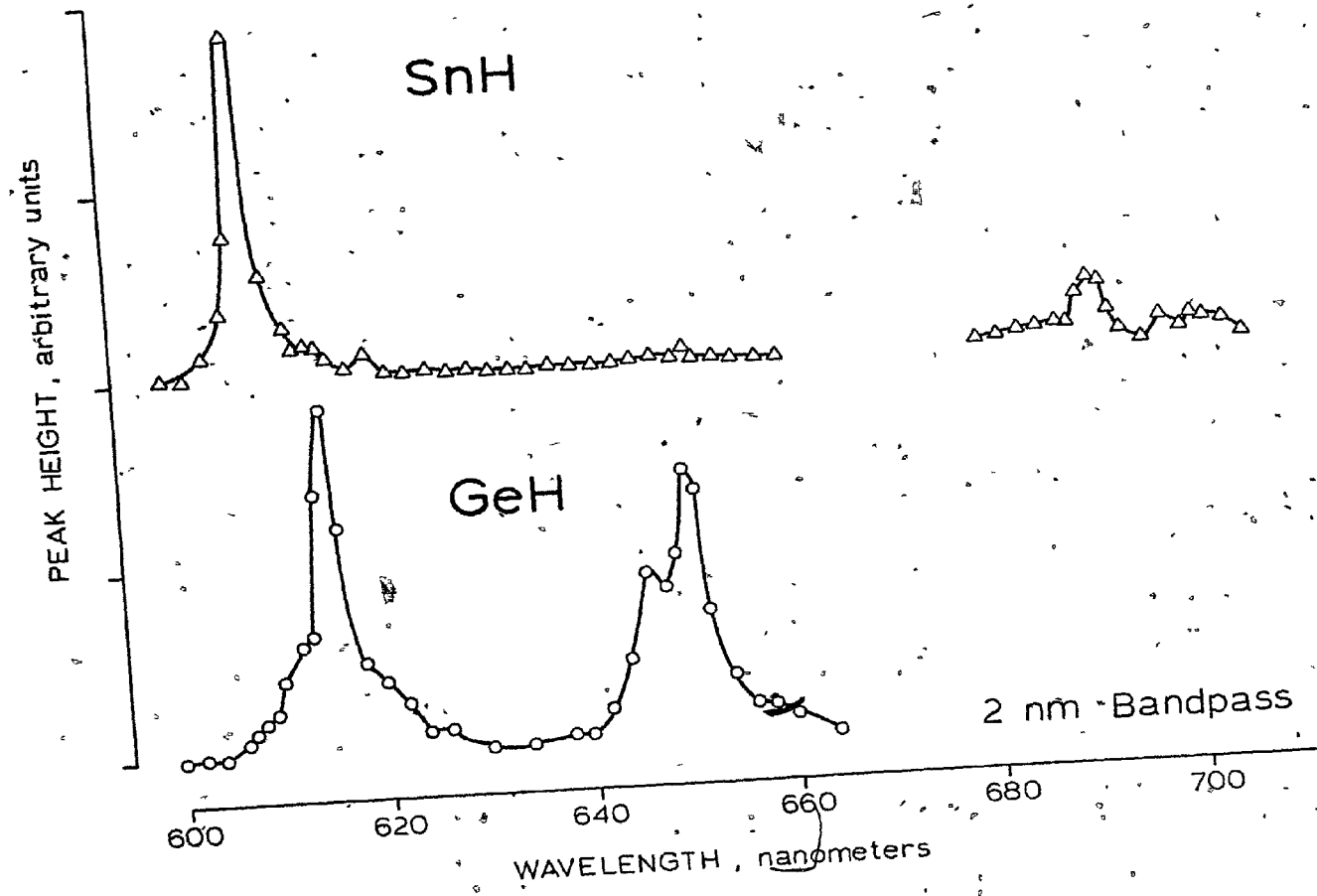


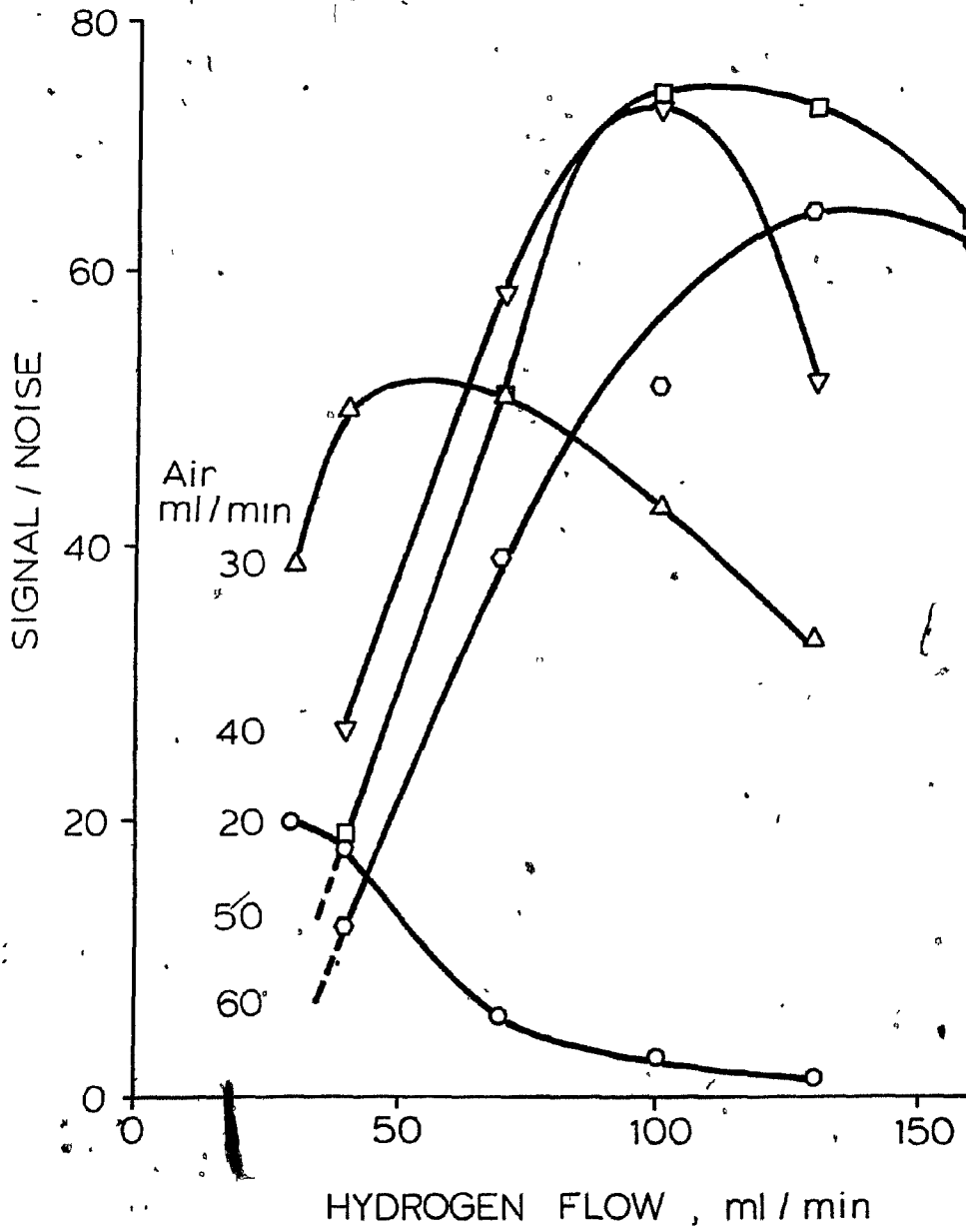
Figure 46

Sensitivity Versus Air and Hydrogen Flow Rates for
"GeH" Emission

Column used as in Figure 44, 600 nm cut-off filter,
normal flame enclosure and R1104 PM tube.

"GeH" EMISSION

(above 600 nm)



germanium emission by monitoring the 650.4 nm band using a 650 nm interference filter. A close inspection of Figure 45 shows that tin compounds would produce significant cross-talk on an optical detector channel monitoring germanium emission at 615 nm, but would do so much less at 650 nm. Calibration curves for tetrabutylgermane and tetrabutyltin are shown in Figure 47 using the 650 nm interference filter. The selectivity of germanium versus tin is close to two orders of magnitude, much better than for the surface-induced-emission detector. The calibration curve is linear for more than three orders of magnitude and the detection limit is about 15 picograms of tetrabutylgermane. The selectivity of tetrabutylgermane versus other possible interferents is as follows: octadecane (positive peak), 1.7×10^6 , diphenylsulfide, 3.3×10^2 , diphenylselenide, 4×10^2 (S and Se values are concentration dependent), and diphenylmethylphosphine, 17. All the selectivities listed were determined from a comparison of detection limits of each compound injected. Phosphorous compounds interfere even more than tin compounds due to the extension of the HPO band system into the red. The main drawback of gas phase emission is that it is an order of magnitude less sensitive than the surface emission. In its favour are its reproducibility and good selectivity versus tin and hydrocarbons.

6.3 Tin and Germanium in the FPD: A Comparison

Tin and germanium show many parallels in behaviour in

Figure 47

Calibration Curves for Tetrabutylgermane and Tetra-
butyltin Using a 650 nm Interference Filter

Both compounds chromatographed isothermally at 110°C.
Flow rates and column as indicated in Figure 44 except
 $H_2 = 100$ ml/min.

GeH GAS-PHASE EMISSION DETECTOR

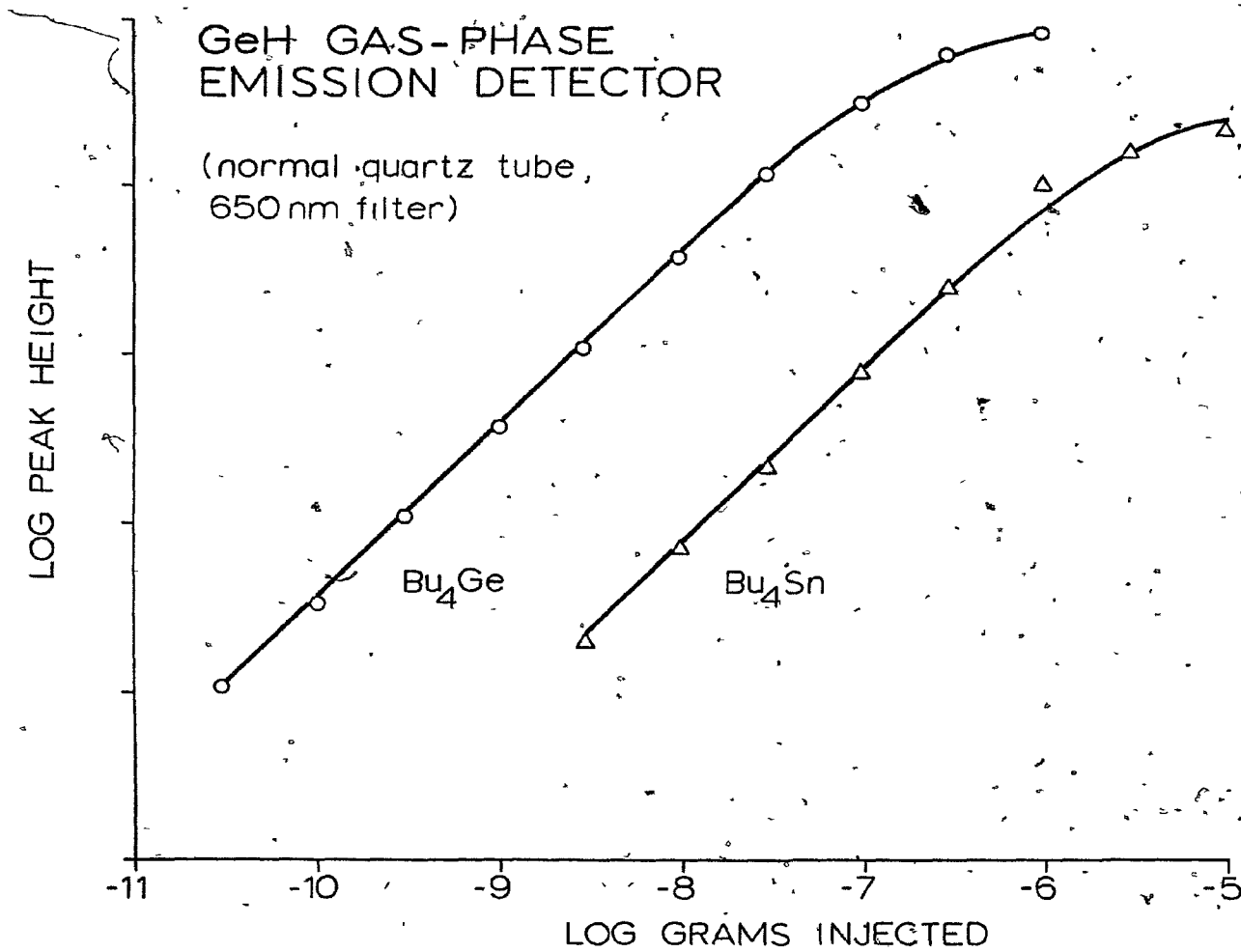
(normal quartz tube,
650 nm filter)

LOG PEAK HEIGHT

LOG GRAMS INJECTED

Bu_4Ge

Bu_4Sn



the FPD. This is not surprising in that they are both Group IVb elements. The most interesting parallel is their surface-induced luminescence occurring on quartz (or pyrex) which contains their fellow congener, silicon. Their surface emission spectra are almost identical; even their gas-phase emission spectra are very close in appearance and wavelength. The reaction mechanisms by which they produce their surface and gas-phase spectra respectively are thus likely to be similar.

A few minor differences have been noted. Germanium peaks are generally broader and tail more than do tin peaks and their response maximum occurs at different flow rates of the combustion gases in the surface emission detector. There is an order of magnitude difference in the sensitivity in the surface emission detector in favour of tin.

7. Selectivity

Selectivity measures the extent to which a particular detector favours one type of compound over another. Quite a variety of definitions of selectivity are in common use, depending on the analytical problem, the chromatographic system, and the selective detector involved. Often selectivity is confused with specificity. A specific detector has infinite selectivity. Selectivity is often represented by a single number which corresponds to a ratio of responses of two compounds or species in the detector for the same amount of compound introduced, or the amounts of compounds that give the same response, or some similar definition. This is fine where all species producing some response give linear calibration curves so that the response per gram or per mole is a constant throughout the linear range. (Measurements beyond linear range are sometimes reported but are obviously of little use.) In the case of linear calibration curves, the selectivity calculated for equal response (SL_R) and the selectivity calculated from equal amounts injected (SL_A) are equivalent. This is illustrated in Figure 48 as case one. The case of non-linear (e.g. quadratic) response is clearly different. A very clear example is sulfur and selenium response in the FPD where both give rise to quadratic calibration curves (in the absence of chalcogen impurities in the background). In filterless mode, sulfur can be said to have a selectivity close to 100 versus selenium as calculated from equal amounts (SL_A). However

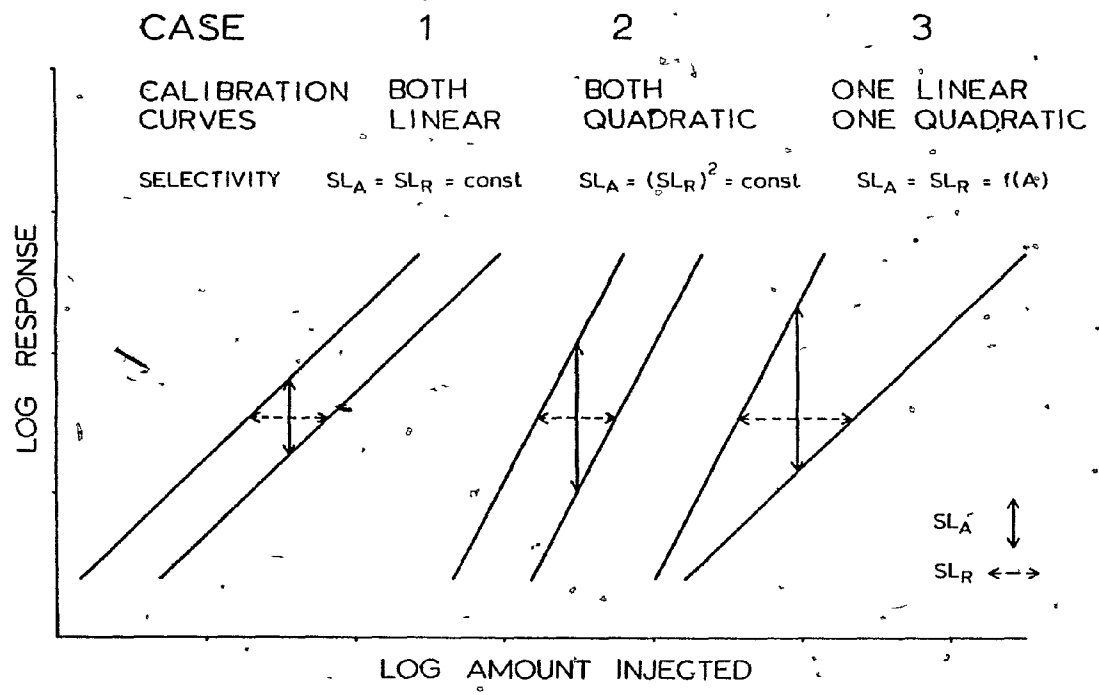
Figure 48

Illustration of Selectivity Measurements Between Calibration Curves. Case 1: Both Linear, Case 2: Both Quadratic, Case 3: One Linear, One Quadratic.

SL_A = Selectivity calculated for equal amounts.

SL_R = Selectivity calculated for equal response.

const. = a constant



the response selectivity (as described by detection limits) is only a factor of ten. This is illustrated as case two in Figure 48. The situation can be further complicated, as is the case for the FPD, when the detector gives rise to both linear and non-linear calibration curves. The use of a single number to represent selectivity becomes of little value. Both forms of expressing selectivity, SL_A and SL_R , become concentration dependent when comparing a linear to a non-linear calibration curve. This is illustrated as case three in Figure 48. Selectivity can then be expressed by giving a range of values to indicate concentration dependence, or by making selectivity comparisons only at the detection limits (and stating them to be such). By far the clearest method is to show calibration curves of all species involved, determined under the same conditions. This presents an overall view of detector performance, giving selectivity as well as sensitivity and linear range data.

Increasing selectivity for one species against potential interferences is often an important goal. The most common case is one in which there is one major interfering species which must be suppressed. Nearly always, flow rate adjustments (e.g. for the flame gases of a FPD) can be optimized for the species of choice. Optical methods, e.g. flame photometric detection, can take advantage of devices such as monochromators, interference and cut-off filters, masks, etc.

In the FPD, different species emit characteristic spectra (often more than one band system) in different areas of the UV and visible region. Filters can be successfully used to gain selectivity, most notably if the species of interest and the prominent interfering species have very different emission spectra. Masks can be used to gain selectivity if different species such as S_2 and HPO emit in different regions above the flame.

In the case of surface-induced versus gas-phase emissions, proper masking can be used to favour one species over others (e.g. tin and germanium versus all other species except hydrocarbons). Tin and germanium emit strongly after interaction with a clean quartz surface, but produce little emission in the gas-phase in the low concentration range. The dual-masked bisected quartz flame enclosure shown in Figure 5, with gas-phase and surface emission channels as indicated, was developed to take advantage of the geometric selectivity possible with surface reactions. As can be seen from the graph in the same Figure, the principle works well in practice.

Selectivity can be enhanced by chemical means (a) where the addition of a suitable reagent to the detector selectively reduces the response of the interfering species but affects the species of interest only marginally and (b) where the reagent enhances selectively the response of the analyte. A good example of the first case is the

action of methane gas which drastically reduces sulfur response in the FPD but does not reduce selenium response to a significant degree. This is well documented in Figures 29 and 32. An example of the second case is the enhancement of, say, selenium response by adding sulfur which leaves P, Sn and Ge response unchanged.

An inherent problem with selective detectors is differentiating between a peak representing a large amount of compound of low response and a low amount of a compound with high response. This is essentially a problem of qualitative analysis. Whether or not a peak is due to tin or germanium versus other species can be determined using the dual-masked bisected flame enclosure. Peaks containing sulfur, selenium and tellurium can be identified by checking for quadratic response or their dependence on a sulfur background. A detector operating in dual-channel mode, using different filters for each channel, can be helpful by producing response ratios at different pairs of wavelengths. Chemical dopants can provide qualitative information by enhancing or depressing the response of certain species but not of others. It should be noted that these various techniques used in combination could provide simple and rapid qualitative information.

8. Conclusions

The analytical utility of a flame photometric detector has been successfully extended to the organic compounds of tin, selenium, germanium and tellurium. Tin and germanium were found to respond via surface luminescence on quartz that had been suitably treated and positioned above the flame. Tin and germanium were the two most sensitive elements which could be determined by FPD with detection limits of 5.3×10^{-16} g/sec and 1×10^{-14} g/sec, respectively. Environmentally important but difficult-to-chromatograph organotin compounds were derivatized by two methods: A) Reduction to the corresponding hydrides with silane and B) Halogenation in a gas chromatograph conditioned with HCl or HBr. Selenium photometric response was found to parallel that of sulfur in almost all respects. The selectivity of selenium versus sulfur could be greatly enhanced by addition of methane to the carrier gas.

Chemical linearization of chalcogen (sulfur, selenium and tellurium) response via sulfur doping appears to be a promising technique for circumventing their quadratic calibration curves and may replace, in many applications, other means of linearization (e.g. electronic) now in common use. Mathematical models, developed to predict the degree of linearization of sulfur and selenium response with sulfur doping conditions, gave satisfactory agreement

between observed and calculated calibration curves. A spectroscopic search provided strong evidence for the existence of the molecules SeS and TeS.

Monitoring a gas-phase GeH band at 650 nm gave nearly two orders of magnitude of selectivity for germanium versus tin. The use of the word selectivity in describing a detector with both linear and non-linear response must be done with a clear description of how it has been derived. Comparison of quadratic and linear calibration curves require a range of selectivity values to be given.

Qualitative analysis of FPD peaks must be a future problem for investigation as many elements have been found to respond and more are likely to follow. Attention should be paid to possible derivatization reactions for compounds that can now be analysed only by relatively insensitive techniques to take advantage of the sensitivity and selectivity the FPD can provide for several elements.

Appendix

Is the Sulfur Emission Mechanism Consistent with Experimental Data?

The question arose during the author's preliminary oral examination whether or not the proposed sulfur emission mechanism was consistent with collision theory. In other words, will enough collisions take place between sulfur atoms to account for the number of photons produced? The response data for 100 nanograms of diphenylsulfide, taken from a set of data used in Chapter Five, was picked as an example for this calculation. The temperature of the emission region of the detector was measured with a chromel-alumel thermocouple (fine wire) to be about 200°C on the average for the optimum flame conditions for sulfur response. It is realized that this temperature value is lower than the actual temperature but was considered to be accurate enough for the type of calculation involved.

Using collision theory, relevant data from equipment specifications and several assumptions, the maximum number of collisions which could take place and the number of photons produced by the injected compound are calculated.

Part One: Collision Theory

Let the sulfur atom density at time t be $N(t)\text{cm}^{-3}$.

Therefore the # collisions in time interval " dt " = $Z(t)$

$$Z(t) = \frac{\pi \sigma^2 \bar{c} N(t)^2}{\sqrt{2}} dt \text{ cm}^{-3} \quad (254) \quad (1)$$

where σ = collision diameter
 \bar{c} = average velocity of sulfur atoms

As a slug of gas passes the observation zone, the number of collisions occurring during time "dt" is as follows:

$$\# \text{ collisions} = Z(t) \cdot V$$

$$\text{Therefore } C_T \text{ (total collisions)} = \frac{1}{2} \int_0^{\infty} Z(t) \cdot V dt \quad (2)$$

The factor of $\frac{1}{2}$ takes into account the assumption of a point source.

$$C_T = \frac{\pi \bar{c} \sigma^2 V}{2 \sqrt{2}} \int_0^{\infty} N(t)^2 dt \quad (3)$$

(during the passage of the peak)

If F is the volume flow rate and N the total number of sulfur atoms, then

$$N = \int_0^{\infty} N(t) dV \quad (4)$$

$$\text{and } F = \frac{dV}{dt} \quad (5)$$

$$\text{Therefore } N = F \int_0^{\infty} N(t) dt \quad (6)$$

A Gaussian distribution of sulfur atoms entering the detector from the column is now assumed

$$N(t) = N_0 e^{-k^2(t-t_0)^2} \quad (7)$$

Substituting equation (7) into equation (6)

$$N = FN_0 \int_0^{\infty} e^{-k^2(t-t_0)^2} dt \quad (8)$$

$$\int_0^{\infty} e^{-a x^2} dx = \frac{1}{2a} \sqrt{\pi} \quad (255) \quad (9)$$

Using the definite integral of equation (9) in equation (8)

$$N = \frac{FN_0 \sqrt{\pi}}{2k} \cdot 2 \quad (10)$$

the factor of 2 in equation (10) accounts for integrating over the entire Gaussian peak with t_0 set equal to 0.

$$N_0 = \frac{kN}{F \sqrt{\pi}} \quad (11)$$

Substitution of equation (7) in equation (3) gives

$$C_T = \frac{\pi \bar{c} \sigma^2 V}{2\sqrt{2}} \int_0^{\infty} N_0^2 e^{-2k^2(t-t_0)^2} dt \quad (12)$$

Substitution of equation (11) for N_0 and after integration, equation (12) becomes

$$C_T = \frac{\sqrt{\pi} \bar{c} \sigma^2 V k N^2}{4F^2} \quad (13)$$

At this point, it is necessary to solve for \bar{c} , σ , k , N , F and V

Calculation of Volume of Gas Observed:

$$V(\text{volume of gas observed}) = \pi R_1^2 H \quad (14)$$

where R_1 = radius of flame enclosure

H = height above burner observed by PM tube

$$\therefore V = \pi (0.6\text{cm})^2 \cdot 2.0\text{ cm}$$

$$V = 2.26\text{ cm}^3$$

Calculation of Average Velocity:

$$\bar{c} = \sqrt{\frac{8RT}{\pi M}} \quad (15)$$

$$T = 473^\circ\text{K} \quad M = 32.06\text{g mole}^{-1}$$

$$R = 8.31 \times 10^7 \text{ ergs deg}^{-1} \text{ mole}^{-1}$$

Solving equation (15),

$$\bar{c} = 5.4 \times 10^4 \text{ cm sec}^{-1}$$

Calculation of Collision Diameter:

$$\sigma = \sqrt{\frac{\bar{c} \cdot m}{2 \sqrt{2} \pi \eta}} \quad (16)$$

The viscosity of sulfur atoms is assumed to be equal to that of oxygen molecules at 473°K . m = the mass of one atom;
 η = viscosity

$$\eta_S = \eta_{O_2} = 2.88 \times 10^{-4} \text{ poise}$$

$$\text{hence } \sigma = 3.41 \times 10^{-8} \text{ cm}$$

Calculation of Total Gas Flow

The total gas flow rate before combustion at room temperature is the sum of the air, hydrogen and carrier gas flow rates which is 100 ml/min as controlled by mass flow controllers. From the stoichiometry of the combustion reaction and knowing air = 30 ml/min and H₂ = 40 ml/min, the total flow rate after combustion is 94 ml/min.

$$F_{473^{\circ}\text{K}} = F_{298^{\circ}\text{K}} \times \frac{473^{\circ}\text{K}}{298^{\circ}\text{K}} \quad (17)$$

$$F = 94 \text{ cm}^3 \text{ min}^{-1} \times \frac{473}{298}$$

$$F = 149 \text{ cm}^3 \text{ min}^{-1} \text{ or } 2.49 \text{ cm}^3 \text{ sec}^{-1}$$

Calculation of the Number of Sulfur Atoms:

$$\text{Grams diphenylsulfide} = 1.00 \times 10^{-7}$$

$$\text{g sulfur} = 1.72 \times 10^{-8}$$

$$\text{Therefore } N(\text{atoms sulfur}) = 3.23 \times 10^{14}$$

Determination of k

$$\frac{R(t)}{R_0} = \left(\frac{N(t)}{N_0} \right)^2 = e^{-2k^2(t-t_0)^2} \quad (18)$$

When $R_0/R(t) = 2$ (at half peak height)

$$t - t_0 = 4.7 \text{ sec}$$

$$\text{therefore } k = 0.12 \text{ sec}^{-1}$$

Substituting the following data into equation(13), the number of collisions can be calculated.

$$\begin{aligned} \sigma &= 3.41 \times 10^{-8} \text{ cm} & N &= 3.24 \times 10^{14} \\ \bar{C} &= 5.6 \times 10^4 \text{ cm sec}^{-1}, & F &= 2.49 \text{ cm}^3 \text{ sec}^{-1} \\ V &= 2.26 \text{ cm}^3 & k &= 0.12 \text{ sec}^{-1} \end{aligned}$$

$$C_T = 1.32 \times 10^{17} \text{ collisions}$$

The total number of collisions as calculated here is higher than the actual number. This is because when $S + S$ reacts to form S_2 , further collisions of the S atoms involved are fictional, i.e. collision rates involve non-reacting particles.

Calculation of number of photons produced from
experimental data

The charge collected at the final dynode of the PM tube follows a squared Gaussian function.

$$Q_T \text{ (total charge)} = I \text{ peak} \int_0^{\infty} e^{-2k^2(t-t_0)^2} dt \quad (19)$$

Where $I \text{ peak}$ = current in amperes corresponding to the peak height. Integration of equation (19) leaves it in the form

$$Q_T = I \text{ peak} \frac{\sqrt{\pi}}{\sqrt{2} k}$$

Determination of $I \text{ peak}$:

$I \text{ peak}$ can be determined knowing that a full scale

signal at attenuation 1 x 1 of 24 cm is produced when a signal of 10^{-12} amperes is recorded.

$$\text{Therefore } I_{\text{peak}} = \frac{17.3 \text{ cm}}{24.0 \text{ cm}} \times 256 \times 10^4 \times 10^{-12} \text{ amperes}$$

$$I_{\text{peak}} = 1.84 \times 10^{-6} \text{ amperes}$$

Determination of Total Charge:

$$Q_T = I_{\text{peak}} \frac{\sqrt{T}}{\sqrt{2} k}$$

$$Q_T = 1.92 \times 10^{-5} \text{ coulombs}$$

Determination of Electrons at Final Dynode:

Knowing the charge per electron is 1.60×10^{-19} coulombs, the total number of electrons can be calculated.

$$E_T = 1.20 \times 10^{14}$$

Determination of Electrons at First Dynode:

$$E_1 = \frac{E_T}{G} \quad (20)$$

where the photomultiplier tube gain $G = 1.8 \times 10^5$

$$\text{Therefore, } E_1 = 6.67 \times 10^8$$

Determination of Photons Arriving at First Dynode:

$$P_1 = \frac{E_1}{QE}$$

where $QE = \text{quantum efficiency} = 0.09$

$$\text{therefore, } P_1 = 7.41 \times 10^9$$

Determination of the Aperture of the Optical System:

$$A(\text{Aperture}) = \frac{\text{PM tube window area}}{4\pi R_2^2}$$

where R_2 = distance from emission zone to PM tube window. The assumption of the sulfur emission as a point source and isotropic light distribution is now made.

$$A = \frac{0.48 \text{ cm}^2}{4\pi(10.3)^2 \text{ cm}^2}$$

$$A = 3.61 \times 10^{-4}$$

Determination of the Total Number of Photons Produced:

$$P_T = \frac{P_1}{A}$$

$$P_T = \frac{7.41 \times 10^9}{3.61 \times 10^{-4}}$$

$$P_T = 2.05 \times 10^{13}$$

Note: 3.24×10^{14} sulfur atoms could produce a maximum of 1.62×10^{14} S_2 molecules, and hence, photons (if one assumes that only one photon can be produced per S_2 molecule). According to this calculation only 12.7% of this maximum number of photons are produced. The number of photons produced, 2×10^{13} is approximately ten thousand times smaller than the number of theoretical collisions, 2.65×10^{17} .

Conclusion:

According to collision theory, there would be more than enough possible collisions to account for the very good sulfur response of the FPD. Hence the mechanism for this emission proposed by Sugiyame (94) cannot be rejected out of hand. The number of photons produced is entirely reasonable for the number of sulfur atoms present.

Obviously a number of factors have been neglected but must still be important. Certainly not every collision between sulfur atoms will result in an excited diatomic sulfur molecule being formed and because of deactivating collisions not every excited diatomic sulfur molecule will produce a photon. It is known that carbon quenches S_2 emission and the compound used for the calculation, diphenylsulfide, possesses 12 carbon atoms. The conversion of the organosulfur compound to sulfur atoms is likely less than 100% with the formation of species such as SO also a possibility in the flame. Visual experience shows that not all sulfur atoms have yet reacted at the upper end of the viewing area, since the blue S_2 glow extends well beyond it. Several other assumptions, as outlined in the appendix, are not completely accurate but lent simplicity to the calculations. However, an affirmative answer can be provided to the original question brought up during the author's preliminary examination: Collision rates do allow the pro-

posed sulfur emission mechanism by a wide margin.

References

1. Wolf, W.R., Coupled Gas Chromatography-Atomic Absorption Spectrometry, *J. Chromatogr.*, 134(1977) 159.
2. Fernandez, F.J., Atomic Absorption Determination of Gaseous Hydrides Utilizing Sodium Borohydride Reduction, *At. Absorption Newslett.*, 12(1973) 93.
3. Freeman, H.C., and Uthe, J.F., An Improved Hydride Generation Apparatus for Determining Arsenic and Selenium by Atomic Absorption Spectroscopy, *At. Absorption Newslett.*, 13(1974) 75.
4. Watling, R.J., The Use of a Slotted Quartz Tube for the Determination of Arsenic, Antimony, Selenium and Mercury, *Anal. Chim. Acta*, 94(1977) 181.
5. Flemming, H.D., and Ide, R.G., Determination of Volatile Hydride-Forming Metals in Steel by Atomic Absorption Spectrometry, *Anal. Chim. Acta*, 83(1976) 67.
6. Chao, T.T., Sanzolone, R.F., and Hubert, A.E., Flame and Flameless Atomic-Absorption Determination of Tellurium in Geological Materials, *Anal. Chim. Acta*, 96(1978) 251.
7. Brodie, K.G., A Comparative Study: Determining Arsenic and Selenium by AAS, *Amer. Lab.*, 9(3) 1977) 73.
8. Cutter, G.A., Species Determination of Selenium in Natural Waters, *Anal. Chim. Acta*, 98(1978) 59.
9. Chau, Y.K., Wong, P.T.S., and Goulden, P.D., Gas Chromatography-Atomic Absorption Method for the Determination of Dimethyl Selenide and Dimethyl Diselenide, *Anal. Chem.*,

47(1975) 2279.

10. Trachman, H.L., Tyberg, A.J., and Branigan, P.D., Atomic Absorption Spectrometric Determination of Sub-Part-Per-Million Quantities of Tin in Extracts and Biological Materials with a Graphite Furnace, *Anal. Chem.*, 49(1977) 1090.
11. Segar, D.A., Flameless Atomic Absorption Gas Chromatography, *Anal. Lett.*, 7(1974) 89.
12. Sighinolfi, G.P., Santos, A.M., and Martinelli, G., Determination of Tellurium in Geochemical Materials by Flameless AA, *Talanta*, 26(1979) 143.
13. Vijan, P.N., and Chan, C.Y., Determination of Tin by Gas Phase Atomization and Atomic Absorption Spectrometry, *Anal. Chem.*, 48(1976) 1788.
14. Fiorino, J.A., Jones, J.W., and Capar, S.G., Sequential Determination of Arsenic, Selenium, Antimony and Tellurium in Foods Via Rapid Hydride Evolution and Atomic Absorption Spectrometry, *Anal. Chem.*, 48(1976) 120.
15. Parris, G.E., Blair, W.R., and Brinkman, F.E., Chemical and Physical Considerations in the Use of Atomic Absorption Detectors Coupled with a Gas Chromatograph for Determination of Trace Organometallic Gases, *Anal. Chem.* 49(1977) 378.
16. Freeman, S.K., "Gas Chromatography and Infrared and Ramon Spectroscopy", Chapter 6 in, *Ancillary Techniques of Gas Chromatography*, Ed.: Ettre, L.S., and McFadden, W.H., Wiley-Interscience, 1969.

17. Saferstein, R., and Manura, J.J., Routine Analysis of Drugs of Abuse by GC/IR, Amer. Lab., 10(2)(1978) 125.
18. Lephardt, J.O., and Bulkin, B.J., On-the-Fly Gas Chromatography-Infrared Spectrometry Using a Cholesteric Liquid Crystal-Effluent Interface, Anal. Chem., 45(1973) 706.
19. Penzias, G.J., Gas Chromatograph Peaks Identified On-Line by a New Grating Infrared Spectrometer, Anal. Chem., 45(1973) 890.
20. Gallaher, K.L., and Grasselli, J.G., Analysis by Optimized Gas Chromatography/Infrared/Nuclear Magnetic Resonance Techniques, Appl. Spectrosc., 31(1977) 456.
21. Shaps, R.H., and Varano, A., GC(Gas Chromatography) /IR as an Accessory for an IR Spectrometer, Amer. Lab., 7 (11)(1975) 77.
22. Shaps, R.H., Simons, W., and Varano, A., A New Analytical Tool, GC/IR and GC/NMR, Amer. Lab., 9(3)(1977) 95, 98.
23. Brady, Jr., R.F., Analysis of Microgram Quantities of Organic Vapours by Combined Capillary-Column Gas Chromatography and Vapour-Phase Infrared Spectrometry, Anal. Chem., 47(1975), 1425.
24. Kizer, K.L., GC(Gas Chromatography)/IR On-Line Analysis, Amer. Lab., 5(6)(1973) 40, 44.
25. Hausdorff, H.H., Selective Infrared Detectors for Chromatography, J. Chromatogr., 134(1977) 131.
26. Hausdorff, H.H., Infrared Group-Specific Detectors for GC, Amer. Lab., 10(5)(1978) 86.

27. Gomez-Taylor, M.M., and Griffiths, P.R., On-Line Identification of Gas Chromatographic Effluents by Dual Beam Fourier Transform Infrared Spectrometry, Anal. Chem., 50(1978) 422.
28. Coffey, P., Mattson, D.R., and Wright, J.C., A Programmable GC/FT-IR System, Amer. Lab., 10(5)(1978) 126.
29. Azarraga, L.V., and McCall, A.C., Infrared Fourier Transform Spectrometry of Gas Chromatography Effluents, Environ. Prot. Technol. Ser., EPA-660/273-034(1974) 61 p CA #105985W, Vol. 82, (1975).
30. Kreuzer, L.B., Laser Optoacoustic Spectroscopy for GC Detection, Anal. Chem., 50(1978) 597A.
31. Wood, L.L., Apparatus for Analysing the Atomic Spectra of Gas Samples, U.S. Patent No. 3,610,759, filed(1967), CA #20988a, 76(1972).
32. West, C.D., Modification of a 30 MHz Plasma Torch for Gas Analysis and Comparison to a 2450 MHz Plasma, Anal. Chem., 42(1970) 811.
33. McCormack, A.J., Tong, S.C., and Cooke, W.D., Sensitive Selective Gas Chromatography Detector Based on Emission Spectrometry of Organic Compounds, Anal. Chem., 37(1965) 1470.
34. Bache, C.A., and Lisk, D.J., Determination of Organophosphorous Insecticide Residues Using the Emission Spectrometric Detector, Anal. Chem., 37(1965) 1477.
35. Bache, C.A., and Lisk, D.J., Simple Tuning Device for

Microwave Tapered Matching Cavity, Anal. Chem., 40(1968) 2224.

36. Braun, W., Peterson, N.C., Bass, A.M., and Kurylo, M.J., A Vacuum Ultraviolet Atomic Emission Detector. Quantitative and Qualitative, Chromatographic Analysis of Typical C, N and S Containing Compounds, J. Chromatogr., 55(1971) 237.
37. Bache, C.A., and Lisk, D.J., Gas Chromatographic Determination of Organic Mercury Compounds by Emission Spectrometry in a Helium Plasma: Application to the Analysis of Methylmercury Salts in Fish, Anal. Chem., 43(1971) 950.
38. Dagnall, R.M., and Whitehead, P., Microwave-Excited Detectors for Gas Chromatography, Proc. Soc. Anal. Chem., 9(1972) 201.
39. Dagnall, R.M., West, T.S., and Whitehead, P., Simple Atmospheric Microwave-Excited Emissive Detector for Gas Chromatography, Anal. Chim. Acta, 60(1972) 25.
40. Dagnall, R.M., West, T.S., and Whitehead, P., Use of the Microwave-Excited Emissive Detector for Gas Chromatography for Quantitative Measurement of Interelement Ratios, Anal. Chem., 44(1972) 2074.
41. Lowings, B.J., Selective Detector for Gas Chromatography, Analysis, 1(1972) 510; CA #66652f, Vol. 82, (1973).
42. Dagnall, R.M., West, T.S., and Whitehead, P., Determination of Volatile Metal Chelates by Using a Microwave-Excited Emissive Detector, Analyst, 98(1973) 647.

43. McLean, W. R., Microwave Plasma Detector (MPD) for Gas Chromatography, Proc. Soc. Anal. Chem., 10(1973) 144.
44. McLean, W.R., Stanton, D.L., and Penketh, G.E., A Quantitative Tunable Element-Selective Detector for Gas Chromatography, Analyst, 98(1973) 432.
45. Serravallo, F.A., and Risby, T.H., A Metal Selective Microwave Emissive Detector for Gas Chromatography, J. Chromatogr. Sci., 12(1974) 585.
46. McLean, W.R., Microwave Plasma Detector System, Recent Anal. Dev. Pet. Ind., (1974) 139; CA #157527p, 83, (1975).
47. Simpson, C.F., Multielement-Selective Detector for Gas Chromatography, Process. Biochem., 10(1975) 13; CA # 98910d, 84(1976).
48. Serravallo, F.A., and Risby, T.H., Effect of Doping Gases on Microwave-Induced Emissive Spectrometric Detectors for Gas Chromatography, Anal. Chem., 47(1975) 2141.
49. Houpt, P.M., Physical Phenomena and Analytical Applications of Helium Microwave Discharges, Anal. Chim. Acta, 86(1976) 129.
50. Von Dalen, J.P.J., De Lezenne Coulander, P.A., De Golan, L., Optimization of the Microwave-Induced Plasma as an Element Selective Detector for Non-Metals, Anal. Chim. Acta, 94(1977) 1.
51. Beenaker, C.I.M., Evaluation of a Microwave-Induced Plasma in Helium at Atmospheric Pressure as an Element

Selective Detector for Gas Chromatography, *Spectrochim. Acta*, 32B(1977) 173.

52. Quimby, B.D., Uden, P.C., and Barnes, R.M., Atmospheric Pressure Helium Microwave Detection System for Gas Chromatography, *Anal. Chem.*, 50(1978) 2112.

53. Robbins, W.B., Caruso, J.A., and Fricke, F.L., Determination of Germanium, Arsenic, Selenium, Tin and Antimony in Complex Samples by Hydride Generation Microwave-Induced Plasma Atomic Emission Spectrometry, *Analyst*, 104(1979) 35.

54. Braman, R.S., and Dynako, A., Direct Current Discharge Spectral Emission-Type Detector, *Anal. Chem.*, 40(1968) 95.

55. Braman, R.S., and Tompkins, M.A., Atomic Emission Spectrometric Determination of Antimony, Germanium, and Methylgermanium Compounds in the Environment, *Anal. Chem.*, 50(1978) 1088.

56. Houpt, P.M., and Baalhuis, G.H.W., Combination of a Second Derivative Ultraviolet Spectrophotometer and a Gas Chromatograph, *Appl. Spectrosc.*, 31(1977) 473.

57. Burchfield, H.P., Wheeler, R.J., and Bernos, J.B., Fluorescence Detector for Analysis of Polynuclear Arenes by Gas Chromatography, *Anal. Chem.*, 43(1971) 1976.

58. Freed, D.J., and Faulkner, L.R., Characterization of Gas Chromatographic Effluents via Scanning Fluorescence Spectrometry, *Anal. Chem.*, 44(1972) 1194.

59. Cooney, R.P., Vo-Dinh, T., and Winefordner, J.D., The SIT Image Vidicon as a Gas Phase Fluorescence Detector for Gas Chromatography, *Anal. Chim. Acta*, 89(1977) 9.
60. Cooney, R.P., and Winefordner, J.D., Instrumental Effects on Limits of Detection in Gas Phase Fluorescence Detection of Gas Chromatographic Effluents, *Anal. Chem.*, 49(1977) 1057.
61. Robinson, J.W.; and Goodbread, J.P., A Selective Gas Chromatographic Detector for Polynuclear Aromatics Based on Ultraviolet Fluorescence, *Anal. Chim. Acta*, 66(1973) 239.
62. Glover, J.H., Chemiluminescence in Gas Analysis and Flame-Emission Spectrometry, *Analyst*, 100(1975) 449.
63. Fontijn, A., Golomb, D., and Hodgeson, J.A., "A Review of Experimental Measurement Methods Based on Gas-Phase Chemiluminescence" reprinted from, *Chemiluminescence and Bioluminescence*, Ed. Cormier, M.J., Hercules, D.M., and Lee, J., Plenum Publishing Corporation, 1973.
64. Bruening, W., and Concha, F.J.M., Selective Detector for Gas Chromatography Based on the Chemiluminescence of Ozone Reactions, *J. Chromatogr.*, 112(1975) 253.
65. Bruening, W., and Concha, F.J.M., Improved Gas Chromatography Ozone Chemiluminescence Detector, *J. Chromatogr.*, 142(1977) 191.
66. Mielniczuk, Z., Flinn, C.G., and Aue, W.A., Photometric Detection of Oxygen, *Anal. Chem.*, 50(1978) 684.

67. Mielniczuk, Z., and Aue, W.A., Construction and Characteristics of a "Cold Flame" Photometric Detector, *J. Chromatogr.*, 166(1978) 1.
68. Grant, D.W., in *Gas Chromatography 1958*, Ed. Desty, D.H., Butterworths, London, (1958) p. 153.
69. Zado, F.M., and Juvet, Jr., R.S., A New Selective-Non Selective Flame Photometric Detector for Gas Chromatography, *Anal. Chem.*, 38(1966) 569.
70. Juvet, Jr., R.S., and Durbin, R.P., Flame Photometric Detection of Metal Chelates Separated by Gas Chromatography, *J. Gas Chromatogr.*, 1 (Dec.)(1963) 14.
71. Braman, R.S., Flame Emission and Dual Flame Emission-Flame Ionization Detectors for Gas Chromatography, *Anal. Chem.*, 38(1966) 734.
72. Belcher, R., Bogdanski, S.L., Burguera, M., Henden, E., and Townshend, A., Molecular Emission Cavity Analysis, Part 12. Evaluation for Gas Chromatographic Detection, *Anal. Chim. Acta*, 100(1978) 515.
73. Belcher, R., Kouimtzis, T., and Townshend, A., Molecular Emission Cavity Analysis - A New Flame Analytical Technique: Part II. The Determination of Selenium and Tellurium, *Anal. Chim. Acta*, 68(1974) 297.
74. Belcher, R., Bogdanski, S.L., Rix, I.H.B., and Townshend, A., Molecular Emission Cavity Analysis: Stimulation of Metal Halide Emissions, *Anal. Chim. Acta*, 81 (1976) 325.

75. Salet, G., Bull. Soc. Chim. France, 13 (1870) 289, as cited in reference 110.
76. Brody, S.S., and Chaney, J.E., Flame Photometric Detector, The Application of a Specific Detector for Phosphorous and Sulfur Compounds - Sensitive to Sub-Nanogram Quantities, J. Gas Chromatogr., 4(1966) 42.
77. Winnett, G., A Simplified Reignition System for Flame Photometric Detectors, J. Chromatogr. Sci., 8 (1970) 554.
78. Watts, R.R., Note on a Simple Solvent Vent System for the GLC-Flame Photometric Detector, Journal of the AOAC, 53(1970) 787.
79. Burgett, C.A., and Green, L.E., An Improved Flame Photometric Detector Gas Chromatography, Spectrochim. Acta, 30B(1975) 55.
80. Hasinski, S., Design of an Unextinguishable Flame Photometric Detector and its Measurement Properties, J. Chromatogr., 119(1976) 207.
81. Moye, H.A., Nonextinguishing Flame Photometric Detector Burner and Housing for Gas Chromatography, Anal. Chem., 41(1969) 1717.
82. Gibbons, P.A., and Goode, K.A., Sulfur-Selective Detector in Natural Gas Chromatography, Gas J., 336(5476) (1968) 27.
83. Rupprecht, W.E., and Phillips, T.R., The Utilization of Fuel-Rich Flames as Sulfur Detectors, Anal. Chim. Acta, 47(1969) 439.

84. Patterson, P.L., Howe, R.L., and Abu-Shumays, A., Dual-Flame Photometric Detector for Sulfur and Phosphorous Compounds in Gas Chromatographic Effluents, *Anal. Chem.*, 50(1978) 339.
85. Patterson, P.L., Comparison of Quenching Effects in Single and Dual-Flame Photometric Detectors, *Anal. Chem.*, 50(1978) 345.
86. Joanson, V.A., and Loog, E.P., A Dual-Channel Flame Photometric Detector with a Separate Combustion Chamber, *J. Chromatogr.*, 120(1976) 285.
87. Greenhalgh, R., and Wilson, M.A., Optimization and Response of the Pye Flame Photometric Detector to Some Insecticides in the Phosphorous and Sulfur Modes, *J. Chromatogr.*, 128(1976) 157.
88. Aldous, K.M., Dagnall, R.M., and West, T.S., The Flame-Spectroscopic Determination of Sulfur and Phosphorous in Organic and Aqueous Matrices by Using a Simple Filter Photometer, *Analyst*, 95(1970) 417.
89. Veillon, C., and Park, J.Y., Use of the Salet Phenomenon in the Determination of Sulfur and Phosphorous in Aqueous and Organic Samples, *Anal. Chim. Acta*, 60(1972) 293.
90. Syty, A., and Dean, J.A., Determination of Phosphorous and Sulfur in Fuel Rich Air-Hydrogen Flames, *Appl. Optics*, 7(1968) 1331.
91. Von H. Hawb, Herrmann, R., and Kolb, M., Residue Analyses of Phosphorous-Containing Insecticides with a

- Filter-Flame Photometer, Deut. Lebensm-Rundsch., 66(1970) 317; CA #130055q, 73, (1970).
92. Laidler, K.J., and Shuler, K.E., Elementary Reactions in the Gas Phase Involving Excited Electronic States, Chem. Rev., 48(1951) 153.
93. Aue, W.A., and Hastings, C.R., Response of a Filterless Flame Photometric Detector to Hetero-Organics, J. Chromatogr., 87(973) 232.
94. Sugiyama, T., Suzuki, Y., and Takeuchi, T., Characteristics of S₂ Emission Intensity with a Flame Photometric Detector, J. Chromatogr., 77(1973) 309.
95. Mizany, A.I., Some Characteristics of the Melpar Flame Photometric GC Detector in the Sulfur Mode, J. Chromatogr. Sci., 8(1970) 151.
96. Sugiyama, T., Suzuki, Y., and Takeuchi, T., Intensity Characteristics of S₂ Emission for Sulfur Compounds with Flame Photometric Detector, J. Chromatogr. Sci., 11(1973) 639.
97. Pecsar, R.E., and Hartmann, C.H., Automated Gas Chromatographic Analysis of Sulfur Pollutants, J. Chromatogr. Sci., 11(1973) 492.
98. Maruyama, M., and Kakemoto, M., Behaviour of Organic Sulfur Compounds in Flame Photometric Detectors, J. Chromatogr. Sci., 16(1978) 1.
99. Eckhardt, J.G., Denton, M.B., and Moyers, J.L., Sulfur FPD Flow Optimization and Response Normalization with a Variable Exponential Function Device, J. Chromatogr. Sci.,

- 13(1975) 133.
100. Retention Times, 2(2)(1975) 2, Tracor Instruments, Austin, Texas 78721, as cited in Ref. 102.
101. Perkin-Elmer Bulletin, Flame Photometric Detector for Gas Chromatography, Norwalk, Conn., August (1975), as cited in Ref. 102.
102. Burnett, C.H., Adams, D.F., and Farwell, S.O., Potential Error in Linearized FPD Responses for Sulfur, J. Chromatogr. Sci., 15(1977) 230.
103. Attar, A., Forge, R., Horn, J., and Corcoran, W.H., Quantitative Evaluation of Chromatographic Data from Non-Linear Detectors and the Sulfur Flame Photometric Detector, J. Chromatogr. Sci., 15(1977) 222.
104. Marcelin, G., Gas Chromatographic Determination of Trace Sulfur. Standard Addition Coupled with Flame Photometric Detection, J. Chromatogr. Sci., 15(1977) 560.
105. Crider, W.L., and Slater, Jr., R.W., Flame-Luminescence Intensification and Quenching Detector (FLIQD) in Gas Chromatography, Anal. Chem., 41(1969) 531.
106. Maitlen, J.C., McDonough, L.M., and Beroza, M., Determination of Residues of 2-Methyl-2-(methylthio) propionaldehyde O-(Methylcarbamoyl) oxime (UC-21149, Temik), Its Sulfoxide, and Its Sulfone by Gas Chromatography, J. Agri. Food Chem., 16(1968) 549.
107. Moss, A.R.L., Theoretical Considerations and the Design of a Flame Photometric Detector, Scan, 4(1974) 5.

108. Zehner, J.M., and Simonaitis, R.A., Improved Technique for Gas Chromatographic Analysis of S-Containing Organic Compounds Using the Flame Photometric Detector, *J. Chromatogr. Sci.*, 14(1976) 348.
109. Sugiyama, T., Suzuki, Y., and Takeuchi, T., Interferences of S₂ Molecular Emission in a Flame Photometric Detector, *J. Chromatogr.*, 80(1973) 61.
110. Gilbert, P.T., in *Analytical Flame Spectroscopy*, Ed.; Mavrodineanu, R., MacMillan, London, 1970, p.279-320.
111. Onley, J.H., Giuffrida, L., Ives, N.F., Watts, R.R., and Storherr, R.W., Gas-Liquid Chromatography and Liquid Chromatography of Ethylenethiourea in Fresh Vegetable Crops, Fruits, Milk and Cooked Foods, *J. of the AOAC*, 60 (1977) 1105.
112. Bowman, M.C., Gas Chromatographic Analysis of Pesticide Residues Containing Phosphorous and/or Sulfur with Flame Photometric Detection and Some Ancillary Techniques for Verifying Their Identities, *Prog. Anal. Chem.*, 5(1973) 175.
113. Devine, J.M., and Siskin, H.R., Use of the Flame Photometric Detector for Determining Residues of Omite [2-(p-tert-Butylphenoxy) cyclohexyl Propargyl Sulfite] in various Crops, *J. Agri. Food Chem.*, 20(1972) 59.
114. Bowman, M.C., Beroza, M., and Hill, K.R., Chromatograms of Foods for Multicomponent Residue Determinations of Pesticides Containing Phosphorous and/or Sulfur

by GLC with Flame Photometric Detection, J. of the AOAC, 54(1971) 346.

115. Gabica, J., Wyllie, J., Watson, M., and Benson, W. W., Example of Flame Photometric Analysis for Methyl Parathion in Rat Whole Blood and Brain Tissue, Anal. Chem., 43 (1971) 1102.

116. Ishikawa, K., Shinohara, R., and Akasaki, K., Behaviour of Thiocarbamate Herbicides in Soil. Part I: Gas Chromatographic Determination of 4-Chlorobenzyl-N, N-diethylthiolcarbamate (Benthiocarb) in Soil, Agri. Biol. Chem., 35(1971) 1161.

117. Ivey, M.C., and Claborn, H.V., Gas Liquid Chromatographic Determination of Ronnel (O, O-Dimethyl O-2,4,5 trichlorophenyl-phosphorothioate) and the Oxygen Analog of Ronnel (Dimethyl 2,4,5 trichlorophenyl phosphate) in Tissues of Cattle, J. Agri. Food Chem., 19(1971) 1256.

118. Williams, I.H., Kore, R., Findlayson, D.G., Determination of Residues of Dasanit and Three Metabolites by Gas Chromatography with Flame Photometric Detection, J. Agri. Food Chem., 19(1971) 456.

119. Bowman, M.C., and Beroza, M., and Gentry, C.R., GLC Determination of Residues of Disulfoton, Oxydemetonmethyl, and Their Metabolites in Tobacco Plants, J. of the AOAC, 52 (1969) 157.

120. Bowman, M.C., and Beroza, M., Determination of Me-s-urol and Five of Its Metabolites in Apples, Pears, and Corn by Gas Chromatography, J. of the AOAC, 52(1969) 1054.

121. Bowman, M.C., and Beroza, M., Rapid GLC Method for Determining Residues of Fenthion, Disulfoton, and Phorate in Corn, Milk, Grass, and Feces, J. of the AOAC, 52(1969) 1231.
122. Bowman, M.C., Beroza, M., and Harding, J.A., Determination of Phorate and Five of Its Metabolites in Corn, J. Agri. Food Chem., 17(1969) 138.
123. Ivey, M.C., and Claborn, H.V., GLC Determination of Dichlorovos in Milk, Eggs, and Various Body Tissues of Cattle and Chickens, J. of the AOAC, 52(1969) 1248.
124. Stanley, C.W., and Morrison, J.I., Identification of Organophosphate Pesticides by Gas Chromatography with the Flame Photometric Detector, J. Chromatogr., 40(1969) 289.
125. Bowman, M.C., and Beroza, M., Determination of Fenthion and Five of Its Metabolites in Corn, Grass and Milk, J. Agri. Food Chem., 16(1968) 399.
126. Bowman, M.C., Beroza, M., and Leuck, D.B., Procedures for Extracting Residues of Phosphorous Insecticides and Metabolites from Field-Treated Crops, J. Agri. Food Chem., 16(1968) 796.
127. Beroza, M., and Bowman, M.C., Gas Chromatography of Pesticide Residues Containing Phosphorous or Sulfur with the Flame Photometric Detector, Envir. Sci. and Tech., 2 (1968) 450.
128. Bowman, M.C., and Beroza, M., Gas Chromatographic Detector for Simultaneous Sensing of Phosphorous and Sulfur-Containing Compounds by Flame Photometry, Anal.

- Chem., 40(1968) 1448.
129. Clay, D.A., Rodgers, C.H., and Jungers, R.H., Determination of Total Sulfur in Gasoline by Gas Chromatography with a Flame Photometric Detector, Anal. Chem., 49(1977) 126.
130. Bentz, A.P., Oil Spill Identification, Anal. Chem., 48(1976) 454A.
131. Wentzel, B., presented at the 27th Pittsburgh Conference on Analytical Chemistry and Applied Spectroscopy, Cleveland, Ohio, March 3, 1976.
132. Garza, Jr., M.E., and Muth, J., Characterization of Crude, Semi-Refined, and Refined Oils by Gas-Liquid Chromatography, Envir. Sci. and Tech., 8(1974) 249.
133. Moshika, Y., and Iida, Y., Gas Chromatographic Determination of Sulfur Compounds in Town Gas, J. Chromatogr., 134(1977) 423.
134. Pearson, C.D., The Determination of Trace Mercaptans and Sulfides in Natural Gas by a Gas Chromatography-Flame Photometric Detector Technique, J. Chromatogr. Sci., 14(1976) 154.
135. Black, M.S., Herbst, R.P., and Hitchcock, D.R., Solid Adsorbent Preconcentration and Gas Chromatographic Analysis of Sulfur Gases, Anal. Chem., 5 (1978) 848.
136. Braman, R.S., Ammons, J.M., and Bricker, J.L., Preconcentration and Determination of Hydrogen Sulfide in Air by Flame Photometric Detection, Anal. Chem., 50(1978) 992.

137. Rasmussen, R.A., Analysis of Trace Organic Sulfur Compounds in Air, Amer. Lab., 4(12)(1972) 55,58,60.
138. Bruner, F., Liberti, A., Possanzini, M., and Allegrini, I., Improved Gas Chromatographic Method for the Determination of Sulfur Compounds at the PPB Level in Air, Anal. Chem., 44(1972) 2070.
139. Bruner, F., Ciccio, P., and DiNardo, F., Further Developments in the Determination of Sulfur Compounds in Air by Gas Chromatography, Anal. Chem., 47(1975)141.
140. Baumgardner, R.E., Clark, T.A., and Stevens, R.K., Increased Specificity in the Measurement of Sulfur Compounds with the Flame Photometric Detector, Anal. Chem., 47(1975) 563.
141. Todd, T.M., Interference-Free Automatic Air Pollutant Chromatographic Analysers, Amer. Lab., 3(10)(1971) 51.
142. Stevens, R.K., and O'Keefe, A.E., Modern Aspects of Air Pollution Monitoring, Anal. Chem., 42(1970) 143A.
143. Blomberg, L., Gas Chromatographic Separation of Some Sulfur Compounds on Glass Capillary Columns Using Flame Photometric Detection, J. Chromatogr., 125(1976) 389.
144. Ronkainen, R., Denslow, J., and Leppänen, O., The Gas Chromatographic Analysis of Some Volatile Sulfur Compounds, J. Chromatogr. Sci., 11(1973) 384.
145. Crider, W.L., Applications of Hydrogen Flame Emission Spectrophotometry to the Analysis of Air Pollutants, Amer. Lab.; 1(11)(1969) 10,16,19.

146. Prager, M.J., and Seitz, W.R., Flame Emission Photometer for Determining Phosphorous in Air and Natural Waters, *Anal. Chem.*, 47(1975) 148.
147. Addison, R.F., and Ackman, R.G., Direct Determination of Elemental Phosphorous by Gas-Liquid Chromatography, *J. Chromatogr.*, 47(1970) 421.
148. Struble, D.L., Quantitative Determination of Elemental Sulfur by GLC with an Electron Capture Detector or a Flame Photometric Detector, *J. Chromatogr. Sci.*, 10(1972) 57.
149. Darlage, L.J., Block, S.S., and Weidner, J.P., The Use of a Flame Photometric Detector for the Analysis of Coal Sulfur, *J. Chromatogr. Sci.*, 11(1973) 272.
150. Pease, H.L., and Holt, J., Manganese Ethylenebis (dithiocarbamate) (Maneb)/Ethylenethiourea(ETU) Residue Studies on Five Crops Treated with Ethylenebis (dithiocarbamate) (EBDC) Fungicides, *J. Agric. Food Chem.*, 25(1977) 561.
151. Nurok, D., Anderson, J.W., and Zlatkis, A., Profiles of Sulfur Containing Compounds Obtained from Arabica and Robusta Coffees by Capillary Column Gas Chromatography, *Chromatographia*, 11(1978) 188.
152. Kawabata, M., Ohtsuki, K., Kokura, H., and Wakahara, Y., Determination of Dimethylsulfide in the Head Space Vapor of Green Tea by Gas Chromatography, *Agric. Biol. Chem.*, 41(1977) 2285.
153. Robinson, W.H., and Hilton, H.W., Gas Chromatography of Phosphine Derived from Zinc Phosphide in Sugarcane, *J.*

- Agri. Food Chem., 19(1971) 875.
154. Kaji, H., Hisamura, M., Saito, N., and Murao, M., Gas Chromatographic Determination of Volatile Sulfur Compounds in the Expired Alveolar Air in Hepatopathic Subjects, J. Chromatogr., 145(1978) 464.
155. Gearhart, H.L., Pierce, S.K., and Payne-Base, D., A Sampling Technique for Organic Components in Human Breath, J. Chromatogr. Sci., 15(1977) 480.
156. Blanchette, A.R., and Cooper, A.D., Determination of Hydrogen Sulfide and Methyl Mercaptan in Mouth Air at the Parts-per-Billion Level by Gas Chromatography, Anal. Chem., 48(1976) 729.
157. Crider, W.L., Hydrogen-Air Flame Chemiluminescence of Some Organic Halides, Anal. Chem., 41(1969) 534.
158. Dagnall, R.M., Smith, D.J., Thompson, K.C., and West, T.S., Emission Spectra Obtained from the Combustion of Organic Compounds in Hydrogen Flames, Analyst, 94(1969) 871.
159. Dagnall, R.M., Fleet, B., and Risby, T.H., Molecular Emission Characteristics of Various Fluorides in a Low Temperature-Hydrogen Diffusion Flame, Talanta, 18(1971) 155.
160. Sowinski, E.J., and Suffet, I.H., Characterization of a Melpar Flame Photometric-Gas Chromatographic System for Application to Boron Hydrides, J. Chromatogr. Sci., 9 (1971) 632.

161. Ref. 110, pp. 188-213.
162. Sowinski, E.J., and Suffet, I.H., Gas Chromatographic Detection and Confirmation of Volatile Boron Hydrides at Trace Levels, *Anal. Chem.*, 46(1974) 1218.
163. Ross, R., and Shafik, T., The Determination of Chromium in Human Urine by Gas Chromatography Using a Flame Photometric Detector with a 425.4 nm Filter, *J. Chromatogr. Sci.*, 11(1973) 46.
164. Bowman, M.C., and Beroza, M., A Copper-Sensitized Flame Photometric Detector for Gas Chromatography of Halogen Compounds, *J. Chromatogr. Sci.*, 7(1969) 484.
165. Gunther, F.A., Lopez-Roman, A., Asai, R.I., and Westlake, W.E., Expanded Utility of the Beilstein Flame Test for Organically Bound Halogens as a Sensitive and Specific Flame Photometric Detector in the Gas Chromatographic Determination of R-X Compounds as Illustrated with Organochlorine Pesticides, *Bull. Envir. Contam. Toxicol.*, 4(1969) 202.
166. Ševčík, J., Selective Detection of Sulfur, Chlorine and Nitrogen with the Help of the Combination of Flame Ionization and Flame Photometric Detectors, *Chromatographia*, 4(1971) 195.
167. Gilbert, P.T., Flame Photometric Determination of Chlorine by Indium Chloride Band Emission, *Anal. Chem.*, 38(1966) 1920.
168. Bowman, M.C., and Beroza, M., An Indium-Sensitized,

- Flame Photometric Detector for Gas Chromatography of Halogen Compounds, *J. Chromatogr. Sci.*, 9(1971) 44.
169. Roseman, R.F., and Aue, W.A., A Dual-Mode Indium Flame Detector, *J. Chromatogr.*, 63(1971) 229.
170. Versino, B., and Rossi, G., Dual Flame Photometric Detector (DFPD) for the Simultaneous G.C. Determination of P-, S- and Cl-Containing Organic Compounds, *Chromatographia*, 4(1971) 331.
171. Gutsche, B., and Herrmann, R., Jod-spezifischer Detektor für einen Gas-Chromatographen, *Z. Anal. Chem.*, 253(1971) 257.
172. Gutsche, B., and Herrmann, R., Ein spezifischer Detektor für den Bromnachweis hinter einem Gas-Chromatographen, *Z. Anal. Chem.*, 249(1970) 168.
173. Overfield, C.V., and Winefordner, J.D., The Selective Indium Halide Flame Emission Detector - A Potentially Useful Detector for Gas Chromatography, *J. Chromatogr. Sci.*, 8 (1970) 233.
174. Dagnall, R.M., Thompson, K.C., and West, T.S., Molecular-Emission Spectroscopy in Cool Flames. Part IV. The Determination of Chloride, Bromide and Iodide by Thermal-Emission Spectroscopy in the Presence of Indium Salts, *Analyst*, 94(1969) 643.
175. Herrmann, R., and Gutsche, B., Improvement of Detection Limits of Flame-Spectrophotometric Determination of Chlorinated Organic Pesticide Residues, *Analyst*, 94(1969) 1033.

176. Gutsche, B., and Herrmann, R., Über eine Kombinationsmöglichkeit der Gas-Chromatographie mit der Flammenphotometrie für den Chlornachweis, Z. Anal. Chem., 245(1969) 274.
177. Novak, A.V., and Malustadt, H.V., Selective Gas Chromatographic Detection Utilizing Emitted Radiation from a Sensitized Flame, Anal. Chem., 40(1968) 1108.
178. Aus, W.A., and Roseman, R.E., presented in the Second International Congress of Pesticide Chemistry, Tel Aviv, Israel, February, 1971.
179. Price, J.W., Tin in the World Today, Fresenius Z. Anal. Chem., 288(1977) 257.
180. Organotin Compounds: New Chemistry and Applications, Symposium at the 171st Meeting of the ACS, New York, April 1976; Adv. Chem. Ser., 157(1976), as cited in Ref. 229.
181. Thayer, J.S., Biological Aspects of Organometallic Chemistry, J. Chem. Educ., 48(1971) 806.
182. Anonymous, C and EN News, Sept. 27(1976) 15, as cited in Ref. 229.
183. O'Sullivan, D.A., C and EN News, Feb. 28(1977) 17, as cited in Ref. 229.
184. Vetterazzi, G., State of the Art of the Toxicological Evaluation Carried Out by the Joint FAO/WHO Expert Committee on Pesticide Residues III. Miscellaneous Pesticides Used in Agriculture and Public Health, Residue Rev., 66(1977) 137.
185. Anonymous, C and EN News, April 25(1977) 23.
186. Piver, W.T., Environ. Health Perspect., June (1973) 61, as cited in Ref. 229.

187. Crompton, T.R., *Chemical Analysis of Organometallic Compounds, Elements of Group IV B*, Academic Press, London, New York, San Francisco, 1974.
188. Kumpulainen, J. and Koivistoinen, P., *Advances in Tin Compound Analysis with Special Reference to Organotin Pesticide Residues*, *Residue Rev.*, 66(1977) 1.
189. Filer, T.D., *Fluorometric Determination of Submicrogram Quantities of Tin*, *Anal. Chem.*, 43(1971) 1753.
190. Patel, B.M., Reeves, R.D., Browner, R.F., Molnar, C.J., and Winefordner, J.D., *Atomic Fluorescence Spectrometry with a Graphite Rod Atomizer and Thermostatted Electrodeless Discharge Lamps*, *Appl. Spectrosc.*, 27(1973) 171.
191. Dagnall, R.M., Thompson, K.G., and West, T.S., *Molecular-Emission Spectroscopy in Cool Flames. Part III. The Emission Characteristics of Tin in Diffusion Flames*, *Analyst*, 93(1968) 518.
192. Stegman, H.B., Uber, W., and Scheffler, K., *Analytik von Di- und Triorgano-Zinn-Verbindungen durch Elektronen-Spin-Resonanz*, *Z. Anal. Chem.*, 286(1977) 59.
193. National Research Council, *Committee on Medical and Biological Effects of Environmental Pollutants, Subcommittee on Selenium*, National Academy of Sciences, Washington, D.C. (1976) , as cited in Ref. 236.
194. Rosenfeld, I., and Beath, A.O., *Selenium, Geobotany, Biochemistry, Toxicity and Nutrition*, Academic Press, New

- York, London, 1964, as cited in Ref. 236.
195. Selenium in Biomedicine, Ed.: Muth, O.H., Avi Publication Co., Westport, Conn., 1967.
196. Anonymous, C and EN News, 55(3)(1977) 35, as cited in Ref. 236.
197. Crosby, N.T., Determination of Metals in Foods, Analyst, 102(1977) 225.
198. Poole, C.F., Evans, N.J., Wibberley, D.G., Determination of Selenium in Biological Samples by Gas-Liquid Chromatography with Electron-Capture Detection, J. Chromatogr., 136(1977) 73.
199. Meyer, A., Grallath, E., Kaiser, G., and Tölg, G., Extrem Nachweisstarkes Gas-Chromatographisches Bestimmungsverfahren für Selen nach Abtrennung durch Verdampfen in Sauerstoffstrom I. Bestimmung in Reinstkupfer, Z. Anal. Chem., 281(1976) 201.
200. Kawashima, T., Kai, S., and Takashima, S., Catalytic Determination of Ultratrace Amounts of Selenium (IV), Anal. Chim. Acta, 89(1977) 65.
201. Berti, M., Buso, G., Colautti, P., Moschini, G., Stievano, B.H., and Tregnaghi, C., Determination of Selenium in Blood Serum by Proton-Induced X-ray Emission, 49 (1977) 1313.
202. Akiba, M., Shimoishi, Y., and Tōei, K., Gas-Chromatographic Determination of Selenium in Pure Elemental Arsenic and Arsenic (III) Oxide with 4-Nitro-1,2-diaminobenzene, Analyst, 101(1976) 644.

203. Shimoishi, Y., Some 1,2-Diaminobenzene Derivatives as Reagents for Gas Chromatographic Determination of Selenium with an Electron-Capture Detector, *J. Chromatogr.*, 136(1977) 85.
204. Nazarenko, I.I., and Ermakov, A.N., *Analytical Chemistry of Selenium and Tellurium*, English Translation, Israel Program for Scientific Translations, Jerusalem, 1973.
205. *Handbook of Chemistry and Physics*, CRC Press, Cleveland, Ohio, 56th Edition, (1975-1976), B-16 to B-17.
206. Van DerKerk, G.J.M., in "Pesticide Chemistry in the 20th Century", a Symposium Sponsored by the Division of Pesticide Chemistry at the 171st Meeting of the ACS, New York, N.Y., April 6, 1976.
207. Lussi-Schlatter, B., and Brandenberger, H., "Trace Detection of Some Inorganic Hydride such as Arsine, Germanium Hydride, Stibene and Tin Hydride by Gas Chromatography with Mass Specific Detection (GC-MD)", in *Advances in Mass Spectrometry in Biochemistry and Medicine*, Volume 2, Spectrum Publications.
208. Sutton, D.G., Melzer, J.E., and Capelle, G.A., Determination of Trace Amounts of Alkyls and Hydrides by Metastable Transfer Emission Spectrometry, *Anal. Chem.*, 50 (1978) 1247.
209. Ref. 205, B-36.
210. Masson, M.R., Determination of Selenium and Tellurium in Organic Compounds and Organic Materials - A Review,

- Mikrochim. Acta, I(4-5) (1976) 419.
211. Guiochon, G., and Pommier, C., Gas Chromatography in Inorganics and Organometallics, Ann Arbor Science, Ann Arbor (1973), 182-184.
212. Poller, R.G., The Chemistry of Organotin Compounds, Logos Press Limited, and Elek Books Limited, London, (1970) pp. 105-129.
213. Lipowitz, J., and Bowman, S.A., Use of Polymethylhydrosiloxane as a Selective, Neutral Reducing Agent for Aldehydes, Ketones, Olefins, and Aromatic Nitro Compounds, J. Org. Chem., 38(1973) 162.
214. Geissler, H., and Kreigsman, H., Separation Solvents for the Gas Chromatographic Investigation of Certain n-Butyltin Compounds, Z. Chem., 5(1965) 423; CA #11834d, 64(1966).
215. Tonge, B.L., The Gas Chromatographic Analysis of Butyl-, Octyl- and Phenyltin Halides, J. Chromatogr., 19 (1965) 182.
216. Gauer, W.O., Seiber, J.N., and Crosby, D.G., Determination of Organotin Residues from Plictran in Fruit Crops by Gas-Liquid Chromatography, J. Agri. Food Chem., 22(1974) 252.
217. Mainema, H.A., Burger-Wiersma, T., Versluis-deHaan, G.V., and Gevers, E.C., Determination of Trace Amounts of Butyltin Compounds in Aqueous Systems by Gas Chromatography/Mass Spectrometry, Environ. Sci. Technol., 12(1978) 288.

218. Hill, Jr., H.H., and Aue, W.A., Performance of a Silicon-Doped Hydrogen Atmosphere Flame Ionization Detector for Gas Chromatography, *J. Chromatogr.*, 122(1976) 515.
219. Figge, K., Koch, J., and Lubba, H., Beitrag Zur Gaschromatographischen Analyse Von Organozinn-Stabilisatoren Fur Polyvinylchlorid, *J. Chromatogr.*, 131(1977) 317.
220. Birnbaum, E.R., and Javora, P.H., The Reaction of Organotin Chlorides with Sodium Borohydride: A New Preparation of Organotin Hydrides, *J. Organometal. Chem.*, 9 (1967) 379.
221. Hayashi, K., Iyoda, J., and Shihara, I., Reaction of Organotin Oxides, Alkoxides and Acyloxides with Organosilicon Hydrides, New Preparative Method of Organotin Hydrides, *J. Organometal. Chem.*, 10(1967) 81.
222. Itoi, K., and Kumano, S., Synthesis of Organotin Hydrides by the Hydrogen Exchange Reaction with Silicon Hydrides, *Kogyo Kagaku Zasshi*, 70(1967) 82; CA #11556v, 67(1967).
223. Considine, W.J., and Ventura, J.J., Reduction of Bis-Tributyltin Oxide with Lithium Aluminium Hydride, *Chem. Ind.*, Part 3 (1962) 1683.
224. Zorin, A.D., Devyatykh, G.G., Dudorov, V. Ya., and Amel'chenko, A.M., Analysis of Mixtures of Certain Volatile Inorganic Hydrides by Gas-Liquid Partition Chromatography, *Russ. J. Inorg. Chem.*, 9(1964) 1364.
225. Kadeg, R.D., and Christian, G.D., Gas Chromatographic Determination of Selected Group IV-VI Element Hydrides,

- Anal. Chim. Acta, 88(1977) 117.
226. Evans, C.S., and Johnson, C.M., The Separation of Some Alkyl Selenium Compounds by Gas Chromatography, J. Chromatogr., 21(1966) 202.
227. Ref. 211, pp. 163-169, pp. 174-178.
228. Snegova, A.D., Markov, L.K., and Ponomarenko, V.A., The Use of Gas Liquid Chromatography for the Analysis of Halogen-Containing Silicon and Germanium Organic Compounds, J. Anal. Chem. USSR, 19(1964) 564.
229. Aue, W.A., and Flinn, C.G., A Photometric Tin Detector for Gas Chromatography, J. Chromatogr., 142(1977) 145.
230. Pearce, R.W.B., and Gaydon, A.G., The Identification of Molecular Spectra, Chapman and Hall Ltd., London, (1963), p. 289.
231. Herrmann, R., and Alkemade, C.T.J., Chemical Analysis by Flame Photometry, Interscience Publishers Inc., New York and London, (1963), p. 403-404, p. 562-563.
232. Connelly, F.C., The Band Spectrum of Tin Oxide, Proc. Phys. Soc., 45(1933) 780.
233. Joshi, M.M., and Yamdagni, R., Flame Emission Spectrum of SnO Molecule in the Visible Region, Indian J. Phys., 41(1967) 275.
234. Aue, W.A., and Flinn, C.G., Letter to the Editor, Note added in Proof, J. Chromatogr., 153(1978) 305.
235. Lee, M.L., and Hites, R.A., Characterization of Sulfur-Containing Polycyclic Aromatic Compounds in Carbon Blacks, Anal. Chem., 48(1976) 1890.

236. Flinn, C.G., and Aue, W.A., Photometric Detection of Selenium Compounds for Gas Chromatography, *J. Chromatogr.*, 153(1978) 49.
237. Salet, G., *C. R. Acad. Sci.*, 73(1871) 742; *C. Z.*, 42 (1871) 641; as cited in Ref. 110.
238. Emelius, H.J. and Riley, H.L., *Proc. Roy. Soc. Ser. A*, 140(1933) 378; *CA*, #3400, 27(1933), as cited in Ref. 110.
239. Ref. 110, pp. 296-308.
240. Aue, W.A., and Flinn, C.G., Chemical Linearization of Chalcogen Response in a Flame Photometric Detector, *J. Chromatogr.*, 158(1978) 161.
241. Mohan, H., and Majumdar, K., Absorption Spectrum of Tellurium Monosulfide in the Ultraviolet Region, *Proc. Phys. Soc.*, 77(1961) 147.
242. Joshi, M.M., and Sharma, D., The Ultra-Violet Absorption Spectrum of TeSe, *Proc. Phys. Soc.*, 90(1967) 1159.
243. Barrow, R.F., Dudley, M.A.H., Hitchings, M.R., and Yee, K.K., The Electronic Spectrum of Gaseous TeS, *J. Phys. B*, 5(1972) L172.
244. Ahmed, F., Barrow, R.F., and Yee, K.K., Fluorescence and Absorption Spectra of Gaseous TeSe, *J. Phys. B*, 8(1975) 649.
245. Ahmed, F., and Barrow, R.F., Rotational Analysis of Absorption Bands of Gaseous SeS, *J. Phys. B*, 7(1974) 2256.
246. Ref. 110, pp. 308-320.

247. Sharma, A., and Padur, J.P., A Spectroscopic Study of the Chemiluminescent Reaction of Germanium Tetrahydride with Atomic Oxygen, Proc. Phys. Soc., 90(1967) 269.
248. Meyer, B., Jones, Y., Smith, J.J., and Spitzer, K., The Spectrum of Matrix-Isolated GeO and GeS, J. Mol. Spectrosc., 37(1971) 100.
249. Ref. 230, p. 167.
250. Tewari, D.P., and Mohan, H., Band Spectrum of the Molecule Germanium Monoxide (GeO) in the Visible Region, J. Mol. Spectrosc., 39(1971) 290.
251. Reduction: Techniques and Applications in Organic Synthesis, Ed. Augustine, R.L., Marcel Dekker, Inc., New York, 1968.
252. Moseman, R.F., Rapid Procedure for Preparation of Support-Bonded Carbowax 20M Gas Chromatographic Column Packing, J. Chromatogr., 166(1978) 397.
253. Mitscherlich, A., Ann. Physik, 121(1864) 459, as cited in Ref. 110.
254. Barrow, G.M., Physical Chemistry, 2nd Edition, McGraw-Hill Inc., p. 44.
255. Ref. 205, A-165.